

University of Windsor

## Scholarship at UWindor

---

Electronic Theses and Dissertations

Theses, Dissertations, and Major Papers

---

1989

### An investigation of the effect of fly ash on the entrained-air-void system in concrete using a newly developed image analysis system.

Barbara Yvette. Hughes  
*University of Windsor*

Follow this and additional works at: <https://scholar.uwindsor.ca/etd>

---

#### Recommended Citation

Hughes, Barbara Yvette., "An investigation of the effect of fly ash on the entrained-air-void system in concrete using a newly developed image analysis system." (1989). *Electronic Theses and Dissertations*. 1126.

<https://scholar.uwindsor.ca/etd/1126>

This online database contains the full-text of PhD dissertations and Masters' theses of University of Windsor students from 1954 forward. These documents are made available for personal study and research purposes only, in accordance with the Canadian Copyright Act and the Creative Commons license—CC BY-NC-ND (Attribution, Non-Commercial, No Derivative Works). Under this license, works must always be attributed to the copyright holder (original author), cannot be used for any commercial purposes, and may not be altered. Any other use would require the permission of the copyright holder. Students may inquire about withdrawing their dissertation and/or thesis from this database. For additional inquiries, please contact the repository administrator via email ([scholarship@uwindsor.ca](mailto:scholarship@uwindsor.ca)) or by telephone at 519-253-3000ext. 3208.



National Library  
of Canada

Bibliothèque nationale  
du Canada

Canadian Theses Service

Service des thèses canadiennes

Ottawa, Canada  
K1A 0N4

## NOTICE

The quality of this microform is heavily dependent upon the quality of the original thesis submitted for microfilming. Every effort has been made to ensure the highest quality of reproduction possible.

If pages are missing, contact the university which granted the degree.

Some pages may have indistinct print especially if the original pages were typed with a poor typewriter ribbon or if the university sent us an inferior photocopy.

Reproduction in full or in part of this microform is governed by the Canadian Copyright Act, R.S.C. 1970, c. C-30, and subsequent amendments.

## AVIS

La qualité de cette microforme dépend grandement de la qualité de la thèse soumise au microfilmage. Nous avons tout fait pour assurer une qualité supérieure de reproduction.

S'il manque des pages, veuillez communiquer avec l'université qui a conféré le grade.

La qualité d'impression de certaines pages peut laisser à désirer, surtout si les pages originales ont été dactylographiées à l'aide d'un ruban usé ou si l'université nous a fait parvenir une photocopie de qualité inférieure.

La reproduction, même partielle, de cette microforme est soumise à la Loi canadienne sur le droit d'auteur, SRC 1970, c. C-30, et ses amendements subséquents.

AN INVESTIGATION OF THE EFFECT OF FLY ASH  
ON THE ENTRAINED-AIR-VOID SYSTEM IN CONCRETE  
USING A NEWLY DEVELOPED IMAGE ANALYSIS SYSTEM

by

© BARBARA YVETTE HUGHES

A Thesis  
submitted to the  
Faculty of Graduate Studies and Research  
through the Department of  
Civil Engineering in Partial Fulfillment  
of the requirements for the Degree of  
Master of Applied Science at  
the University of Windsor

Windsor, Ontario, Canada

1989



National Library  
of Canada

Bibliothèque nationale  
du Canada

Canadian Theses Service    Service des thèses canadiennes

Ottawa, Canada  
K1A 0N4

The author has granted an irrevocable non-exclusive licence allowing the National Library of Canada to reproduce, loan, distribute or sell copies of his/her thesis by any means and in any form or format, making this thesis available to interested persons.

The author retains ownership of the copyright in his/her thesis. Neither the thesis nor substantial extracts from it may be printed or otherwise reproduced without his/her permission.

L'auteur a accordé une licence irrévocable et non exclusive permettant à la Bibliothèque nationale du Canada de reproduire, prêter, distribuer ou vendre des copies de sa thèse de quelque manière et sous quelque forme que ce soit pour mettre des exemplaires de cette thèse à la disposition des personnes intéressées.

L'auteur conserve la propriété du droit d'auteur qui protège sa thèse. Ni la thèse ni des extraits substantiels de celle-ci ne doivent être imprimés ou autrement reproduits sans son autorisation.

ISBN 0-315-50513-3

ACB 8915



Barbara Yvette Hughes 1989  
All Rights Reserved

## TABLE OF CONTENTS

	Page No.
ABSTRACT.....	iv
DEDICATION.....	v
ACKNOWLEDGEMENTS.....	vi
TABLES.....	vii
FIGURES.....	ix
CHAPTER	
1 INTRODUCTION.....	1
2 COMPOSITION OF CONCRETE.....	4
Constituents of Concrete.....	4
General	
Paste Structure	
Pore Structure.....	11
Porosity	
Air Voids in Concrete	
Durability of Concrete.....	16
General	
Theory of Frost Action	
Role of Entrained Air in	
Freeze-Thaw Durability	
3 FLY ASH IN CONCRETE.....	25
Introduction.....	25
Pozzolans.....	26
Fly Ash as a Pozzolan.....	29
Physical Properties of Fly Ash	
Chemical Properties of Fly Ash	
Effect of Fly Ash on Properties of	
Concrete.....	39
4 MEASUREMENT OF THE AIR-VOID SYSTEM IN	
CONCRETE.....	48
Introduction.....	48
Parameters of the Air-Void System.	50
Factors Affecting the Air-Void	
System in Fresh Concrete.....	51
Measurement of Air Content in	
Plastic Concrete.....	55
Measurement of Air Content in	
Hardened Concrete.....	57
Image Analysis.....	65

## TABLE OF CONTENTS (cont'd)

	Page No.
5 DEVELOPMENT OF AN IMAGE ANALYSIS SYSTEM USING A PC.....	69
General.....	69
Computerized Hardware.....	70
Stage Unit.....	73
Design of Stage Equipment	
Microscope-Camera	
Lighting Setup	
Computer Software .....	77
Standardization of the Image Analysis System.....	79
6 EXPERIMENTAL PROGRAM.....	86
General.....	86
Mixture Design.....	88
Materials	
Batching	
Sample Preparation.....	95
Casting	
Polishing	
Surface Preparation	
Analysis of Sample Surface.....	99
7 RESULTS.....	101
Introduction.....	101
Presentation of Data.....	102
Statistical Evaluation of Image Analysis Data.....	109
Analysis and Discussion.....	112
Air-Entraining Agent Demand	
Compressive Strength	
Air Content	
Entrained-Air-Void System	
8 CONCLUSIONS AND RECOMMENDATIONS.....	137
APPENDIX A STATISTICAL METHODS.....	140
APPENDIX B IMAGE ANALYSIS SOFTWARE PROGRAM.....	143
REFERENCES	158
VITA AUCTORIS	169

## ABSTRACT

The effect of fly ash on the entrained air void system in concrete was analyzed, in both the plastic and hardened states. To analyze the concrete in the hardened state the plane-intercept method of analysis was applied to a newly developed image analysis system using a personal computer.

Three fly ashes were tested at two nominal air contents. The addition of fly ash to the concrete mixture was found to increase the demand for air entraining agent to attain the required air content. The fly ash concretes also require a longer curing period to attain the same strength as the non-fly ash concretes. However, analysis of the concrete in the hardened state indicates no significant difference in the characteristics of the entrained-air-void system for the fly ash and non-fly ash concretes.

An image analysis system for air content measurement using a personal computer was found to be a good alternative to the more expensive complex image analysis systems on the market today.



I thank my parents for  
giving me the support  
and encouragement to  
attain what appeared at  
times to be the impossible.  
To them I dedicate this  
work.

### ACKNOWLEDGEMENTS

I wish to express my sincere gratitude to Dr. C. MacInnis and Dr. P. Hudec for their interest and guidance during this research.

I would also like to thank the technical staff in both the Civil Engineering and Geological Engineering departments for their cooperation and expertise in conducting the laboratory work. In addition appreciation is extended to Ontario Hydro for supplying the fly ash samples used in this research.

To complete a project such as this requires a tremendous amount of motivation and support. For this I thank my colleagues, Nick Sitar and Tom O'Dwyer. Their generous support and encouragement will be remembered.

Lastly, but most importantly, I thank my husband, Tom, for his patience and understanding throughout the entirety of this project.

# TABLES

	Page No.
2-1 Classification of Pore Sizes in Hydrated Cement Pastes.....	14
3-1 Pozzolanic Materials.....	28
3-2 Chemical Requirements of Fly Ash.....	34
3-3 Chemical Properties of a Class C Fly Ash.....	36
4-1 Class of Exposure of Concrete.....	49
4-2 Effect of Mixture Design and Concrete Constituents on Control of Air Content in Concrete.....	52
5-1 Data Retrieved during Scaling Process.....	81
5-2 Comparison of Air Contents.....	83
5-3 Statistical Comparison of Linear Traverse and Image Analysis Air-Content Results.....	84
6-1 Summary of Test Program.....	87
6-2 Physical and Chemical Analysis of Fly Ash....	92
7-1 Record of Casting .....	104
7-2 Summary of Image Analysis Data.....	105
7-3 Characteristics of the Entrained Air-Void System using the Plane-Intercept Method of Analysis.....	108
7-4 Statistical Comparison of Means of Total Number of Entrained Voids in Table 7-2..	110
7-5 Statistical Comparison of Means of 28-day Compressive Strength for 5 and 8 Percent Nominal Air Content (Table 7-1).....	115
7-6 Statistical Comparison of Paired Means of 28-day Compressive Strength for Fly Ash Concretes (Table 7-1).....	116
7-7 Statistical Comparison of Paired Means of 56-day Compressive Strength for Fly Ash Concretes (Table 7-1).....	116

TABLES (cont'd)

	Page No.
7-8 Comparison of Measured Air Contents.....	121
7-9 Statistical Comparison of % Total Air Content measured in the Plastic State and Hardened State (Table 7-7).....	122
7-10 Statistical Comparison of Means of Entrained Air Content for Control Mix with Fly Ash Concrete (Table 7-3).....	126
7-11 Statistical Comparison of Means of Entrained Air Content for 20% and 30% Fly Ash Mixtures (Table 7-3).....	127
7-12 Statistical Comparison of Paired Means of Entrained Air Content for Fly Ash Concrete (Table 7-3).....	128
7-13 Statistical Comparison of Means of Voids per Volume for Control Concrete and Fly Ash Concrete (Table 7-3).....	129
7-14 Statistical Comparison of Means of Spacing Factor for Control Concrete and Fly Ash Concrete (Table 7-3).....	131
7-15 Statistical Comparison of Means of Specific Surface for Control Concrete and Fly Ash Concrete (Table 7-3).....	132
7-16 Statistical Comparison of Means of Average Void Diameter for Control Mix with Fly Ash Concrete (Table 7-3).....	133
7-17 Size Distribution of Entrained Air Voids.....	135

## FIGURES

	Page No.
2-1 The relation between strength and water/cement ratio of concrete.....	6
2-2 Simplified model of paste structure.....	10
2-3 Schematic model of C-S-H in cement paste...	10
2-4 Volume relationships among constituents of hydrated pastes: (a) constant w/c ratio = 0.50; (b) changing w/c ratio ( = 1.0).	19
2-5 Creation of hydraulic pressure in frozen cement paste: (a) non-air-entrained; 9b) air-entrained paste.....	24
3-1 Typical schematic of coal burning process....	30
3-2 Particle size distributions of two fly ashes, AD-94, collected mechanically, and AD-3, collected electrostatically.....	31
3-3 Laboratory report for a fly ash sample, Lingan, Nova Scotia.....	35
3-4 Comparison of compositions of fly ashes with natural pozzolans and portland cements in the system CaO-SiO <sub>2</sub> -Al <sub>2</sub> O <sub>3</sub> .....	40
4-1 Pressure meter used to measure air content in plastic concrete.....	57
5-1 Image analysis hardware.....	70
5-2 Schematic of Oculus 200 image analysis board.	72
5-3 Printout of Image Analysis for Sample CM057..	78
5-4 Pattern used to scale image analysis.....	80
5-5 Relationship between Image Analysis and Linear Traverse - Air Content.....	85
6-1 Gradation of coarse aggregate.....	89
6-2 Gradation of fine aggregate.....	90
6-3 Concrete mixer.....	94
6-4 Concrete saw.....	96

FIGURES (cont'd)

	Page No.
6-5 Polishing unit.....	97
6-6 Prepared sample surface.....	99
6-7 Pattern of analysis of sample surface.....	100
7-1 Percent Increase in Air Entraining Agent Demand vs LOI of Fly Ash.....	113
7-2 Compressive Strength of Concrete at 5% Nominal Air Content.....	119
7-3 Compressive Strength of Concrete at 8% Nominal Air Content.....	119
7-4 Bar Graph of Percent Distribution of Section Diameters.....	136

## CHAPTER 1

### INTRODUCTION.

Concrete is one of the most widely used and complex building materials used in construction today. The integration of new advanced admixtures with the high quality cements in the concrete industry has produced very favorable results with respect to both strength and durability of concrete elements.

In spite of the many new developments in the concrete industry, the basics of concrete durability and serviceability remain the same. The durability of a concrete structure will depend on the quality of the concrete and on the environment to which it is exposed. The most common cause of deterioration in concrete in temperate climates is exposure to cyclic freezing and thawing. In addition to the aggressive action of freezing and thawing within the concrete, many concrete structures, such as bridges and parking garages, are exposed to deicing salts which accelerate the deterioration process.

The two main characteristics of concrete, which will improve its durability are decreased permeability of the paste and an adequate entrained air-void system. One method of decreasing the permeability of the paste is through the addition of fly ash to the concrete mixture, as a partial replacement of the cement. The fly ash behaves as a

pozzolan where reaction products will produce a less permeable paste through which the passage of aggressive water is inhibited.

The purposeful entrainment of air in concrete was recognized in the 1940's as an effective method of providing protection against freeze-thaw action. The effectiveness of a given the entrained air-void system in increasing concrete durability can be evaluated by correlating the characteristics of the air-void system in the hardened concrete with its freeze-thaw performance in the laboratory or field performance.

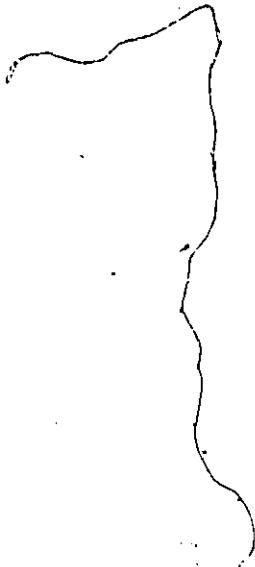
Unfortunately, the addition of fly ash to concrete has been found to inhibit the entrainment of air in concrete. The most prominent characteristic of the fly ash affecting entrained air in concrete is carbon content; however the exact mechanism of this effect is not known.

This research was undertaken to determine what effects fly ash has on the characteristics of the entrained air-void system. The test program included three fly ashes with varying carbon contents batched at two nominal air contents.

To perform microscopical analysis of the concrete, an image analysis system was developed using optics coupled with a desktop personal computer and application software. Computerized analysis of the hardened concrete provided a time-efficient and easy method by which to determine the



characteristics of the entrained air-void system in fly ash-concrete.



## CHAPTER 2

### COMPOSITION OF CONCRETE

#### 2.1 Constituents of Concrete

##### 2.1.1 General

In a civil engineering context, concrete can be defined as a construction material formed by a coalition of a cementing material and a mineral aggregate. Depending on the cementing medium, concretes may include, for example, asphaltic concrete, high alumina cement (HAC) concrete, portland cement concrete, or polymer concrete. The term concrete in this research, refers to portland cement concrete.

Portland cement concrete, in its simplest form is a mixture of portland cement, water, and aggregate, which is combined to form a solid heterogeneous material. The inherent material and structural features of a concrete structure will depend on the individual characteristics of the constituents and the proportions in which they are present. A quality mixture design, as well as good mixing, placing and curing are essential for the production of reliable concrete structures. The Canadian Standard Association (CSA) publishes CAN3-A23.1-M77 [1] and

CAN3-A23.2-M77 [2] which provide guidelines and minimum specifications for quality of concrete materials, methods of concrete construction, and methods for testing concrete.

The most important properties of concrete as a construction material are strength, durability and impermeability. These properties will depend on the quality of the hardened cement paste and on the quality of the aggregate.

The quality of the cement paste is determined by the proportions of cement and water. A minimum water-cement (w/c) ratio is required to provide a workable consistency of the concrete mixture in the plastic state, however the lower the water-cement ratio of the concrete mixture the higher the quality of the paste. Figure 2-1 [3] illustrates the effect of w/c ratio on the compressive strength attained by a concrete mixture. CSA Standard CAN3-A23.1 - 14.3.1 specifies the maximum allowable w/c ratio for a variety of exposure conditions for concrete. The effect of w/c ratio on the durability of concrete will be discussed in Section 2.3.1, which presents the interrelationship of w/c ratio, permeability and durability.

Aggregate occupies approximately three-quarters of the volume of concrete. The primary function of the mineral aggregate in concrete is to add volume to the concrete at less cost than cement. The quality of the aggregate will influence the volume stability, strength and durability of the concrete.

Most concretes produced today contain one or more admixtures. Admixtures are organic or inorganic chemical compounds or finely divided minerals which are used to enhance the characteristics of concrete in both the fresh and hardened states. Specifications for properties and use of admixtures are discussed in CSA Special Publication CAN3-A266.1-M [7]. Two admixtures of interest in this research are fly ash and air-entraining agents.

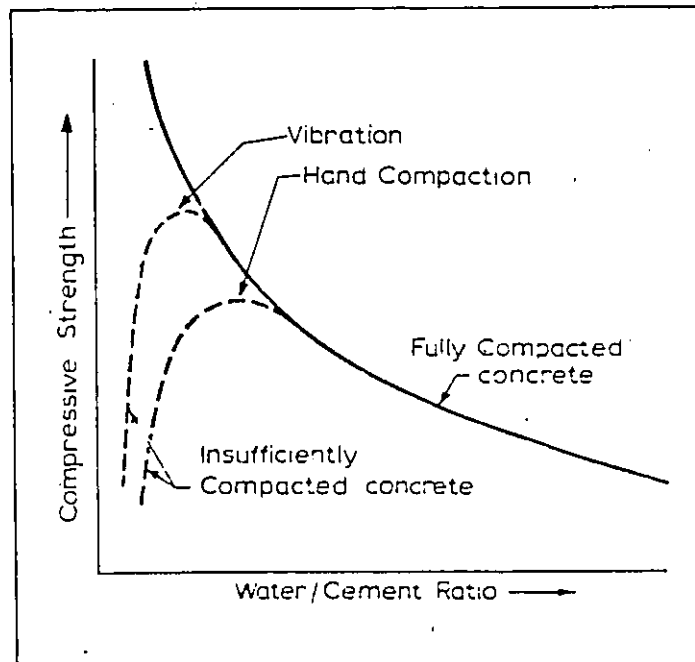


Figure 2-1 : The relation between strength and water/cement ratio of concrete [3]

Fly ash is an artificial pozzolan produced from the burning of coal. A pozzolan is a siliceous and aluminous material that in itself possesses little or no cementitious properties, but will, in finely divided form and in the presence of moisture at ordinary temperatures, react chemically with calcium hydroxide to form stable compounds possessing cementitious properties. [5] The calcium hydroxide fraction of the pozzolanic reaction is derived from the hydration products of portland cement.

Fly ash can be used as a partial replacement of cement, usually in the amount of 15 to 35 per cent by weight. The advantages of using fly ash as a replacement for cement in concrete include reductions in the unit cost, a decrease in heat of hydration and water requirement, and a reduction in the upward migration of water known as bleeding. It can also increase the workability of plastic concrete and improve water tightness and resistance to aggressive environments of the hardened concrete.

The idea of entraining a network of air bubbles in concrete to enhance its freeze-thaw resistance originated in the 1940's and has since become a proven method for protection of concrete against freeze-thaw damage. The presence of the air-entraining admixture results in the distribution of numerous, minute, predominantly spherical air voids in the cement paste to form an air-void system.

The size and distribution of the air voids can be influenced by a number of factors, one of which is the addition of fly ash to the concrete mixture.

### 2.1.2 Paste Structure

The basic mechanism of strength gain in concrete is the hydration of the mineralogical components of cement to form a cementing matrix, bonding the solid constituents of the concrete mixture. The major hydration products which compose the cementing matrix are C-S-H [Calcium-Silica-Hydrate] gel and crystals of  $\text{Ca(OH)}_2$ .

The physical microstructure of these hydration products plays an important role in the mechanical properties of the hardened concrete.

The C-S-H gel comprises approximately one-half to two-thirds of the volume of the hydrated paste. The calcium hydroxide occupies about 20% to 25% of the paste volume. The remaining total volume of paste is composed of other minor hydrates and voids.

A simplified model for the paste structure of concrete is presented by Powers [3] in Figure 2-2. The solid dots represent the gel structure of the paste. The interstitial spaces are gel pores and the spaces marked "C" are capillary cavities. The model shown is not to scale; nor does it represent the true size distribution of pores and cavities.

The gel pores and capillary cavities are the result of the amorphous structure of the solid C-S-H gel. Extensive studies on the structure of C-S-H gel have resulted in a number of models describing or representing the nature of the paste structure. The three most celebrated models of C-S-H are the Powers-Brunauer model, the Feldman-Sereda model, and the Munich model. The validity of any one model has yet to be proven due to the non-existence of equipment that would be required to visually confirm the physical microstructure of the C-S-H gel. Mindess and Young [6] attempt to combine the models into a concept in which they portray the C-S-H gel as being composed of layers of "bread" and "filling". The "bread" is composed of calcium silicate sheets and the "filling" of calcium ions and water. Figure 2-3 [6] illustrates the irregular arrangement of these layers, producing interconnecting interstitial spaces of varying size; hence the creation of micropores or gel pores and capillary pores.

As the second major component of the paste structure, calcium hydroxide has a crystalline structure with a distinct hexagonal prism morphology. Calcium hydroxide crystals will only grow where free space is available, such as capillary pore space. Prior to the utilization of fly ash in concrete, the presence of water soluble calcium hydroxide crystals contributed little to the structural

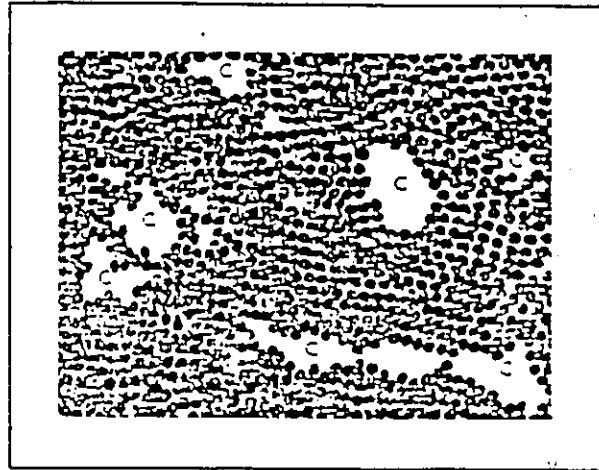


Figure 2-2 : Simplified model of paste structure (3)

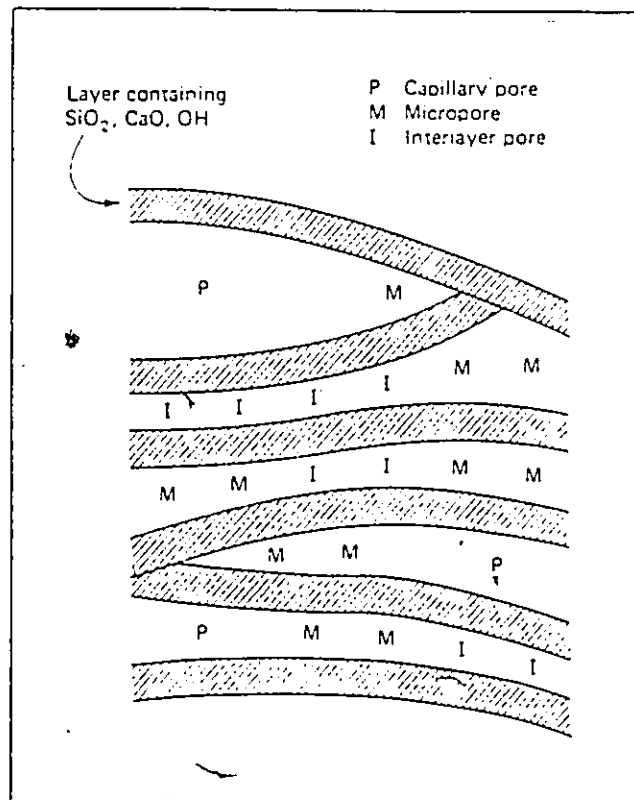


Figure 2-3 : Schematic model of C-S-H in cement paste (6)



properties of the cement paste. In aggressive environments the calcium hydroxide exists as an easy target for the deleterious mechanism of leaching. The introduction of fly ash into concrete allows utilization of the calcium hydroxide, produced by hydration, as an ingredient for further development of the C-S-H gel, producing a less porous concrete with increased durability.

## 2.2 Pore Structure

### 2.2.1 Porosity

Porosity is that portion of the cement paste not occupied by the solid constituents. In essence it is the third major component of the microstructure of cement paste, but its importance to this research warrants a detailed discussion.

Porosity is an extremely difficult characteristic to measure, due to the minute size of the pores. The two most widely used methods for the measurement of porosity are mercury intrusion porosimetry and physical adsorption of gases. Research efforts in this area have resulted in the classification of pores into two general categories, gel

pores and capillary pores. This classification of pores is based on the nature of the water held in the pore and on the size of the pore.

The gel pores within the C-S-H gel structure occupy about 28 per cent of the total volume of gel [3]. The size classification for a gel pore is in the order of 0.5 nm - 10 nm in diameter. As a result, the water contained within the pores is said to be adsorbed and exerts a disjoining pressure on the gel particles. Removal of water from the gel pores requires an ambient relative humidity of less than 50 per cent.[3]

Capillary pores represent the volume of the cement paste not filled by hydration products. A more accurate definition of a capillary pore is one in which capillarity occurs and the water contained within the pore exists in bulk form. Capillary pores may not always contain water.

The size of capillary pores is in the range of 10 nm to 10  $\mu$ m. The extent of capillary pores throughout the cement paste depends on the original w/c ratio and the degree of hydration. Capillary pores exist as an interconnected system and are seen as the main contributor to the permeability of concrete.

Table 2-1, from Mindess and Young [6], summarizes the foregoing description of the classification of pore sizes in hydrated cement pastes.

#### 2.2.2 Air Voids in Concrete

Gel pores and Capillary pores, which develop as a result of the complex process of hydration, represent only a portion of the air voids within the cement paste structure. The remaining voids may be classified as either entrapped or as entrained-air voids.

Entrapped air originates from the accidental inclusion of air bubbles or water filled voids during the mixing and placing of the concrete. It is the presence of these voids which greatly reduces the strength of the concrete. Neville [3] states that for a 5 per cent entrapped air content the strength of the concrete may be lowered by as much as 30 per cent.

The classification of an air void as either entrapped or entrained is based on the shape and size of the void. Entrapped-air voids usually appear as irregularly shaped air voids greater than 1 mm in size and randomly distributed throughout the cement paste. Entrained-air voids are characteristically spherical in shape and are much smaller in size ranging from 0.01 mm to 1.25 mm. Entrained air is

Table 2-1

Classification of Pore Sizes in Hydrated Cement Pastes

Designation	Diameter	Description	Role of Water	Paste Properties Affected
Capillary pores	10-0.05 $\mu\text{m}$	Large capillaries	Behaves as bulk water	Strength; permeability
	50-10 nm	Medium capillaries	Moderate surface tension forces generated	Strength; permeability; shrinkage at high humidities
Gel pores	10-2.5 nm	Small (gel) capillaries	Strong surface tension generated	Shrinkage to 50% RH
	2.5-0.5 nm	Micropores	Strongly adsorbed water; no menisci form	Shrinkage; creep
	< -0.5 nm	Micropores "interlayers"	Structural water involved in bonding	Shrinkage; creep

Mindess and Young (6)

intentionally distributed throughout the cement paste, using air-entraining admixtures to produce millions of minute air bubbles uniformly dispersed throughout the paste. The size, size distribution, and spacing of the entrained air bubbles form the parameters of what is referred to as the entrained-air-void system within the concrete.

The process of entraining air in concrete, begins with the introduction of an air-entraining admixture into the mixing water to promote the formation of a stable foam. The most common forms of air-entraining agents are:

- 1) animal and vegetable fats and oils and their fatty acids.
- 2) natural wood resins, which react with lime in the cement to form a soluble resinate. The resin may be pre-neutralized with NaOH so that a water-soluble soap of a resin acid is obtained.
- 3) wetting agents such as alkali salts of sulphated and suphonated organic compounds.

The air-entraining product contains surface-active substances, or surfactants, which concentrate at the air-water interface lowering the surface tension of the water and stabilizing the bubbles once they are formed. Mindess and Young[6] describe surface-active agents as molecules which are made up of hydrophilic groups and

hydrophobic groups. The molecules tend to align at the air-water interface with the hydrophilic groups in the water phase and the hydrophobic groups in the air phase. It is this stable configuration which allows the air bubbles to remain in the concrete during mixing and setting of the cement paste.

The intentional inclusion of entrained air in concrete contradicts the well known fact that the presence of air voids will reduce the strength of the concrete. However the serviceability of a concrete structure is only partially determined by the strength of the concrete. In temperate climates where concrete structures are subjected to severe fluctuations in temperature and humidity, consideration must also be extended to the durability of the concrete.

## 2.3 Durability of Concrete

### 2.3.1 General

Durability is a measure of how well a structure can withstand the conditions for which it is designed. Strength and durability have long been the key parameters in the design of concrete structures. However in recent years the improvements experienced in the cement industry have

resulted in the production of high quality cements, making it much easier to attain the required design strengths. In North America, the strength of cement for a given w/c ratio, doubled during the period from 1916 to 1936, and since then has increased an additional 60 percent, due to finer grinding techniques and improved quality control in the cement industry.[8] As a result, the cement contents needed for design strength have decreased and w/c ratios have risen. These increased w/c ratios, unfortunately result in a much higher percentage of capillary pores in the hydrated cement paste with resultant detrimental effects on the durability of the concrete.

In a normal service life, concrete must be designed to withstand environmental attack of both a chemical and a physical nature.[9] Chemical attack can take the form of leaching, sulphate attack, alkali-aggregate reaction, acid attack, and corrosion of the reinforcing steel. Physical attack is more commonly seen as freezing and thawing, wetting and drying, temperature changes, and abrasion. The degree to which concrete will be susceptible to any one or a combination of these processes, will depend on the quality of the aggregate, paste, and steel, which together make up the concrete structure.

Permeability of the cement paste is viewed as one of the key characteristics in the susceptibility of concrete to most forms of aggressive attack, both chemical and physical. Permeability is a term used to define the rate at which a solution penetrates the pore system within the concrete.

The permeability is largely determined by the original w/c ratio of the concrete mixture and the degree of hydration. Figure 2-4 [6] illustrates the effect of w/c ratio on the volume of capillary porosity. An increase in the water-cement ratio creates a marked increase in the volume of capillary pores. Water flows easily through larger pores (capillary pores); therefore pastes with high capillary porosities will usually have high permeabilities. Other factors which determine the permeability of a concrete are the size, distribution and continuity of the pores.

### 2.3.2 Theory of Frost Action

The protective capability of entrained-air in concrete can best be appreciated by understanding the destructive mechanisms through which damage occurs in concrete on repeated cycles of freezing and thawing.



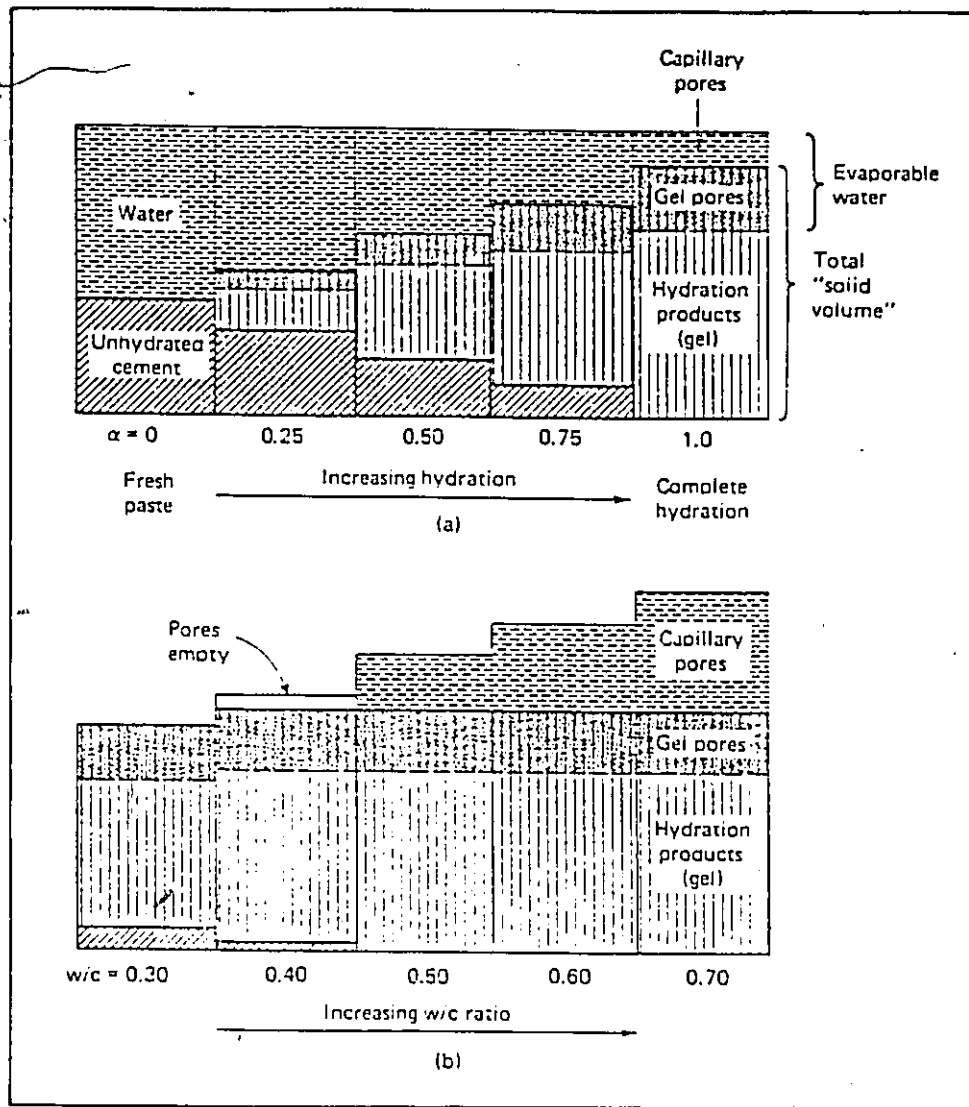


Figure 2-4 : Volume relationships among constituents of hydrated pastes:  
(a) constant w/c ratio = 0.50  
(b) changing w/c ratio with complete hydration

(6)

Due to the porous nature of concrete, it may, in the presence of water, approach saturation. However complete saturation (100 %) is not required for the destructive effects of freeze-thaw to occur. Instead research indicates that the critical degree of saturation for non-air-entrained concrete is approximately 0.80 of the total freezable water which can exist in the concrete pore structure.[6] Concrete saturated beyond the critical degree of saturation is susceptible to the damaging effects of frost attack when exposed to fluctuating freezing and warming temperatures.

Due to the spectrum of pore sizes, from 0.5 nm to 10,000 nm, the water contained within the pore system exists either as adsorbed water in the gel pores or as a combination of adsorbed and absorbed water in capillary pores. Adsorbed water exists as a thin film of water held at the surface of the gel pores by physical (Van-der-Waals forces) and chemi-sorption forces. Absorbed water will occupy the larger capillary pores as bulk water, held by the forces of capillarity. The ambient relative humidity and the size of the pore will determine the type and volume of water held in the porous medium.

Powers [11-14] worked extensively to develop theories for the action of frost in hardened concrete. He proposed two theories based respectively on osmotic and hydraulic pressures.

The hydraulic pressure theory is based on the fact that, as water freezes, it expands by 9% of the original volume. As water freezes in the concrete, residual water is forced to migrate through the capillaries to an area of free space within the paste. If the migration path is too great the capillary will dilate creating destructive tensile forces in the paste.

According to his osmotic theory, ice forming in the larger pores will result in an increase in alkali content in the unfrozen portion of the solution in the remaining pore system. The higher concentration of alkalis in the solution creates an osmotic potential which impels water molecules in the nearby unfrozen pores to begin diffusing into the areas of ice growth. This action further promotes ice growth in the paste, creating dilative pressures which may exceed the tensile strength of the paste and result in failure.

Since Powers' early work in this area, other theories have been presented, the most recent of which is the theory presented by Litvan [15]. Litvan believes that supercooled adsorbed water in the cement paste will coexist with bulk ice in the larger pores, creating a vapor pressure gradient in the cement paste. As a result, the relative humidity is lowered and part of the adsorbed water is released, creating hydraulic pressure within the cement paste

Further work on the mechanism of frost damage in argillaceous rocks, by Dunn and Hudec [66], attributed the damage due to freeze-thaw action as being synonymous to the action of wetting and drying. The destructive expansive forces in the cement paste are believed to be the result of both sorptive interactions with water vapor or liquid water and ice expansion. The result is the deterioration of frost sensitive materials such as non-air-entrained concrete.

While there is controversy as to which theories best explain the mechanisms of freeze-thaw action in concrete, there is general acceptance of the beneficial role of purposefully entrained-air in enhancing the frost durability of concrete. However, the concept that hydraulic pressures do occur in the cement paste when exposed to cooling temperatures and that the path length for migration of mobile water will influence the magnitude of the destructive forces is strongly supported in the literature.

### 2.3.3 Role of Entrained Air in Freeze-Thaw Durability

The presence of air entrainment in concrete was accidentally discovered in the late 1930's. Organic agents, added to aid in the grinding of cement, or in some

instances, the leakage of organic matter from bearings in older grinding equipment, unknowingly served as the first air-entraining agents.

The benefit of air-entrained concrete was recognized as early as 1939. Literature published during that period [16], attributed the increased durability to the reduced amount of bleeding observed with an increase in air content. From those early observations, researchers were soon able to establish the conclusive contribution of entrained air in concrete. The present day understanding of the role of entrained air in concrete, as described by Klieger [17], stems from those early observations by researchers in the field of concrete.

Entrained air exists as a system of well distributed minute spheroids of air introduced into the fresh concrete mixture and remaining as part of the structure of the cement paste after the concrete has set. When concrete is exposed to freezing temperatures, a portion of the bulk water contained within the capillary pores will freeze creating a 9 percent increase in volume from the liquid to the solid phase. The remaining water will tend to migrate through the interconnected capillary pores to larger, unsaturated pores in the system. If the increased volume of ice and the migration of water is not accommodated by a well distributed entrained air-void system, the cement paste will experience

potentially destructive tensile forces. The entrained air-voids are said to act as pressure relief valves through which free water can enter and leave during the freezing and thawing cycle. The entrained-air voids must be well distributed throughout the paste to reduce the migration path of moving water and to accommodate the volume change during ice formation. Figure 2-5 illustrates the destructive mechanism of frost action in non-air-entrained paste and air-entrained paste according to the hydraulic pressure hypothesis .[6]

Air entrainment provides protection for concrete which becomes critically saturated. Entrained air bubbles do not contribute to the permeability of concrete and do not readily fill with water. However, if the entrained air voids become fully saturated during a freezing cycle, the concrete will become highly susceptible to frost damage.

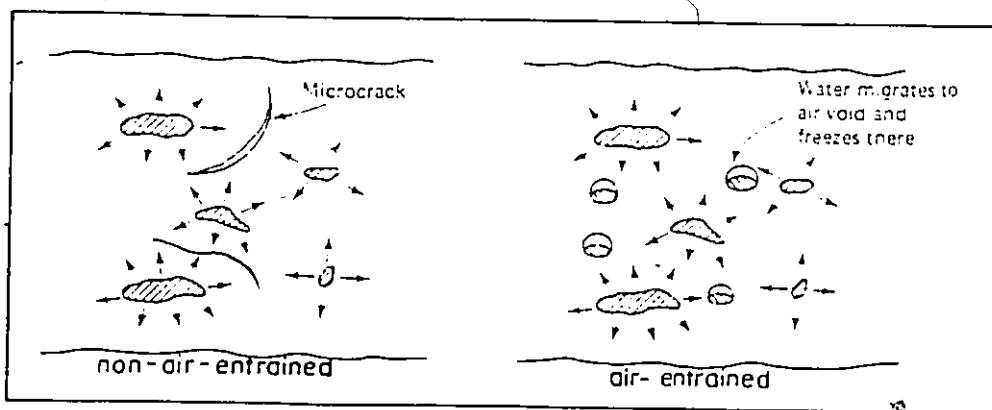


Figure 2-5 : Creation of hydraulic pressure in frozen cement (6)

## CHAPTER 3

### FLY ASH IN CONCRETE

#### 3.1 Introduction

Fly ash is a by-product of the combustion of coal in electric utility power plants. In 1986 Canadian utilities operated 24 coal-fired thermal generating stations, which produced an estimated 3.0 million tonnes of fly ash.[18]

Due to environmental constraints, fly ash emissions from coal-fired generating stations are prohibited. As a result operators are presented with the problem of collection and disposal of the voluminous amounts of fly ash produced each year. Present disposal methods include landfill, lagoon, and mine backfill systems.

As an alternative to the disposal of fly ash as a waste by-product, the construction industry has demonstrated the useful application of fly ash in structural fill, cement and concrete production, and road base stabilization. Further efforts, concentrating on the utilization of fly ash will reduce the costs of developing new ash disposal sites, provide a potential revenue source to utilities and reduce the general level of environmental damage that ultimately results from industrial activity.

The application of fly ash in this research is as a pozzolan, partially replacing the cement in the concrete mixtures. Since the early 1930's, interest in the use of fly ash in concrete has been accompanied by extensive testing and research. Widespread acceptance of fly ash in the concrete industry will require a better understanding of the advantages and limitations associated with the utilization of fly ash as a pozzolan in concrete.

Fly ash is a heterogeneous material whose composition and properties depend on the coal source and the method of operation of the thermal plant. Physical and chemical analysis of fly ash intended for use in concrete is a necessary step towards the standardization of fly ash as a pozzolan. The physical and chemical properties of fly ash will influence its pozzolanic properties. Variations in the physical properties of the fly ash are due to the composition of the coal, the degree of pulverization of the coal, the rate and efficiency of combustion and the fly ash collection system. The chemical composition of fly ash depends on the various types of mineral matter in the coal.

### 3.2 Pozzolans

Lea [19] defines a pozzolan as a "material which will combine with lime at ordinary temperature, in the presence of water, to form stable insoluble compounds possessing



cementing properties". There are many materials that possess this characteristic, each differing considerably from the others in origin, composition and mineralogical constitution. A list of recognized pozzolanic materials is given in Table 3-1.

The ability of a pozzolan to react chemically with calcium hydroxide is beneficial to concrete. In addition, with careful proportioning of concrete mixtures, the addition of fly ash as a partial replacement for portland cement will allow a reduction in cement content. Replacing a portion of the cement by the less expensive fly ash will result in an economical concrete mixture.

The ability of a pozzolan to react with calcium hydroxide in the presence of water is dependent on the pozzolanic activity of the material. To determine the pozzolanic activity, it is necessary to consider the reactive state of the chemical components composing the pozzolan. Silica and alumina are the two main components of a pozzolan. Both are highly reactive to calcium hydroxide when their structural bonds are weak and unstable. If, however, silica and alumina are chemically bound in a semi-stable state, the pozzolanic reaction will occur at a slower rate, or not at all.

A number of investigations have been carried out to compare hydration products of normal portland cement concrete and cement-pozzolan concrete. Researchers [20,21] suggest that, with the exception of a reduction in the

Table 3-1 Pozzolan Materials

<u>Pozzolan</u>	<u>Approximate Composition</u>	<u>Treatment</u>
Pumicite	Acidic volcanic glass with 5% quartz and feldspar	Ground & Calcined
Diatomite	60% opaline silica, 30% quartz & feldspar, 5% montmorillonite, 5% illite and miscellaneous	Ground & Calcined
Kaolinite	Nearly pure kaolinite	Ground & Calcined
Wyoming bentonite	75% sodium montmorillonite, 25% feldspars, quartz and miscellaneous	Ground & Calcined
Illite	75% illite clay, 20% quartz & feldspars, 5% miscellaneous	Ground & Calcined
Gibbsite	Reagent grade powder $\text{Al}_2\text{O}_3 \cdot 3\text{H}_2\text{O}$	-
Quartz	Practically pure quartz	Ground
Flyash	65% glass, 25% magnetite, 10% quartz, carbon	Used as Received

\* Reference [65]

amount of  $\text{Ca(OH)}_2$  present, the cementitious compounds formed by pozzolanic action are of the same type as formed by the hydration of portland cement.

### 3.3 Fly Ash as a Pozzolan

#### 3.3.1 Physical Properties of Fly Ash

Fly ash is transported from the combustion chamber in the coal burning plant through the boiler via the flue gases and is collected either in electrostatic precipitators or in fabric bag type filters. Figure 3-1 is a schematic of a typical coal burning process. The filter bag or mechanical collection system produces a more homogeneous supply of fly ash than the electrostatic precipitator collection system, because a sample with representative particle size is collected in all the filter elements. In the electrostatic precipitator collection system, the size of the ash particles become finer as the gases move from first to second to third electrostatic fields. Figure 3-2 [22] illustrates the variation in particle size distribution of two fly ashes collected mechanically and electrostatically. The fly ash collected by the mechanical collection system is coarser.

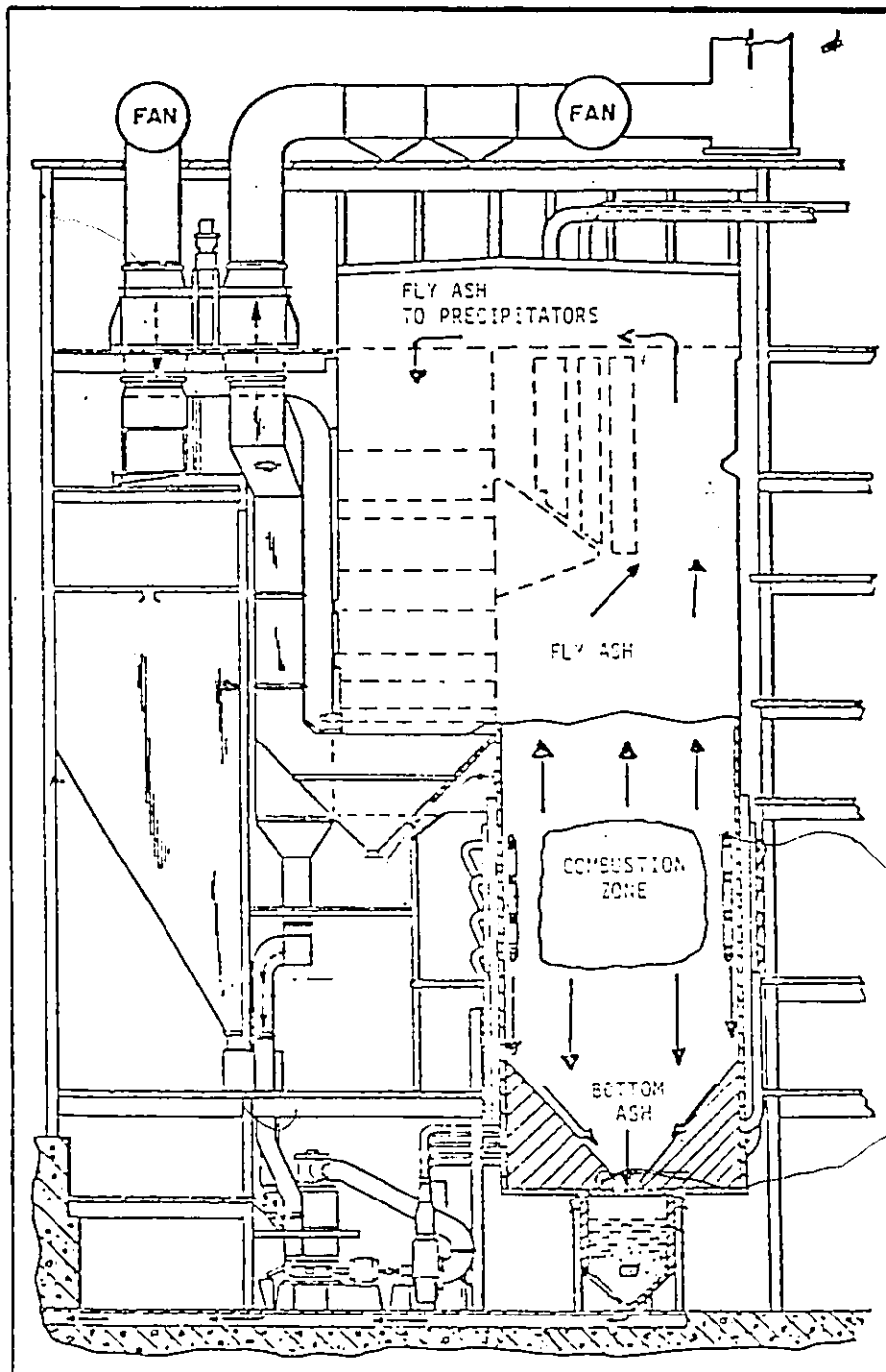


Figure 3-1 : Typical schematic of coal burning process (66)

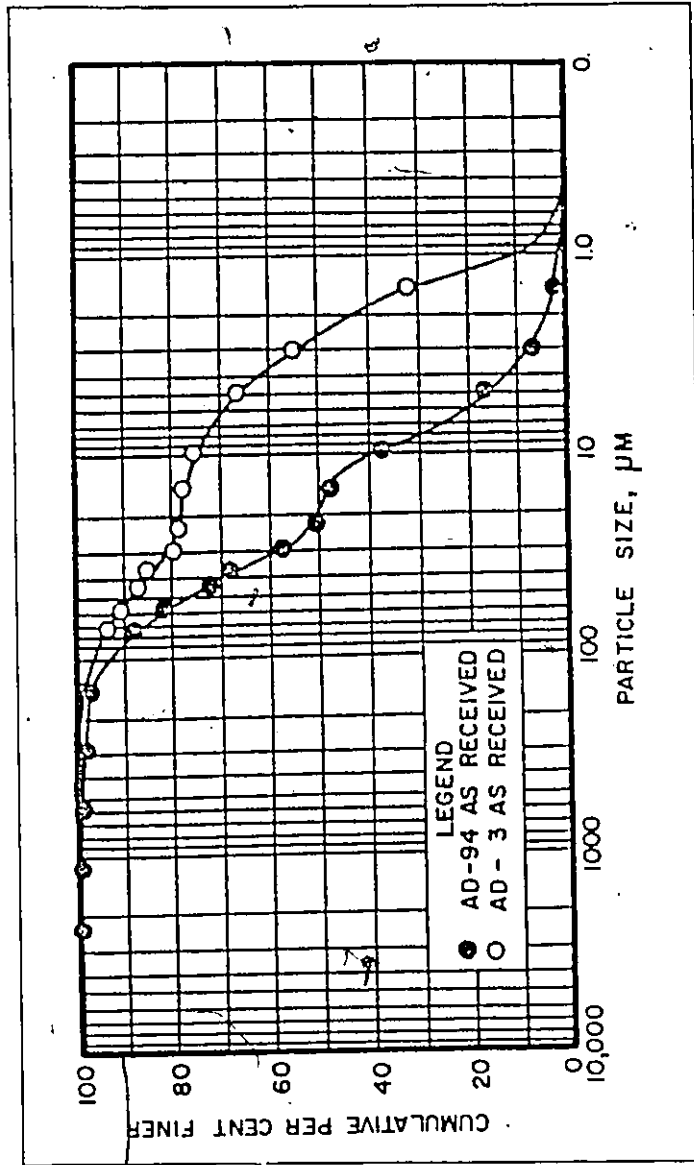


Figure 3-2 : Particle size distribution of two fly ashes  
AD-94, collected mechanically, and AD-3,  
collected electrostatically (22)

Fly ash particles are typically spherical in shape, ranging in diameter from 1 to 150  $\mu\text{m}$ . The pozzolanic activity of fly ash increases as the fineness of grain size increases; therefore the coarser material in the first field of an electrostatic precipitator, which constitutes about two-thirds of the total output, is less likely to meet the specifications for a pozzolanic material than the material in the other fields.

The density of fly ash can be indicated by the bulk density, average apparent density, or by specific gravity. Average values for existing fly ash supplies range from 0.54 to 0.86  $\text{g/cm}^3$  for bulk density, 1.90 to 2.40  $\text{g/cm}^3$  for apparent density and 2.65 to 2.80  $\text{g/cm}^3$  for specific gravity.[22]

Fly ash consists mostly of solid or hollow spherical glassy particles, reddish-brown particles high in iron content and irregularly shaped, porous, carbon particles. Watt and Thorne [23] distinguished eight classifications of particles by microscopic examination.

Researchers [23,19] have concluded that the pozzolanic activity exhibited by a fly ash correlates well with the glass content and the fineness of the fly ash.

### 3.3.2 Chemical Properties of Fly Ash

Fly ash is classed by the American Society of Testing Materials (ASTM) as either a Class F or Class C pozzolan based on the chemical composition. ASTM C618-80 "Fly Ash and Raw or Calcined Natural Pozzolan for use as a Mineral Admixture in Portland Cement Concrete" [5] defines the chemical requirements pertaining to each class. Table 3-2 illustrates the percentage of components for each classification. The requirement for CaO content is not specified in the standards, however Class C fly ash has a higher percentage of CaO and a lower percentage of carbon.

Fly ash consists principally of the oxides of silicon and iron with varying amounts of constituents containing aluminum and some unburned coal or carbon. Other trace elements such as potassium, phosphorus, cobalt, molybdenum, boron or manganese may be present [24]. The particular composition of a specific fly ash sample must be analyzed by the fly ash supplier to determine the classification of a sample. Figure 3-3 contains a typical laboratory report for a fly ash sampled at Lingan, Nova Scotia. The test results shown in Figure 3-3 illustrate the regiment of physical and chemical testing programs carried out to monitor fly ash produced for marketing.

Class C fly ash will result, usually, from a lignite or subbituminous coal source and, in addition to having pozzolanic properties, will also have some cementitious

Table 3-2  
Chemical Requirements of Fly Ash

Standard	$\text{SiO}_2$	$+\text{Al}_2\text{O}_3$	$+\text{Fe}_2\text{O}_3$	$\text{CaO}$	$\text{MgO}$	$\text{Na}_2\text{O}$	$\text{SO}_3$	M.C.%	LOI%
<u>ASTM C618</u>									
	<u>Maximum % by Weight</u>								
Class F	(min) 70	-	5.0	1.50	5.0	3.0	12.0		
Class C	(min) 50	-	5.0	1.50	5.0	3.0	6.0		
<u>CSA CAN3 - A23.5 - M82</u>									
Class F	-	-	-	-	5.0	3.0	12.0		
Class C	-	-	-	-	5.0	3.0	6.0		

(5)



# Nova Scotia Research Foundation Corporation

100 Fenwick Street, Box 790, Dartmouth, Nova Scotia, Canada, B2Y 3Z7

Tel: (902) 424-8670



## CHEMISTRY DIVISION

### ANALYTICAL LABORATORIES REPORT

**CLIENT:** Nova Scotia Power Corporation  
Box 910  
Halifax, Nova Scotia  
B3J 2W5

**DATE SUBMITTED:** Sept. 13, 1983

Attn: T. Kumanan

**MATERIAL:** Fly Ash

**DATE REPORTED:** Sept. 28, 1983

LAB NO.	DESCRIPTION	% Ignition Loss		% Ignition Loss		% SiO <sub>2</sub>		% SO <sub>3</sub>	
		@500°C		@1000°C					
K174/1	Lingan Fly Ash From North Silo Sampled 83-09-08	1.07		2.94		43.14		0.85	
		% Total Carbon	% CaO	% Fe <sub>2</sub> O <sub>3</sub>	% MgO	% Al <sub>2</sub> O <sub>3</sub>	% Na <sub>2</sub> O	% K <sub>2</sub> O	
K174/1		2.50	0.46	22.22	0.90	23.45	0.51	2.60	
		Cu (ppm)	Mn (ppm)	Ni (ppm)	Cr (ppm)	Pb (ppm)	Cd (ppm)	Zn (ppm)	V (ppm)
K174/1		125	530	22	27	77	1.0	78	71
								As (ppm)	Hg (ppb)
								227	55

**Figure 3-3** : Laboratory report for a fly ash sample, Lingan, Nova Scotia

properties due to the calcium oxide content. A typical chemical analysis of a Class C fly ash, originating from a subbituminous coal ash is shown in Table 3-3.

Table 3-3

Typical Chemical Properties of a Class C Fly Ash

<u>Chemical Property</u>	<u>Percent by Weight</u>
SiO <sub>2</sub>	34.29
Al <sub>2</sub> O <sub>3</sub>	16.90
Fe <sub>2</sub> O <sub>3</sub>	5.80
SO <sub>3</sub>	3.63
MgO	4.50
CaO	30.29
Na <sub>2</sub> O	1.45

---

Reference (70)

Silicon dioxide, aluminum oxide and iron oxide are grouped together for classification purposes because it is believed that a direct relationship exists between the pozzolanic activity of a fly ash and the percentages of these three elements. The pozzolanic activity of the fly ash will depend on the individual percentage of these elements and whether the elements are present in the fine or coarse fractions of the ash.

The specifications limit the amount of magnesium oxide in fly ash to prevent expansion caused by the formation of magnesium hydroxide. Although the hydration of  $MgO$  is a relatively slow process, the resulting hydration product occupies a greater volume than the  $MgO$ , creating deleterious effects. In contrast, the content of sulfur trioxide ( $SO_3$ ) in fly ash does not appear to have an adverse effect on concrete durability. At one time it was believed to influence the drying shrinkage of cement-fly ash mortars, but through cooperative tests performed by 15 laboratories, Lane and Best [24] report that the combination of high  $SO_3$  content in both the cement and fly ash produces expansion equal to those in the control mixture. The  $SO_3$  in fly ash exists mainly in the form of calcium sulphate [22].

The specified maximum allowable percentage of available alkalis in a fly ash is 1.5 percent. This limit is most critical in concrete with aggregate known to be alkali reactive and when the use of low-alkali cement is stipulated. According to Lane and Best [24] the available alkali content in most ashes is less than 1.5 percent and has been found to have little effect on concrete properties. Tests have shown, however, that alkalis in larger amounts in fly ash continue to dissolve in water after 28 days and may affect expansion resulting from alkali-silica reaction. For these reasons, the 1.5 percent, expressed as  $Na_2O$  content is stated as an optional specification.

Loss on ignition (LOI) is a term often used to indicate carbon content in a fly ash sample. LOI is among the most variable of the fly ash properties and is one of the criteria used to classify fly ash as either Class C or Class F. A fly ash with a high LOI usually requires a higher dosage of air-entraining admixture. Some fly ashes with more than 6 percent carbon have been observed to produce a black, oily film on the surface of concrete, producing a poor aesthetic effect and occasionally preventing bonding of successive concrete lifts. [24].

The content of CaO in a fly ash is reflected in the ability of a fly ash to exhibit cementitious properties of its own. Fly ashes of this type are a Class C fly ash from a lignite or subbituminous coal source. Berry [22] documents a report by Manz [26] in which he has termed ashes from subbituminous and lignite sources as "basic ashes". The distinguishing characteristic for a basic ash is that the sum of percent CaO and percent MgO is greater than the percent  $\text{Fe}_2\text{O}_3$ . If the CaO content is excessively high, the CaO will exist as free CaO, which is referred to as the "dead burnt" lime. Previous experience in the concrete industry has shown that free CaO in cement clinker has led to unsoundness in hydrated cement.

Comparison of the chemical composition of a normal portland cement with a typical fly ash would indicate a close similarity in the types of compounds present, but great differences in the proportions of each compound. A

graphical illustration of the compositions of fly ash, natural pozzolans and portland cement, with respect to the system,  $\text{CaO-SiO}_2\text{-Al}_2\text{O}_3$ , is shown in Figure

3-4 [22]. It is evident that fly ash is very similar in composition to natural pozzolans, while being considerably different in CaO content from portland cement. From a strictly chemical viewpoint, its behavior as a pozzolanic material is to be expected.

#### 3.4 Effect of Fly Ash on Properties of Concrete

In 1937, Davis et al[26], conducted an extensive testing program including fly ashes from 15 different sources and portland cements of seven compositions. They investigated properties such as strength, elasticity, volume change, plastic flow, heat of hydration, and durability as indicated by resistance to freezing and thawing and by resistance to the action of sodium sulfate. They observed that fly ash concrete:

- (1) needed about the same water requirement to produce a given consistency;

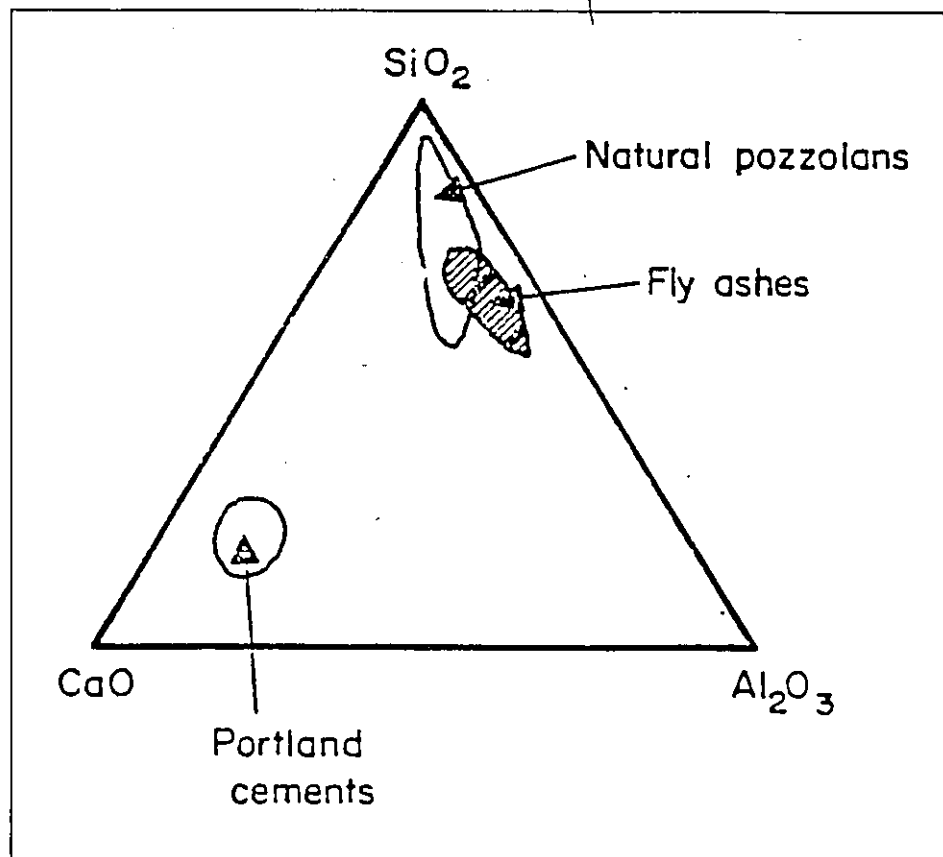


Figure 3-4 : Comparison of compositions of fly ashes with natural pozzolans and portland cements in the system  $\text{CaO-SiO}_2\text{-Al}_2\text{O}_3$  . (22)

- (2) produced somewhat lower compressive strengths at the early ages but substantially higher compressive strengths at the later ages under normal conditions of moist curing (21° C);
- (3) had compressive strengths which were substantially higher even at the relatively early age of 28 days when the temperature of curing is 38° C;
- (4) had shrinkage characteristics for sections of normal thickness and normal drying conditions which was likely to be no more and may be less than plain concrete;
- (5) had lower heat of hydration;
- (6) had about the same or somewhat less resistance to freezing and thawing; and
- (7) had greater resistance to sulfate action.

Davis et al[26] concluded that the incorporation of 30% fly ash in a concrete mix would not adversely affect the quality of the concrete. They also acknowledged that the fly ashes derived from various coals possess a variation in chemical composition, particularly in carbon content. As well they concluded that, a fly ash of moderately low carbon content and moderately high fineness would produce the most favorable concrete. They determined that, fly ashes originating from different sources display varying properties and that consistent quality control could only be attained through the establishment of a standard. This standard should specify requirements concerning the chemical composition, fineness, and activity of the fly ash in the

presence of lime. Davis continued to investigate the use of fly ash in concrete, producing reports both in 1941[27] and 1950[28]. His subsequent investigations led to the same general conclusions.

The first large scale application of fly ash in concrete was in the construction of the Hungry Horse Dam in 1950, using a fly ash produced in Illinois. Blanks [29] reported that the concrete containing fly ash showed improvements in workability and durability and reductions in permeability, heat of hydration, and alkali-aggregate reactivity. The specified air content was 3% and no problems were reported in obtaining this level. However in 1954, Minnick [30] produced a report which summarized the results of a number of investigations conducted at that time on the use of fly ash as a pozzolanic material and as an admixture in portland cement concrete. The findings of the study show a definite correlation between loss on ignition (LOI) of fly ash and the amount of air-entraining agent required to produce a given air content. Mather[31] confirmed Minnick's conclusion, that increase in LOI increases the air-entraining admixture requirement.

In 1962, Clendenning and Durie [32] investigated the variability of fly ash produced from a coal-fired thermal generating station operating under a variable production load. The high LOI levels and high fineness found in fly ash are attributed to the poorer combustion conditions accompanying operation of generating stations at low load.



Variability in quality of ash appeared as a major deterrent to its use at that time, due to the resulting inconsistency in the properties of the concrete containing the fly ash. They again confirmed the adverse affect of increased LOI on air entraining agent requirements and disproved the earlier suggestions, that the fineness of the ash was contributing to the reduction in air-entrainment.

In addition to studying air-entraining agent requirements, Clendenning and Durie also conducted freeze-thaw tests to determine the effect of fly ash on the frost durability of the concrete. Their tests showed that the freeze-thaw weight loss of a mixture utilizing 12% carbon ash at 30% replacement was approximately 2% higher than that of the control mix. They attributed this small increase in deterioration to the possibility that the porous carbon particles may act as centers for water entrapment and subsequent ice formation; in addition, the carbon may alter the air-void structure in the vicinity of the carbon particles. This was the first time it was suggested that the addition of fly ash of high carbon content may adversely affect the air-void system of the concrete.

In the 1950's and 1960's, a number of U.S. Highway Departments conducted experimental research on fly ash concrete in highway pavements, comparing sections of fly ash pavement design with regular portland cement control sections exposed to the same environmental conditions.

Results of studies [33-37] showed comparable or better behavior for concrete pavements containing fly ash. The observation periods varied anywhere from 1 to 8 years. Of particular interest is a report by Legg [37], on an experimental fly ash concrete pavement in Michigan. The fly ash used in the concrete had an LOI value of 13-14% and, as a result, the fly ash concrete required large amounts of air-entraining agent to attain the required air content. After 8 years of exposure to a northern environment, the fly ash concrete showed no signs of deterioration. Similar results were found by Stirrup and Clendenning [38] in their outdoor exposure specimens.

The inhibiting effect which carbon has on the air-entraining capabilities of an air-entraining agent (AEA) is due to the high surface area of the carbon particles, which tend to adsorb AEAs. Mardulier [39] reported in 1948 that particle size of carbon-black was a significant factor affecting its selective adsorption of AEAs in concrete. By using a relatively coarse fly ash material it was possible to avoid the depressing effects on air content. Larson [40], in an extensive study, confirmed the following observations:

- (1) the AEA must satisfy the initial carbon adsorption demand of a particular combination of fly ash;
- (2) air entrainment should occur in a normal fashion after the demand is satisfied; and

(3) since adsorption (Van der Waals) bond forces are very large, the agent used to satisfy adsorption capability should be permanently associated with the carbon and should have no unique effect on the concrete.

Larson[40] also investigated Clendenning and Durie's suggestion, that the addition of fly ash of high carbon content may be affecting the air-void system within the hardened cement paste. Using the linear traverse method for analysis, he determined that no apparent difference existed in the size and distribution of air voids, even in the proximity of large carbon particles. Tests were conducted on concrete samples containing three types of fly ash at 30% replacement.

The more recent and significant collection of papers dealing with fly ash in concrete was presented at an international conference sponsored by CANMET (Canada Centre for Minerals and Energy Technology) in 1983. In an article authored by Gebler and Kleiger [41] the effect of fly ash on air-void stability in concrete was evaluated. They investigated ten fly ashes with a wide range of chemical and physical properties and geographical origins. Tests indicated that air contents of concretes containing Class C fly ash appear to be more stable than those in concretes containing Class F fly ash. The fly ashes were classified according to ASTM C618 [5], where fly ashes with CaO content greater than 10 percent were designated as a Class C fly

ash. Class C fly ashes are associated with LOI less than 6 percent. They found that even though the air volume is reduced, the spacing factor, specific surface, and number of voids are not affected.

Gebler and Kleiger also investigated the validity of the Foam Index test, introduced by Dodson [42] and modified by Meininger [43]. The Foam Index test is a new rapid test for estimating the air-entraining admixture requirement of mixtures containing cement and fly ash. The "Foam Index" of a cement-fly ash combination is the minimum amount of air entraining admixture necessary to produce a stable foam over the entire cross-sectional area of a wide mouth jar, following a vigorous shaking. Gebler and Kleiger concluded that the Foam Index test using the modified method appeared to be a good rapid test to predict relative air-entraining admixture dosage requirements for concrete.

Other papers in the symposium dealt with the many qualities of concrete which are affected by the addition of fly ash. The findings agree closely with the early findings of Davis and other researchers of the 40's, 50's and 60's. Of particular interest is an article by Stirrup, Hooton and Clendenning [44]. They suggested that the total air content required for adequate resistance to freezing and thawing action in fly ash concrete may be less than for non-fly ash concrete since fly ash, by providing additional workability, had reduced the entrapped air content to

approximately 0.5 percent in laboratory tests. As a result a lower air content in a fly ash mix could provide an equivalent volume of beneficial entrained air.

A second international conference on "Fly Ash; Silica Fume, Slag, and Natural Pozzolans in Concrete" sponsored by CANMET was held in Madrid, Spain in 1986. Included in the proceedings is an article by Gebler and Klieger [45] on the effect of fly ash on the durability of air-entrained concrete. Their findings led to the conclusion that air-entrained concretes with or without fly ash, moist cured at 23 C generally showed good resistance to freezing and thawing; however when cured at low temperatures (4.4 C), air-entrained concretes with Class F fly ash showed slightly less resistance to freezing and thawing than concrete made with Class C fly ash. The performance of concrete containing Class F fly ashes varied in the freezing and thawing tests. Class F fly ashes having high silica content showed the most significant weight losses compared with the other fly ash concretes.

The fact that concretes containing Class F fly ash show less resistance to freezing and thawing than concretes with Class C fly ash or concretes without fly ash is consistent with the fact the Class F fly ash concrete is slower to mature. Gebler and Klieger [45] did not associate the poor performance of the Class F fly ashes with an inadequate air-void system.

## CHAPTER 4

### MEASUREMENT OF THE AIR-VOID SYSTEM IN CONCRETE

#### 4.1 Introduction

For the purpose of durability the required air content of a concrete mixture will depend on the severity of exposure of the concrete structure. CSA CAN3 A23.1 - M77 [1] classifies the exposures into four categories, A through D. Class A exposure represents the most severe condition, which would include concrete structures subjected to frequent cycles of freezing and thawing with the application of de-icing chemicals or in a marine environment. Class D exposure represents concrete not exposed to freezing and thawing or the application of de-icing chemicals. Table 8 from this standard, included in Table 4-1, is an outline of the recommended range of total air content for various classes of exposure and maximum size of coarse aggregate. As an example, a bridge deck constructed with a 20 mm nominal maximum size coarse aggregate and subjected to freeze-thaw cycles and deicer salts, would require a total air content of 5 to 8 percent. Studies have shown that a 9 percent volume of air in the mortar fraction of the concrete will effectively protect the concrete under a Class A exposure condition. Current field control testing methods for fresh concrete provide a means for measuring the air

volume as a percentage of the whole concrete mixture. The lower value of the range specified in Table 4-1 represents an air-void system which would provide the critical 9 percent volume of air in the mortar fraction.

The air entraining admixture is introduced with the mixing water during the batching sequence. The quantity of admixture required to achieve a specified air content is determined by manufacturers recommendations or, more accurately, by trial mixtures.

Table 4-1 Range of Total Air Content for  
Various Classes of Exposure

<u>Class of Exposure</u>	<u>Range of Total Air Content for</u> <u>Nominal Size Coarse Aggregate</u>			
	<u>10 mm</u>	<u>14 mm</u>	<u>20 mm</u>	<u>40 mm</u>
A, exposed to deicing chemicals	7-10	6-9	5-8	4-7
B, not exposed to deicing chemicals	6-9	5-8	4-7	3-6
C	5-8	4-7	3-6	3-6
D	<5	<4	<3	<3

Reference [1]

#### 4.2 Parameters of the Air-Void System

The air-void system within a concrete specimen is usually characterized by the air content, specific surface, diameter of voids, spacing factor, and number of air voids per linear measurement in the sample. The air content is defined as "the volume of air voids in cement paste, mortar, or concrete, exclusive of pore space in aggregate particles, usually expressed as a percentage of total volume of paste, mortar, or concrete" [47]. Specific surface is a measure of the surface area of air voids contained in a unit volume of hardened concrete expressed as square millimeters per cubic millimeter. The void spacing factor indexes the maximum distance of any point in a cement paste or in the cement paste fraction of mortar or concrete from the periphery of an air-void [47]. Diameter of voids and number of air voids per linear measurement are, as the respective terminology implies, a measurement of the diameter and frequency in which the voids occur along a line, taken as an average for a sample. To provide an air-void system with adequate freeze-thaw resistance the following limits are suggested [48].

- (1) Air content - minimum 9% of the volume of paste;
- (2) Spacing factor ( $\bar{L}$ ) - Less than 0.2 mm (200  $\mu$ m);
- (3) Specific surface ( $\alpha$ ) - 25 mm<sup>2</sup> of air-void surface per mm<sup>3</sup> of air-void volume or greater; and
- (4) Diameter - in the range of 0.025 - 0.05 mm.



The total air content is determined in the field for the plastic concrete and is adjusted accordingly, to meet the requirements of the project specifications. The spacing factor, specific surface and diameter of the air voids must be determined after the concrete has hardened. Analysis of the air-void parameters in hardened concrete using conventional methods is time consuming and involves highly technical equipment and personnel expertise.

#### 4.3 Factors Affecting the Air-Void System in Fresh Concrete

The properties of the concrete mixture and the method of batching and placing the concrete will largely affect the quantity and distribution of the air voids. When designing an air-entrained concrete mixture, consideration should be given to the physical and chemical properties of cement, aggregate, and admixtures; the required slump and temperature of the mixture; the type of equipment used for batching; and the method of vibration during concrete placement. Table 4-2 [65] gives a detailed description of the effect of mixture design and concrete constituents on the control of air content in concrete. The following is a discussion of those factors most commonly observed in the field placement of concrete.

Table 4-2 :

**Effect of Mixture Design and Concrete Constituents on Control of Air Content in Concrete**

Type of constituent	Effects on		Corrective action
	Air content	Air-void system	
Accelerators	Calcium chloride increases air content. Other types have little effect	Unknown	Decrease AEA* when calcium chloride is used
Cement composition	Higher fineness (Type III) requires more AEA. Alkali increases air content	Effects not well defined	Use 50% to 100% more AEA for Type III. Decrease AEA dosage 20% to 40% for high alkali
Cement contaminants	Oxidized oils increase air. Unoxidized oils decrease air	Little apparent effect	Obtain certification on cement. Test for contaminants if problems develop
Cement content in mix design	Decreases with increase in cement	Smaller voids and greater number with increasing cement content	Increase AEA 50% for 200 lb per cubic yard increase in cement. Increase AEA 10 times or more for very rich, low-slump mixtures
Coarse aggregate	Decreases as maximum size of aggregate increases. Crusner fines on coarse aggregate decreases air content	Little effect	No action needed as required air decreases with increase in aggregate size. Hold percentage (fines below 4%)
Fine aggregate	Increases with increase in sand content. Organic impurities may increase or decrease air content	Surface texture may affect specific surface of voids	Decrease AEA as sand content increases. Check sand with ASTM C-40 prior to acceptance
Fly ash	High loss on ignition or carbon decrease air content. Fineness of ash may have effect	Little effect	Increase AEA. May need up to 5 times more with high-carbon ash. Foam Index test is useful. check procedure. Air reduction with long mixing times (90 minutes) can be significant with high-carbon ash. Add more AEA
Mix-water contaminants	Truck mixer wash water decreases air. Extreme water hardness may decrease air. Algae increases air	Unknown	Test water supplies for algae and other contaminants prior to acceptance
Pigments	Carbon-black and black iron oxide based pigments may absorb AEA, depress air content	Unknown	Prequalification of pigment with job materials
Slump	Increases 1/2 to 1 percentage point per 1-in. slump increase for slumps up to 6 or 7 in., then higher slumps result in decreased air	Becomes coarser with higher slumps	Reduce AEA dosage
Superplasticizers (high-range water reducers)	Melamine-based materials may decrease air or have little effect. Naphthalene and lignosulfonate-based materials increase air content. Highly fluid mixtures may lose air	Produces coarser air-void systems. Spacing factors increase	Use less AEA with naphthalenes. Specify 1% to 2% higher air content if possible
Water content in mix design	Increases with increase in water content about 1/2 to 1 percentage point per gallon of water. Fluid mixes show loss of air	Becomes coarser at high water content	Decrease AEA accordingly
Water reducers, retarders	Lignosulfonates increase air. Other types have less effect	Spacing factors increase at higher dosages	Decrease AEA 50% to 90% for lignosulfonates especially at lower temperatures. Decrease AEA 20% to 40% for other types. Do not mix admixtures prior to batching

The amount of air-entraining agent required in a given mixture is usually specified as a dosage rate per unit of cement. As the cement content increases for a particular concrete mixture, the air content decreases for a set quantity of air-entraining admixture. Fortunately, setting a dosage rate per unit of cement, decreases the air-void spacing factor and increases the specific surface, thereby creating a more durable concrete.

Air-entraining agents will react differently with cements from different sources and different types of cement. In Canada, cement is classified into five categories, Type 10 to Type 50, based on the physical and chemical properties[1]. Changes in the type of cement or cement source may alter the demand for air-entraining agent to produce an equivalent volume of entrained air.

Variations in coarse and fine aggregate supply will have a marked effect on the air content of concrete. As the maximum size of coarse aggregate is decreased the air content will increase for a constant dosage rate. This is attributed to the increase in relative mortar volume. An increase in the percentage of fine aggregate to total aggregate will increase the air content; aggregate with a large percentage of fines, however, will tend to cause a reduction of entrained air [48].

Variation in the air content with changes in slump of a concrete mixture is frequently observed in the field testing of plastic concrete. As the slump increases, a constant dosage of air-entraining admixture will produce a greater volume of air.

This is generally true for slumps up to  $170 \pm$  mm; however as the slump continues to increase beyond this point, the air content will decrease. Slump of concrete reflects the workability of the concrete and will influence the amount of vibration required for proper consolidation. Longer vibration times at high frequencies will have the most detrimental effect on the volume of air and spacing factor. The adverse effect on air entrainment associated with lengthy agitation of the concrete during batching and mixing is also observed during field testing of the plastic concrete. Prolonged mixing will tend to decrease the amount of stable entrained air in the concrete.

The use of admixtures in concrete mixture designs has become common practice in the concrete industry; however, the compatibility of other admixtures with the air-entraining agents will vary. Particular to this research is the effect of fly ash on the air-void system. Extensive field experience by others has shown that fly ash concrete requires a much higher dosage of air-entraining agent to achieve the same air content as an equivalent non-fly ash concrete mixture. The mechanism of the effect on the air-void system of the addition of fly ash in concrete is not entirely understood.

#### 4.4 Measurement of Air Content in Plastic Concrete

The three test methods specified by ASTM to measure the total air content of plastic concrete are the gravimetric, volumetric and pressure methods.

The gravimetric method of determining the air content is described in ASTM C138 [50]. For this method the unit weight of concrete containing air is compared to the calculated unit weight of air-free concrete. The air content is calculated using the following formula:

$$A = \frac{T - W}{T} \times 100$$

where: T = theoretical unit weight of air-free concrete computed from the proportions and specific gravities of the mix components.

W = measured unit weight of concrete.

To calculate the theoretical unit weight, relative density and the absolute volumes of the concrete ingredients must be accurately determined. As a result, this test method is suitable for laboratory use only.

The volumetric method of determining the air content in concrete is described in ASTM C173 [51]. This method is based on comparing the volume of fresh concrete containing air with the new volume of the same concrete after the air

has been expelled. The concrete is placed in a measuring bowl and agitated vigorously until all the air seems to have been removed. The reading of the air content is correlated with the volume of water which has replaced the expelled air. This method is particularly useful for concretes made with lightweight and porous aggregates when determining the total air content.

The third and most common method for measuring the air content of fresh concrete in the field or laboratory is the pressure method. The principle of this test is the measurement of the change in volume of the concrete when subjected to a given pressure. The test method is described in ASTM C231 [52]. Figure 4-1 illustrates the equipment used in the test method. This method is very practical for field testing all concretes, except those made with highly porous and lightweight aggregates.

The three test methods described here facilitate the measurement of total air content in fresh concrete; however no information is provided about the nature of the air-void system. The purpose of these tests is to provide a quick means of determining the air content of a concrete before placement. With the use of proper and familiar air-entraining agents a general assumption can be made with respect to a proper air-void system development in the concrete, when using these tests as a quantitative measure.

To determine accurately the characteristics of the air-void system the concrete must be analyzed in the hardened state, using microscopic techniques.

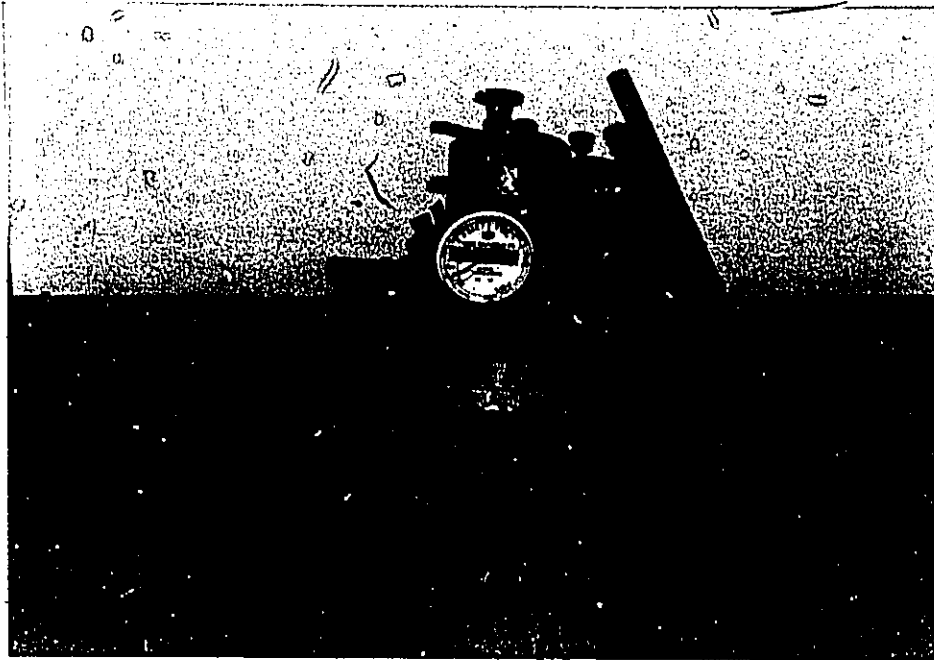


Figure 4-1 : Pressure meter used to measure air content in plastic concrete.

#### 4.5 Measurement of Air Content in Hardened Concrete

The determination of air-void content and parameters of the air-void system in hardened concrete is made possible through the microscopic examination of prepared concrete sections. The two most commonly used microscopic techniques are the Point Count Method, developed by Chayes [53] in 1949

and the Linear Traverse Method, based on procedures described by Rosiwal in 1898. A third method for determining air-void characteristics in hardened concrete, developed by Verbeck [58] in 1947 is called the areal traverse method.

The key to accurate and consistent analysis of a concrete sample is careful preparation of the concrete surface prior to analysis. ASTM C457 [54] describes the standard procedure for preparation of concrete sections for microscopic examination. The concrete section should be ground, using a series of abrasive grits, until the surface is considered satisfactory when observed under the test magnification. It is equally important to determine the required area of the concrete sample to be analyzed in order to produce results which are statistically representative of the hardened concrete. Recommended areas for concrete test sections and length of traverse for measurement of various characteristics of hardened concrete are also outlined in ASTM C457.

The modified point count method is a reasonably accurate technique and is less time consuming than the other manual methods. The technique determines the frequency at which regularly spaced points along a line of traverse, observed through a microscope, intersect with air voids on the prepared concrete section. The device used is a specially constructed manually operated mechanical stage with movement in two perpendicular directions.



The data collected by the operator include:

- 1) total number of air voids intersected;
- 2) the frequency with which regularly spaced points on the line coincide with the location of an air-void;
- 3) the total number of points coinciding with the paste.

From the data obtained the parameters of the air-void system can be calculated.

The linear traverse technique has become the most widely accepted method for the analysis of air-void parameters in hardened concrete. As a result this method is used as a basis for comparison of results of newly developed systems of analysis. The linear traverse method was originally developed by Brown and Pierson [55], but received further study and modification by Powers [11], Willis [56], and Lord and Willis [57].

The apparatus requires a specially designed stage mounted on a carriage block and accompanied by a stereoscopic microscope. The prepared concrete sample is mounted on the carriage which travels beneath the microscope. The sample is traversed along a line until an air-void is encountered, at which time a counter records the chord length across the void. The traverse is continued until a second air-void is contacted and the chord length is again recorded. At the completion of the traverse the operator has recorded the total length of traverse across

the sample, the total length of traverse across the air voids, and the number of air voids encountered. From this data the desired parameters of the air-void system can be readily calculated using the following mathematical relationships [11].

$$A = nl$$

where:

A = total volume of air voids, expressed as a fraction of the concrete volume;

n = number of voids intersected per unit length of traverse;

l = average distance across intersected voids along the line of traverse.

$$\alpha = 4/l$$

where:

$\alpha$  = specific surface of air voids, expressed as boundary area per unit volume of air.

and

$$\bar{L} = P/4n \quad \text{for } P/A < 4.33$$

or

$$\bar{L} = 3/\alpha [1.4(P/A + 1)^{1/3} - 1] \quad \text{for } P/A > 4.33$$

where:

$\bar{L}$  = spacing factor

P = paste content

The mathematical significance of these relationships is discussed exhaustively by Willis [59]. In his discussion, Willis explains that Powers' treatment of chord length data is mathematically valid for a system of air bubbles of uniform size. In contrast, the system of air voids observed microscopically in air-entrained concrete is represented by bubble sizes distributed over a wide range. Willis' final comments state that the true void properties can be determined statistically from the section diameters obtained by the areal traverse method and not the chord lengths determined in the linear traverse method. Unfortunately the areal traverse method was at that time a manual and tedious operation and received little recognition in concrete research.

The areal traverse or plane-intercept method for analyzing voids in concrete was first employed by Verbeck [58] who measured the area of the void sections in camera lucida drawings of a prepared concrete surface. Rexford [59] adopted a similar idea using photographs of the concrete surface, on which to measure air-void characteristics. The application of this method to determine characteristics of the entrained-air voids in

concrete was eventually developed by Willis [60] and Warren [61]. On the basis of their work, this author developed a computerized image analysis system using the principles of the areal traverse technique.

Warren recognized the need to determine the following properties of the voids in concrete:

- (1) Average void diameter;
- (2) Specific surface of the voids;
- (3) Number of voids per unit volume of concrete;
- (4) Total volume of voids per unit volume of concrete;
- (5) Void spacing factor;

The basic technique of the plane-intercept method, was to pass a plane through the concrete specimen and then record the diameters of the air-void sections exposed on the surface.

In Warren's work the sample preparation consisted of cutting and polishing a representative plane section of concrete. The section voids exposed were then filled with a fluorescent material and photographed under ultraviolet light. This produced a contrasting image between the air voids and the surrounding paste. The size distribution and number of voids appearing on the photographed section were measured and a mathematical analysis of the data was carried out.

Warren derived the equations relating the void properties as measured on a plane passing through the voids to the actual properties of the voids using the methods of mathematical statistics.

A mathematical relation exists which states: if in a distribution of scalar quantities, there is a number  $a_1$  of  $m_1$  magnitude,  $a_2$  of  $m_2$  magnitude,  $a_3$  of  $m_3$  magnitude, etc., the arithmetic mean of the magnitudes is defined as

$$\begin{aligned} [m]_1 &= \frac{a_1 m_1 + a_2 m_2 + a_3 m_3 + \dots + a_n m_n}{a_1 + a_2 + a_3 + \dots + a_n} \\ &= \frac{\sum (a m)}{\sum a} \end{aligned}$$

In mathematical statistics, this relation would be referred to as the first moment of the series of magnitudes  $m_1$ ,  $m_2$ ,  $m_3$ , etc. This approach is similar to the approach taken by Willis [60], when attempting to explain the statistical significance of the equations developed by Powers [11], for the linear traverse method.

The recording of individual air-void section diameters may be grouped into particular size classes. Each circle falling within a particular size is assumed equal to the average size of the size class. The nth moment of the void diameter,  $l$ , is defined as

$$[ll]_n = \frac{\sum (a l^n)}{\sum a}$$

where:

a = the number of section diameters, l, on the concrete surface.

For the purpose of this study it is necessary to determine the harmonic mean,  $[ll]_{-1}$ , the first moment,  $[ll]$ , and the second moment,  $[ll]_2$ , of the section diameters.

The equations relating the true void properties to the properties of the section diameters on the interception plane were derived by Warren as follows:

$$D_a = \frac{\pi}{2[ll]_{-1}}$$

where  $D_a$  = average diameter of the spheres in the distribution of sphere sizes.

$$\alpha = \frac{16[ll]}{\pi[ll]_2}$$

where  $\alpha$  = specific surface of the distributed spheres.

$$M = \frac{2h[ll]_{-1}}{\pi}$$

where  $M$  = number of spheres per unit volume of concrete.

$n$  = number of voids intercepted per unit area of the intercepting plane.

$$V_t = \frac{\pi n l^3}{4}$$

where  $V_t$  = air content per unit volume of concrete.

$$\bar{L} = \frac{\sqrt{3}}{2} \left( \frac{p + V_t}{M} \right)^{1/3} - \frac{Da}{2}$$

where  $\bar{L}$  = void spacing factor

$p$  = paste content

#### 4.6 Image Analysis

In 1949, Willis commented that although a more statistically valid representation of the air-void system in concrete could be obtained by the areal traverse method, the method was much too tedious to be used in research. Unfortunately Willis and Powers did not have the advantage of the technical age of image processing which is available today.

In this technological age, image processing has found diversification into many areas of scientific research and development. The application of image processing or image analysis has progressed from the more complicated hardwired systems to the simpler and more effective software controlled systems of today.

Image analysis is simply the manipulation of a digital image to enhance existing features to create a clearer image. To digitize an image, the image is divided into a large number of small picture elements, or pixels. Each pixel has a particular brightness value, or digital intensity associated with it. The computer sees this image as a rectangular array of numbers, each of which indicates the brightness or intensity for that pixel. The spectrum of digital intensities range from 0 to 255, representing a range of grey levels from black to white, respectively. The resolution of the image is usually defined by a 512 x 512 array of pixels; however higher resolution image processors are available.

The most useful tool in image enhancement is the histogram, showing the number of pixels at each digital intensity. The histogram contains useful information regarding the contrast of the image and the distribution of grey levels in the image. Of particular interest to the analysis of air voids in concrete is the bimodal histogram. This type of histogram would have two peaks representing an image having two distinct groups of grey levels such as air



voids filled with white powder against a darkened background surface. The bimodal histogram provides us with the means of locating a subject's boundary such as an air void. To further define the image a threshold can be set so as to create a binarized image. A binarized image displays only black or white pixels with no intermediate grey levels. The threshold will determine at which grey level the transition between black and white will occur.

The contrast enhancement is effected through look-up tables (LUT) which are built into the digitizing hardware system. LUT's are a user friendly way of controlling all pixels in an image to attain an enhanced image.

The amount and type of information retrieved from an enhanced image is particular to the application of the image analysis system and is facilitated through compatible computer software. The most versatile image analysis systems will allow the user to develop the software so as to fully implement the particular application.

The application of image analysis in the microscopic examination of hardened concrete has been documented by Chatterji and Gudmundsson [62], 1977, Meyer [67], and Racic [68]. The image analysis technique works on the same principle as the Rosiwal technique; however with the use of an automatic image analyzing microscope they were able to characterize the air-void system within a much shorter time frame and with more accuracy.

The image analysis system developed for this research employs the technique of the areal traverse method for determining air-void parameters. The method is quick and efficient in determining the distribution of section-void diameters on a prepared concrete sample which was clearly stated by Willis 35 years previously, as a necessary development in concrete research. ✓

## CHAPTER 5

### DEVELOPMENT OF AN IMAGE ANALYSIS SYSTEM USING A PC

#### 5.1 General

Prior graduate research projects, using image analysis equipment, conducted within the Civil Engineering department of the University of Windsor, utilized a system developed by Lemont Scientific. The system consisted of a central unit (which included a computer, digital scan generator, threshold selector, and image selector), an optic system, an automatic stage control, a cathode ray tube (CRT), printer and a dual floppy disk data storage unit. The researchers, Meyer [67] and Racic [68], experienced numerous operating problems with an eventual malfunction in the computer hardware. The equipment was rendered inoperative and the complexity of the outdated hardware made it futile to attempt to rectify the problem. The recent advances in microcomputer technology provided the basis for the present development of a new image analysis system which proved more efficient from both a cost and application point of view.

National Library  
of Canada

Canadian Theses Service

Bibliothèque nationale  
du Canada

Service des thèses canadiennes

NOTICE

AVIS

THE QUALITY OF THIS MICROFICHE  
IS HEAVILY DEPENDENT UPON THE  
QUALITY OF THE THESIS SUBMITTED  
FOR MICROFILMING.

UNFORTUNATELY THE COLOURED  
ILLUSTRATIONS OF THIS THESIS  
CAN ONLY YIELD DIFFERENT TONES,  
OF GREY.

LA QUALITE DE CETTE MICROFICHE  
DEPEND GRANDEMENT DE LA QUALITE DE LA  
THESE SOUMISE AU MICROFILMAGE.

MALHEUREUSEMENT, LES DIFFERENTES  
ILLUSTRATIONS EN COULEURS DE CETTE  
THESE NE PEUVENT DONNER QUE DES  
TEINTES DE GRIS.

## 5.2 Computerized Hardware

The computerized image analysis setup is shown in Figure 5-1. The system consists of an Oculus 200 real-time video digitizer board installed in a Tandy 1200HD (IBM compatible) microcomputer. The Oculus 200 board can also be installed in any other IBM-PC compatible machine.

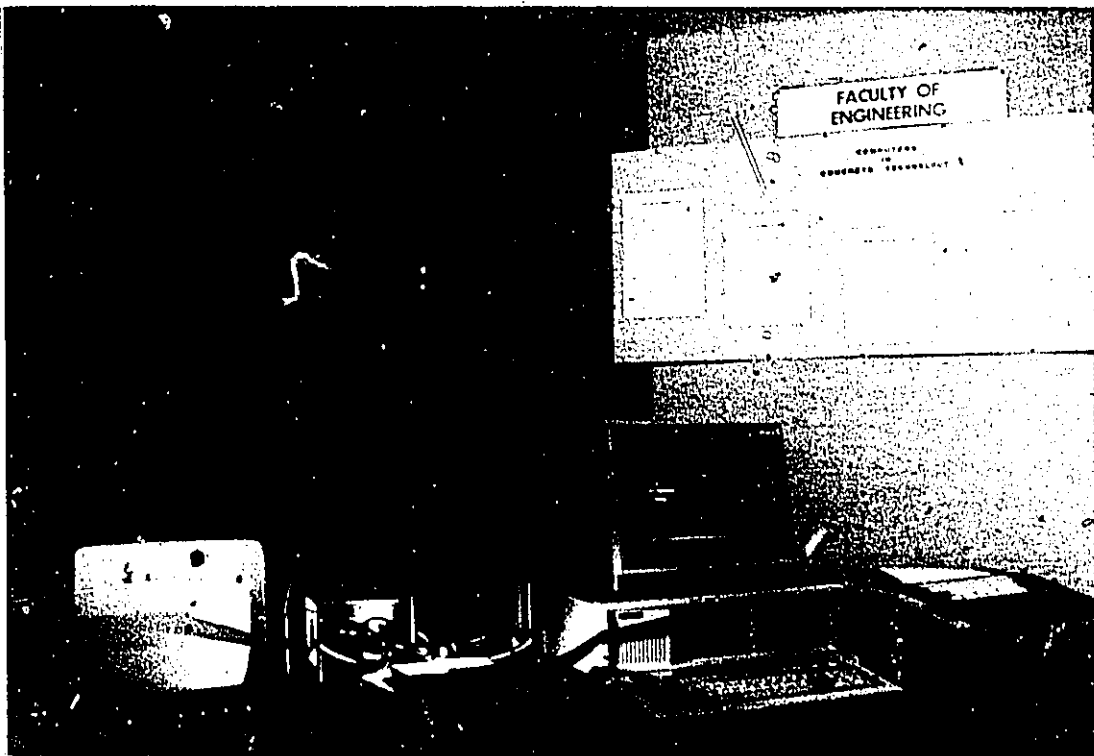


Figure 5-1 : Image Analysis Hardware

The personal computer is equipped with a standard floppy disk drive, 10 Mbyte hard disk drive, and 640K RAM (Random Access Memory). The 640K RAM was necessary to run the accompanying image analysis software and to process

efficiently the large amounts of data retrieved by the system. The computer is interfaced with a parallel dot-matrix printer for presentation of results.

The Oculus 200 digitizing board was developed and marketed by Coreco Inc., Montreal, Canada. The digitizing board, more commonly referred to as the frame grabber, converts a standard television image into an array of 480 X 512 pixels, at the rate of 30 images per second, and displays the image with the same resolution on an auxiliary monitor seen to the right in Figure [5-1]. The digitized image is written using 256 Kbytes of on-board RAM memory which can be accessed by the processor in the microcomputer.

A schematic of the Oculus 200 frame grabber is shown in Figure 5-2.

The digitization logic allows a standard RS-170 video input to be digitized into an array of 480 X 512 pixels to an accuracy of 7 bits per pixel at a rate of 30 images per second. In the event the images must be retrieved from disk storage the synchronization modes independently produce signals to drive a monitor. This will allow the operator to visually observe the image stored on disk.

The look-up tables reside on-board in 1024 bytes of menu driven memory. These tables are used for histogram expansion, thresholding or other single pixel data related functions.

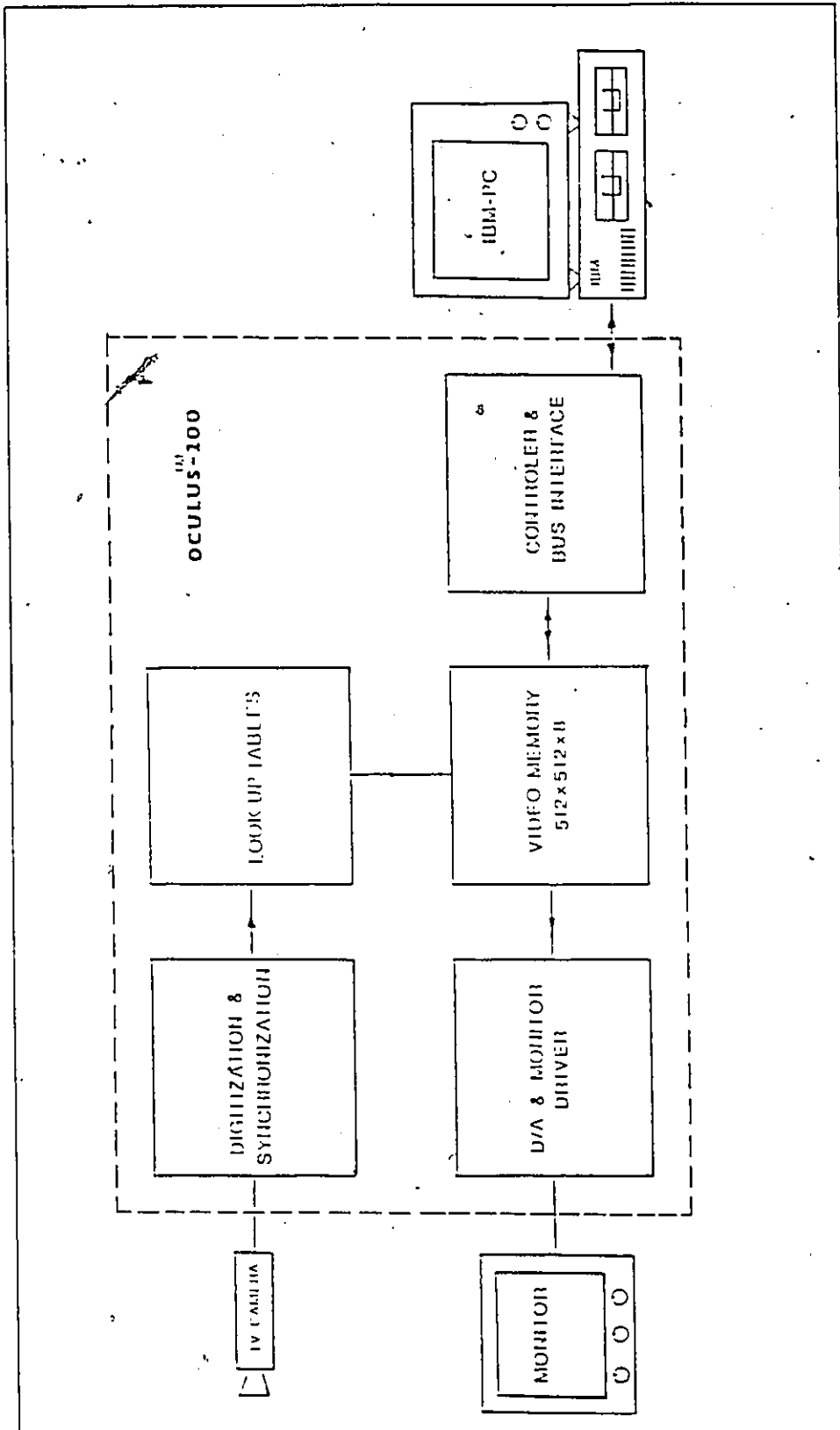


FIGURE 5-2 SCHEMATIC OF OCULUS 200 IMAGE ANALYSIS BOARD

The on-board video memory is 256 Kbytes, designed to allow simultaneous acquisition of data in conjunction with the processing and display operations. Each pixel in an image can be accessed through a coordinate address grid.

The D/A (digital-to-analog) interface and monitor driver displays the image stored in on-board memory on an auxiliary video monitor.

The controller and bus interface contains 5 I/O mapped registers which operate as either read and or write registers for special programming applications.

### 5.3 Stage Unit

#### 5.3.1 Design of Stage Equipment

The stage unit shown in Figure 5-1 consists of a free moving horizontal platform on which the sample is positioned, and a stationary mount to support the binocular microscope and video camera. The setup was designed to meet the following criteria:

- 1) the operator must have complete control and ease in guiding the sample in two perpendicular directions;
- 2) the sample mount must be equipped with a levelling device so as to compensate for samples of varying thickness;



- 3) the microscope-camera unit must be strategically positioned to access the entire sample surface, while maintaining a stable vertical position;
- 4) the microscope-camera mounting rod must permit vertical movement of the optic system to facilitate focusing at different magnifications;
- 5) the base must be compact and portable, while providing a stable platform for mounting the microscope-camera; and
- 6) the stage must not obstruct access of the light source to the sample surface.

The stage equipment developed for the subject research requires manual operation by the user. However for future research projects, the stage design will permit automation of the equipment to transfer control from the operator to the computer software. This would release the operator from manually maneuvering the sample and would ultimately be the most efficient method of analysis.

The sample platform is guided in the X and Y directions by two threaded turn bolts, arranged perpendicularly to one another. The operator effects smooth movement of the sample beneath the microscope-camera using the readily accessible knobs at the end of either turn bolt.

The platform is equipped with a levelling screw at each of the four respective corners. With the aid of a simple bulls eye level placed on the sample surface, the platform can be adjusted to compensate for variation in sample thickness. This eliminates the need for constant focusing of the sample surface as the sample moves beneath the microscope-camera. Due to the shallow depth of field attained at the high magnifications used, it is extremely important to attain precise levelling of the sample surface in order to maintain the resolution of the target boundaries.

#### 5.3.2 Microscope - Camera

The microscope-camera shown in Figure 5-1, consists of a CCTV Panasonic video camera in series with 5X and 6.4X binocular microscopic lenses. The camera was adapted to the binocular microscope using a specially designed single extension tube. Using the lens configuration described above a resolution of 10  $\mu$ m was attainable. The camera is equipped with a highly sensitive separate mesh 2/3 inch pick-up tube also known as a vidicon.

To avoid problems with light scatter reflected by the surface of the prepared sample the microscope lens was equipped with a polarizing filter. Light scatter is common on smooth, reflective surfaces and disrupts the clarity of the signal transmitted by the optic unit, creating background noise in the image. The polarizer filters the plane polarized light reflected from the surface.

The focusing of the sample surface beneath the microscope-camera was achieved by moving the microscope-camera unit vertically along the mounting rod, while simultaneously viewing the image on the auxiliary monitor. The image was focused in and out until the sharpest image was attained. The optic unit was then locked into position throughout the entire period of analysis. Assuming the sample surface had been accurately levelled, each frame retrieved from the sample surface was equally focused. The focusing procedure had to be performed on each new sample surface.

#### 5.3.3. Lighting Setup

The extremely high magnifications required for analysis of the concrete samples demanded intense illumination of the sample surface. The preferred light source was a high quality quartz light source with two flexible fibre optic extenders. The fibre optic extenders were fed into a

plexiglass light guide to ensure a constant lighting angle and intensity on the sample surface. Figure 5-1 illustrates the setup of the light source, the light guide, and the sample surface.

During the initial setup and focusing of the sample the plexiglass light guide was positioned beneath the microscope-camera unit and remained in that position throughout the analysis of the concrete surface. The intense stationary light source ensured maximum illumination of the sample surface and eliminated any variation in lighting intensity between frames.

#### 5.4 Computer Software

The Oculus 200 board is accompanied by a computer package called the Gray Library. The Gray Library contains efficient machine language functions designed to enable a user to configure his own computer vision applications. The desired Gray Library functions are called from a user developed main program, compiled in C language [63].

The main program developed for the application of this research is included in Appendix B. Through a system of keystrokes the operator is guided through a series of user friendly menus until sufficient sample area is analyzed. The operator has complete control of the amount of area

analyzed on the sample and can view the binarized image of the sample during the processing, on the auxiliary monitor . An example of the final printout is shown in Figure 5-3.

```
Sample : CM057
Area of Sample Analysed : 588.0 sq mmms
Number of Frames : 100
Total # of Voids : 1639
Avg Diam of Total Voids : 81.8 um
Percent Total Air : 4.47 %
Number of Entrained Voids : 1153
Avg Diam of Entrained Voids : 71.4 um
Percent Entrained Air : 2.59 %
Classification of Voids
0.0 - 18.8 : 34.3%
18.8 - 47.0 : 19.9%
47.0 - 94.0 : 22.5%
94.0 - 188.0 : 15.7%
188.0 - 282.0 : 4.6%
282.0 - 376.0 : 1.5%
376.0 - : 1.5%
```

Figure 5-3 : Printout of Image Analysis for Sample CM057

The retrieved data was then entered into a spreadsheet. The programming capabilities of the spreadsheet package allowed the operator to compile all the data and perform the mathematical functions of the areal traverse method to arrive at the following true air-void parameters:

- 1) the average diameter of the spheres;
- 2) the specific surface of the spheres;

- 3) the number of spheres per unit volume of concrete;
- 4) the entrained air content per unit volume of concrete; and
- 5) the void-spacing factor;

The amount of data collected by the image analysis program and the extent of the calculations involved in arriving at the air-void system parameters is massive. However, through the use of readily available spreadsheet packages the task was performed accurately in a greatly reduced time frame.

#### 5.5 Standardization of the Image Analysis System

The computerized system for image processing analyzes a pattern as a series of pixels grouped together to form objects of distinct shape and size. To convert the pixel data to actual linear measurements a scale was determined using the test pattern shown in Figure 5-4. Due to the high magnification, a suitable template was not readily available. The test pattern, shown here, was found to be the closest simulation of the pattern of air voids on a prepared specimen surface.

During the scaling process the microscope-camera was focused on the size pattern with a diameter equal to 0.25 mm. Consecutive frames were grabbed using various scales

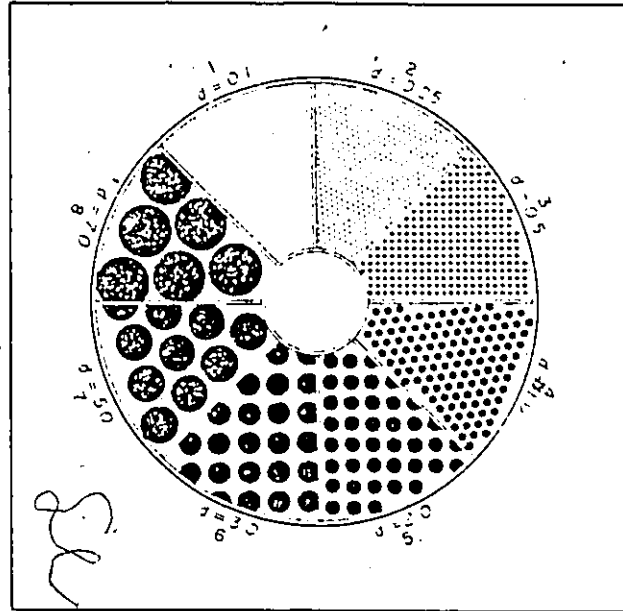


Figure 5-4 : Pattern used to scale image analysis

input in the software, by the operator. A cumulative analysis of the processed data was output for each scale. Through a number of trials a scale of 9 um per pixel produced the closest approximation to the known object diameter. Table 5-1 summarizes the analysis of data retrieved using the 9 um per pixel scale.

TABLE 5-1

Number of Frames	Number of Complete Objects	Average Diameter of Complete Objects
		(mm)
1	12	0.21
2	23	0.22
3	34	0.22
4	44	0.23
5	56	0.23

A total of 56 objects were observed. The known average diameter of the objects is 0.25 mm. The average diameter as determined by the image analysis system is 0.23 mm.

The linear traverse method for analysis of the air-void system in hardened concrete is the most widely used technique in concrete research. To evaluate the newly developed image analysis system, a series of samples was analyzed using both techniques. The comparison of results was for air content only, shown in Table 5-2.

A statistical evaluation of the test results produced by the two methods, shown in Table 5-3, indicates that there were no significant difference. A linear regression analysis of the data revealed the following relationship:



$$y = 0.5x + 2.2$$

where  $y$  = air content by image analysis

$x$  = air content by linear traverse

This relationship has a correlation coefficient of 0.97 at a 99 percent confidence level. A graphical representation of this relationship is illustrated in Figure 5-5.

The high correlation coefficient for this data would indicate the two methods of analysis produce consistent results. However, it can be seen from the graph in Figure 5-5, at 0% air content determined by the linear traverse method, the image analysis method records a 2.2% air content. The initial air content of 2.2% for the image analysis method can be attributed to the ability of the image analysis system to measure the smaller air voids which an operator would find difficult to detect in the linear traverse method.

In addition, beyond the initial air content of 2.2% the image analysis method records 0.5 times the percent air content determined by the linear traverse analysis. Since the operator does not distinguish between the entrapped-air and entrained-air, the air content determined by the linear traverse method is a measure of the total air content of the hardened concrete. With the aid of computerized analysis the air content determined by the image analysis method is

representative of the percent entrained air in the hardened concrete. The flattened slope shown in Figure 5-5 indicates the air content determined by the linear traverse method does not give a true representation of the percent entrained air in concrete. Since it is the entrained air content that contributes to the resistance against frost action in concrete, the image analysis method provides the operator with a much more valuable tool by which to analyze the parameters of the hardened concrete.

TABLE 5-2  
Comparison of Air Contents

<u>Sample</u>	<u>Linear Traverse</u>	<u>Image Analysis</u>
CM082B	4.9	4.5
L2051B	4.0	4.2
L3081C	5.0	4.5
M2081A	4.7	4.8
M3051A	2.3	3.3
H2052A	2.1	3.2

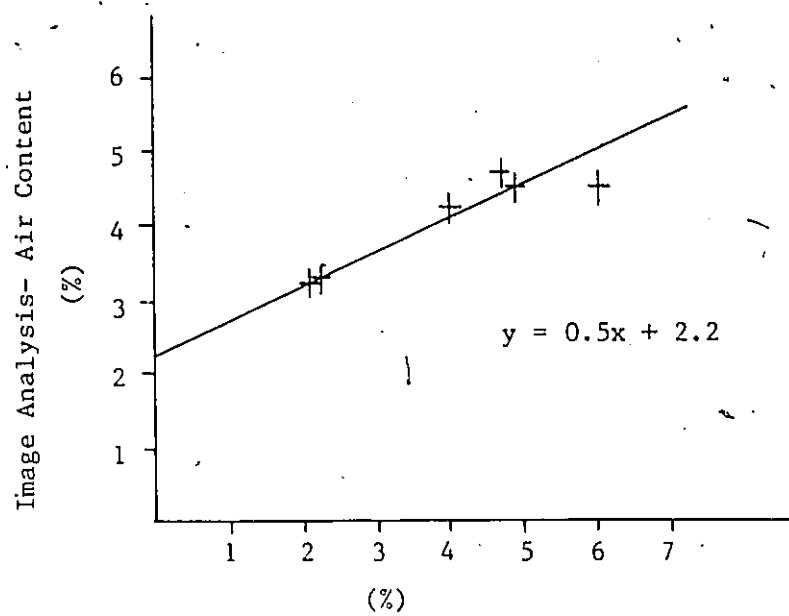
TABLE 5-3

Statistical Comparison of Linear Traverse  
and Image Analysis Air-Content Results

	Linear Traverse	Image Analysis
$\bar{x}$	3.8	4.1
s	1.31	0.67
n	6	6
calculated t	0.52	

"t" critical at 10 significance level = 1.812

Conclusion: No significant difference in test results.



Air Content - Linear Traverse

Figure 5-5 : Relationship between Image Analysis and Linear Traverse - Air Content

## CHAPTER 6

### EXPERIMENTAL PROGRAM

#### 6.1 General

The experimental program was designed to compare the effect of carbon content on the air-void system in concrete using three different fly ashes at 20 and 30 percent replacement and at 5 and 8 percent air content. These air contents define the minimum and maximum limits specified by CSA Standard CAN3 A23.1 [1] for concrete with a 20 mm nominal size aggregate exposed to a Class A exposure. Class A is the most severe exposure condition where seawater or de-icing salts are present and saturated conditions prevail.

A summary of the experimental program is presented in Table 6-1. The percent replacement values for fly ash used in this research are based on the recommended values determined from previous research.

To ensure statistical validity of the results, the test program included two batches for each set of parameters measured. In total, 31 test batches were prepared and 4 samples were procured from each batch for microscopic analysis.

TABLE 6-1  
SUMMARY OF TEST PROGRAM

SAMPLE	% REPLACEMENT	AIR CONTENT	# OF BATCHES	# OF SAMPLES FOR MICROSCOPICAL ANALYSIS
Control	-	5	4	16
Control	-	8	3	12
OHL	20	5	2	8
OHL	20	8	2	8
OHL	30	5	2	8
OHL	30	8	2	8
OHM	20	5	2	8
OHM	20	8	2	8
OHM	30	5	2	8
OHM	30	8	2	8
OHH	20	5	2	8
OHH	20	8	2	8
OHH	30	5	2	8
OHH	30	8	2	8

The OHL, OHM and OHH samples represent low, medium, and high LOI, respectively.

## 6.2 Mixture Design

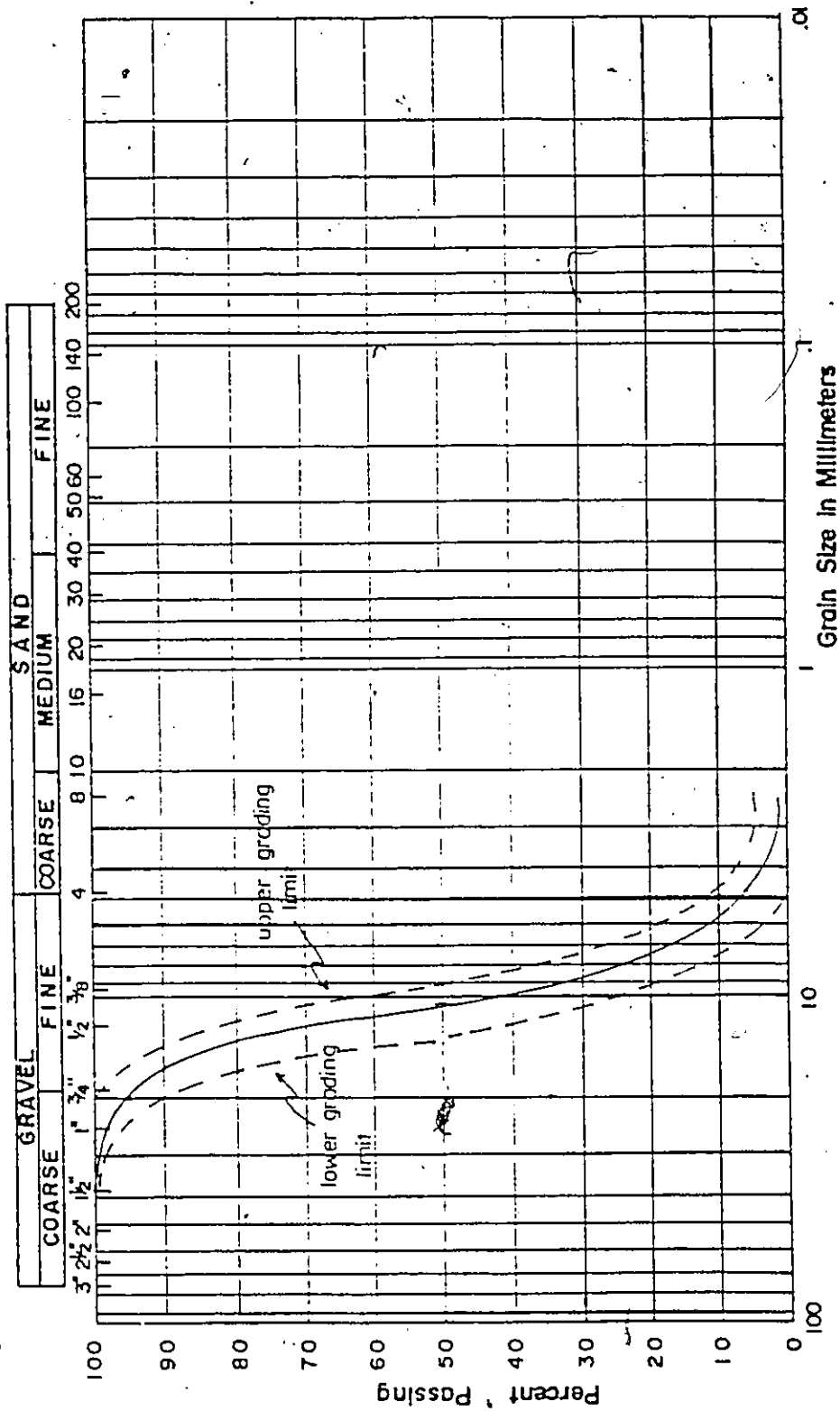
### 6.2.1. Materials

The normal density coarse and fine aggregates were obtained from a local supplier and are used regularly by the ready mix suppliers in the Windsor area. The gradation, by sieve analysis, of both the fine and coarse aggregates was determined in accordance with CSA Test Method A23.2-2A. The results are presented in Figures 6-1 and 6-2, along with the grading limits specified by CSA Standard CAN3-A23.1-M77, Tables 1 and 3[1]. The aggregates were stored in separate bins and were maintained in a protected environment throughout the research program.

The cement was a Normal Type 10 portland cement, conforming to the requirements of CSA Standard CAN3-A5, and was supplied locally. The total amount of cement required to complete the testing program was purchased at one time, to eliminate variation in cement supply. The cement was removed from the bags, intermixed by hand and stored in a dry steel drum.

The water supply was obtained from the City of Windsor supply and a constant temperature was maintained throughout the batching.

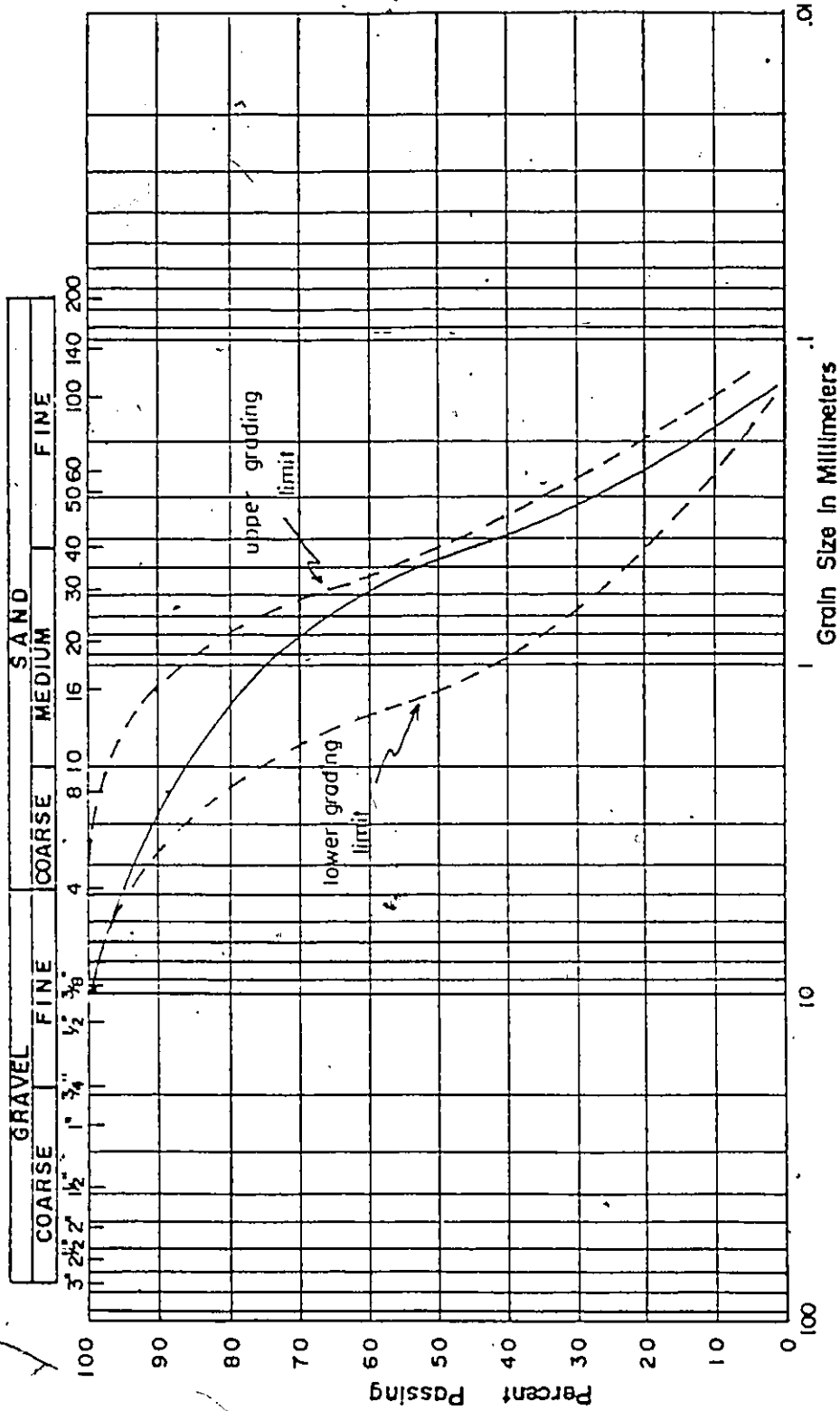
The air-entraining admixture used was Darex, supplied by W.R. Grace Construction; it is an aqueous solution of salts of a sulfonated hydrocarbon. The admixture conforms to the requirements of CSA Standard CAN3-A266.1-M. The



grading limits specified in  
CAN3-A23.1 - M77 Table 3

FIGURE 6-1 GRADATION OF COARSE AGGREGATE





grading limits specified in  
CAN3 - A23.1 - M77 Table 1

FIGURE 6-2 GRADATION OF FINE AGGREGATE

total requirement of admixture to complete the testing program was obtained in one supply and was stored at constant room temperature throughout the batching period.

The fly ash used in this research was obtained from Ontario Hydro's, Lakeview Generating Station (GS). The coal was supplied to Ontario Hydro from various bituminous mines in Pennsylvania and Northwest Virginia. At the Lakeview GS both mechanical and electrostatic equipment are used to collect the ash. A portion of the fly ash collected is marketed and the remainder is land-filled on site. The Lakeview GS has eight boilers with 4 or 5 precipitators in each boiler. The quality of the fly ash will vary depending on the boiler and the elevation level of the precipitator from which the sample was obtained.

The samples received were selected on the basis of LOI percent, ranging from 1 to 12 percent. As discussed in Section 3.3.2, fly ash is categorized as a Class F or C pozzolan based on the chemical composition. To determine the chemical composition of the three fly ashes used in the test program, representative samples of each fly ash were analyzed by an x-ray fluorescence spectrometer. Moisture content, loss on ignition and specific gravity were also determined according to ASTM C 311 [64]. Results of testing are shown in Table 6-2.

Table 6-2 Physical and Chemical Properties of Fly Ash Samples

Sample	% by Weight							M.C.%	LOI%	S.G.	+ #325%
	SiO <sub>2</sub>	Al <sub>2</sub> O <sub>3</sub>	Fe <sub>2</sub> O <sub>3</sub>	CaO	MgO	Na <sub>2</sub> O	SO <sub>3</sub>				
OHL	46.8	24.2	18.5	5.3	0.9	0.7	0.6	0.3	1.4	2.69	1.72
OHM	43.5	22.6	17.5	4.9	0.8	0.8	2.7	0.6	8.2	2.43	28.3
OHH	43.4	23.2	13.8	5.0	0.9	0.8	3.1	0.9	12.1	2.52	12.1

### 6.2.2 Batching

The mixture proportions used for casting specimens were based on a design strength of 30 MPa, a slump of 80 to 100 mm and an air content of either 5 or 8 percent. A number of trial batches were prepared prior to the start of the testing program to establish the following optimum control mixture design:

Coarse aggregate	27.4 kg
Fine aggregate	21.3 kg
Cement	10.1 kg
Water	5.0 kg
AEA - 5 %	8.0 ml
- 8 %	35.0 ml

The above proportions yielded .02 cubic meters of concrete.

The control mixture design was altered for the 20 and 30 percent fly ash replacement concrete mixtures as follows:

#### 20 % Replacement

Cement	8.1 kg
Fly ash	2.0 kg

#### 30 % Replacement

Cement	7.1 kg
Fly ash	3.0 kg

The proportions of coarse and fine aggregate remained the same for all mixtures. The amounts of air-entraining agent and water were adjusted to accommodate the addition of the fly ash.

The concrete was batched in accordance with CSA Standard CAN3 A23.2-2C, "Making Concrete Mixes in the Laboratory". The concrete mixer shown in Figure 6-3 is a power driven tilt drum with a capacity of .04 cubic meters. The dry materials were placed in the mixer and thoroughly



Figure 6-3 : Concrete Mixer

mixed, prior to adding the water. During the dry mix process a lid was placed on the mixer to avoid loss of fines. The air entraining agent and water were mixed before adding to the dry materials. After all materials were combined the mixer was rotated for a period of 3 minutes followed by a 3 minute rest period and then 2 minutes of final mixing. This batching sequence was closely adhered to throughout the testing program. Immediately following discharge from the mixer, the concrete was tested for slump and air content. The air content was determined using a pressure type air meter as shown in Figure 4-1. The air meter is manufactured by Soiltest Inc., Chicago, Illinois and was calibrated prior to the test program. In addition, two test cylinders were cast for compressive strength evaluation.

### 6.3 Sample Preparation

#### 6.3.1 Casting

The concrete test specimens were cast in prisms measuring 100mm x 200mm x 250mm. The concrete was placed in two layers and rodded sufficiently to insure proper consolidation of the specimens. The specimens were sealed and allowed to cure for a 24-hour period before the forms

were removed. The test prisms were then placed in a lime saturated water bath and allowed to cure for a 28 day period.

After curing, four 25 mm thick slices were cut from each test prism perpendicular to the direction in which the concrete was placed. The concrete saw shown in Figure 6-4 built by Clipper Manufacturing Company of Kansas City, is equipped with a 355 mm diameter diamond studded blade. The four cut samples were spaced evenly throughout the sample so as to effectively represent the concrete in the prism.

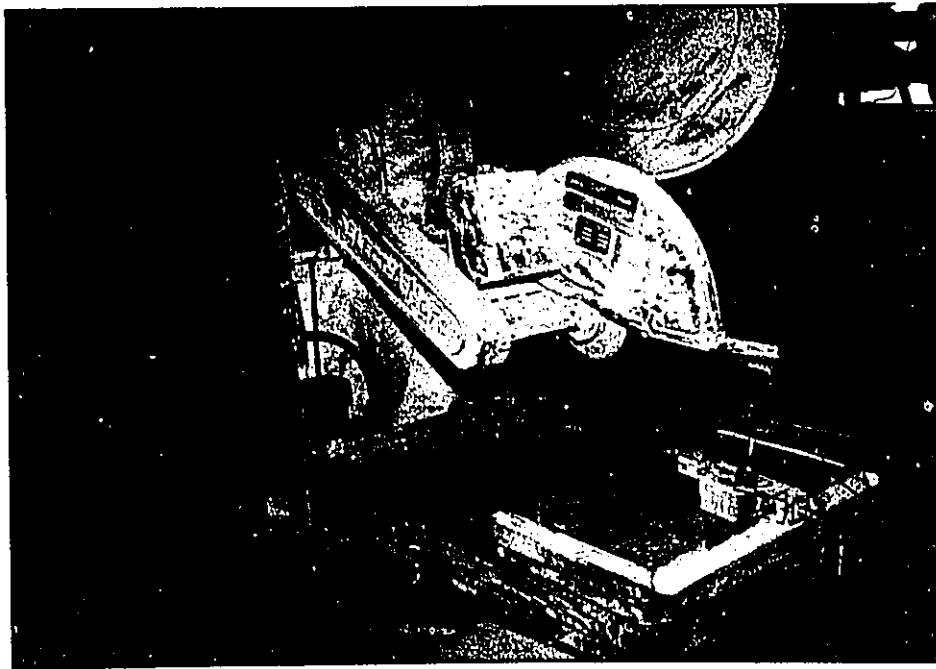


Figure 6-4 : Concrete Saw

### 6.3.2 Polishing

The cut samples were polished on the polishing unit shown in Figure 6-5. The unit, manufactured by Buehler Ltd., consists of a powered flat rotating surface on which specified grinding powders are evenly applied. The polishing was achieved by using a series of grinding powders, supplied by Garway Industrial Supplies, starting with a #100 (122um) and ending with a #1000 (approximately 8um).

Between each successive grit size application the samples required a thorough cleaning to remove remnants of the previous grit from the voids in the concrete surface. This was achieved by ultrasonic cleaning of the samples in a

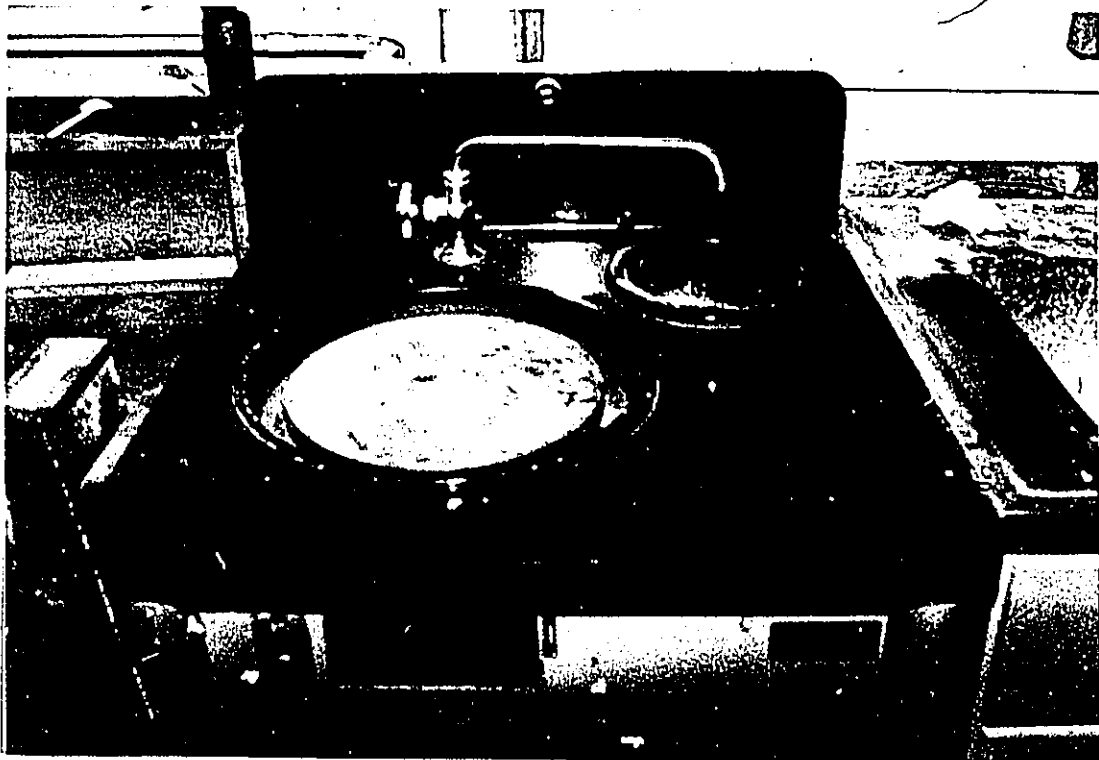


Figure 6-5 : Polishing Unit



water bath. The ultrasonic unit is manufactured by Branson. The samples were placed in the unit for a minimum of 5 minutes or until the surface was visually clean.

### 6.3.3 Surface Preparation

Following the grinding and polishing process the samples were air dried before masking the surface. The purpose of the masking was to provide a darkened background on the sample surface. The masking was done using a fluid of low viscosity so as not to fill the minute air voids. A permanent type black printing ink supplied by Essex Stamp of Windsor, Ontario, was found to be the most suitable. The sample surface was covered with a thin layer of ink and then blotted to remove any excess ink from the voids. The sample was then placed in an oven to dry before another layer of ink was applied. This process was continued until the entire surface was evenly darkened, usually after the second or third pass.

High contrast white finely ground aluminum oxide powder was used to fill the voids. The powder was worked over the darkened surface until all the voids had been filled. To ensure a thorough application, the prepared surface was visually inspected under a binocular microscope. All

excess powder was removed using a moistened fingertip. Figure 6-6 illustrates a prepared specimen surface.



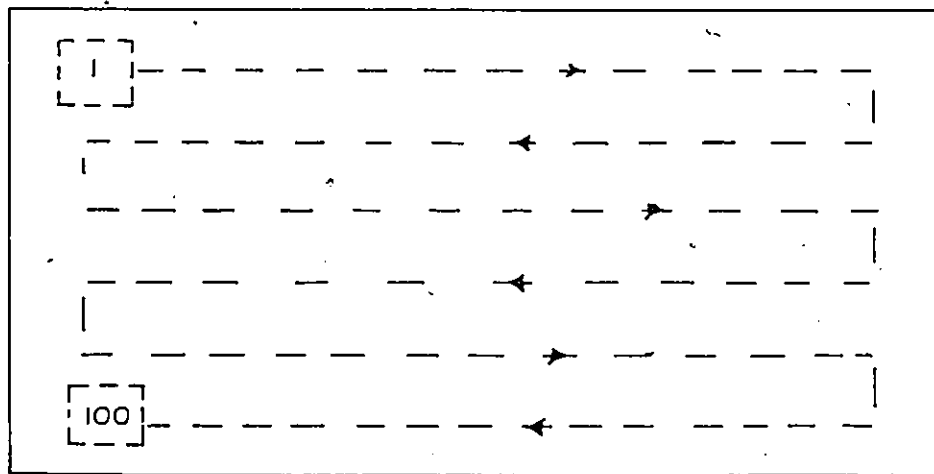
PREPARED CONCRETE SURFACE

Figure 6-6 : Prepared Sample Surface

#### 6.4 Analysis of Sample Surface

The procedure for analyzing the sample surface was as follows. The prepared samples were placed on the traversing stage and levelled using a bulls eye level. With the aid

of the computer software the operator signaled the image processing board to grab an image of the sample surface and display it on the auxiliary monitor. The light source was then aligned under the microscope-camera and its position adjusted, along with the camera focusing, to achieve a clear picture. Following the instructions provided by the program menus, the operator advanced the sample beneath the camera, stopping at evenly spaced intervals for frame analysis. To ensure a representative area of sampling, 100 frames were analyzed on the sample surface, for a total approximate area of 500 square millimetres. The pattern of analysis is shown in the schematic in Figure 6-7. Approximately 1500 to 2000 voids were encountered on each sample surface.



Approximate Sample Size 13,000 mm<sup>2</sup>  
Approximate Area Analyzed 500 mm<sup>2</sup>

Figure 6-7: Pattern of Analysis of Sample Surface

## CHAPTER 7

### RESULTS

#### 7.1 Introduction

In this chapter the results of an experimental program conducted to determine the effect of fly ash on air-entrained concrete are presented and discussed. Three fly ashes, with varying percent LOI, were used in the test program. These fly ash samples were batched at 20% and 30% cement replacement and at nominal air contents of 5% and 8%. In the analysis of the results the following effects are discussed:

- 1) air-entraining agent demand;
- 2) compressive strength;
- 3) air content; and
- 4) entrained-air-void system.

All discussions are accompanied with a statistical analysis of the data obtained. Results are considered significant when the comparison of the means show a variation at the 95% level of significance.

## 7.2 Presentation of Data

A summary of the relevant data recorded during casting is included in Table 7-1. The coding of the samples is as follows.

Example:            I   II   III   IV  
                    L   20   5   1

where:

The 'I' position designates the type of fly ash sample, for example:

CM - Control mix

L - Low LOI (1.4%)

M - Medium LOI (8.2%)

H - High LOI (12.1%)

The 'II' position indicates the percent replacement of cement by fly ash, for example:

0 percent

20 percent

30 percent

The 'III' position indicates the nominal air content in the sample, for example:

5 percent

8 percent

The 'IV' position designates the batch number in the test group, for example:

- 1 - first trial batch
- 2 - second trial batch
- 3 - third trial batch
- 4 - fourth trial batch

For each test batch in Table 7-1, four samples were analyzed using the newly developed image analysis equipment. A summary of the raw data obtained from the computer-aided microscopic analysis of the prepared samples is presented in Table 7-2. Based on the data in Table 7-2 and using the theoretical equations developed for the plane-intercept method of analysis the characteristics of the entrained-air-void system were calculated for the four combined samples of each test group. The characteristics of the entrained-air-void system are included in Table 7-3. These characteristics include:

- 1) the average diameter of the entrained-air-void system ( $\mu\text{m}$ );
- 2) the number of entrained-air voids per volume of concrete;
- 3) percent entrained air in the total volume of concrete (%);

Table 7-1 Record of Casting

TEST BATCH	DATE CAST	AEA QUANTITY (ML)	AIR CONTENT (PLASTIC)	SLUMP (MM)	COMPRESSIVE STRENGTH	
					28 - DAY	56 - DAY
CM051	23/07/85	8	5.0	60	40.3	
CM052	07/08/85	8	4.8	60	32.9	
CM053	08/08/85	8	5.2	110	31.7	
CM054	01/10/85	8	5.1	150	32.4	
CM081	30/07/85	30	7.7	50	28.2	
CM082	13/09/85	30	7.5	110	26.5	
CM083	17/09/85	35	7.5	130	26.3	
L2051	22/09/85	12	5.1	120	30.2	37.1
L2052	18/10/85	12	4.5	100	35.4	37.9
L3051	08/10/85	16	5.3	120	31.0	32.3
L3052	22/10/85	16	4.9	120	30.7	36.6
L2081	11/10/85	45	7.1	120	28.5	33.5
L2082	16/12/85	60	10.0	100	27.9	32.4
L3081	17/10/85	85	7.0	120	28.7	31.6
L3082	17/10/85	100	8.1	120	25.6	29.3
M2051	24/10/85	50	5.8	110	29.9	33.9
M2052	08/11/85	50	5.0	100	29.4	35.2
M3051	24/10/85	65	5.5	110	28.4	32.6
M3052	09/11/85	65	5.6	100	27.2	31.5
M2081	29/10/85	85	8.5	110	21.0	24.6
M2082	08/11/85	85	8.5	100	23.9	27.4
M3081	01/11/85	125	7.0	120	22.9	27.0
M3082	17/12/85	90	8.0	100	21.8	26.7
H2051	21/11/85	55	5.6	110	32.4	35.3
H2052	10/12/85	55	5.8	100	30.2	34.1
H3051	28/11/85	70	6.0	120	28.3	31.5
H3052	11/12/85	65	5.0	100	30.1	33.4
H2081	06/12/85	90	8.0	110	25.7	28.9
H2082	11/12/85	90	8.4	100	23.9	27.2
H3081	06/12/85	95	7.3	110	22.1	25.7
H3082	12/12/85	105	8.4	100	20.1	24.9

Table 7-2 SUMMARY OF IMAGE ANALYSIS DATA

SAMPLE	TOTAL AREA [SQ.MM.]	TOTAL NUMBER OF VOIDS	% TOTAL AIR	TOTAL NUMBER OF ENTRAINED AIR VOIDS
CM051A	588	1843	8.4	1304
CM051B	532	2695	6.6	1924
CM051C	570	2011	5.6	1424
CM051D	534	2998	6.2	2029
CM052A	552	2495	5.2	1750
CM052B	591	1536	3.9	1058
CM052C	588	1639	4.5	1153
CM052D	582	1886	4.1	1290
CM053A	398	2426	8.7	1655
CM053B	551	2077	5.3	1455
CM053C	529	2734	7.0	1904
CM053D	563	2228	5.3	1523
CM054A	468	2772	6.5	1876
CM054B	578	2058	4.1	1376
CM054C	578	1763	5.0	1236
CM054D	537	2488	5.0	1699
CM081A	317	2517	9.0	1643
CM081B	398	1970	8.2	1317
CM081C	412	1999	7.3	1327
CM081D	413	2266	7.5	1476
CM082A	366	1971	9.2	1285
CM082B	408	1984	9.7	1268
CM082C	412	1758	6.4	1131
CM082D	424	1452	6.6	976
CM083A	408	2063	9.1	1088
CM083B	352	2147	9.6	1411
CM083C	358	1957	11.2	1259
CM083D	353	2172	10.8	1412
L2051A	559	2777	5.6	1937
L2051B	497	3014	7.7	2029
L2051C	548	2307	6.9	1567
L2051D	512	2616	6.8	1733
L2052A	544	1779	5.4	1675
L2052B	511	1705	6.5	1705
L2052C	584	1789	4.8	1789
L2052D	415	2060	6.0	1449
L3051A	582	2062	4.8	1407
L3051B	575	1891	5.0	1316
L3051C	442	2693	7.6	1732
L3051D	375	2268	9.1	1425



Table 7-2 Summary of Image Analysis Data (Cont'd)

SAMPLE	TOTAL AREA [SQ.MM.]	TOTAL NUMBER OF VOIDS	% TOTAL AIR	TOTAL NUMBER OF ENTRAINED AIR VOIDS
L3052A	595	1474	4.7	998
L3052B	578	2516	5.7	1658
L3052C	526	2700	6.2	1780
L3052D	589	1904	5.2	1267
L2081A	352	2287	9.4	1575
L2081B	380	2047	8.4	1311
L2081C	358	2522	9.9	1665
L2081D	381	2359	8.9	1549
L2082A	364	2616	9.4	1629
L2082B	265	2641	14.7	1671
L2082C	350	2741	8.9	1787
L2082D	420	1587	6.2	1046
L3081A	408	2141	7.5	1358
L3081B	367	2205	9.1	1448
L3081C	377	2207	9.0	1383
L3081D				
L3082A	322	2409	11.1	1518
L3082B	350	2188	10.8	1434
L3082C	388	1886	9.3	1153
L3082D	373	2486	9.5	1595
M2051A	513	2366	6.7	1609
M2051B	535	2401	6.3	1662
M2051C	517	2675	7.4	1852
M2051D	552	2354	6.1	1610
M2052A	505	2645	5.8	1793
M2052B	460	2939	7.1	2018
M2052C	541	2441	6.6	1649
M2052D	543	1763	5.8	1763
M3051A	468	2589	8.6	1775
M3051B	529	2633	7.2	1711
M3051C	452	2717	8.3	1823
M3051D	518	2661	6.9	1832
M3052A	491	2601	7.2	1850
M3052B	571	2421	6.0	1665
M3052C	531	2310	6.3	1562
M3052D	497	2526	7.0	1714
M2081A	339	2153	10.0	1396
M2081B	349	2055	12.0	1270
M2081C	324	2116	12.5	1352
M2081D	364	2118	10.5	1319

Table 7-2 Summary of Image Analysis Data (Cont'd)

SAMPLE	TOTAL AREA [SQ.MM.]	TOTAL NUMBER OF VOIDS	% TOTAL AIR	TOTAL NUMBER OF ENTRAINED AIR VOIDS
M2082A	399	2415	9.3	1530
M2082B	362	2317	10.7	1486
M2082C	392	2185	8.8	1430
M2082D	404	2271	8.2	1476
M3081A	407	1915	9.9	1270
M3081B	390	2088	8.8	1289
M3081C	412	1960	7.3	1251
M3081D	384	2058	10.4	1323
M3082A	388	2152	9.4	1390
M3082B	404	1799	8.8	1120
M3082C	412	2215	9.6	1340
M3082D	331	2677	9.5	1754
H2051A	513	2457	6.5	1678
H2051B	539	2592	7.5	1824
H2051C	524	2342	5.9	1622
H2051D	573	2330	6.0	1593
H2052A	499	2471	6.9	1678
H2052B	557	2350	5.7	1638
H2052C	540	2598	5.6	1704
H2052D	595	1705	6.1	1207
H3051A	521	2549	7.1	1729
H3051B	518	2543	7.6	1769
H3051C	533	2519	8.0	1777
H3051D	545	2626	6.5	1745
H3052A	591	2203	4.7	1603
H3052B	580	2582	5.1	1834
H3052C	587	2098	4.9	1488
H3052D	572	2273	4.2	1627
H2081A	422	1827	7.9	1170
H2081B	400	1780	8.8	1178
H2081C	381	2080	9.9	1354
H2081D	393	2014	9.8	1336
H2082A	409	2410	9.3	1550
H2082B	393	2162	8.2	1383
H2082C	389	2372	7.3	1510
H2082D	410	1823	8.5	1199
H3081A	395	2284	8.6	1517
H3081B	415	1862	7.8	1199
H3081C	397	2532	8.7	1527
H3081D	401	2082	9.9	1395
H3082A	366	2079	9.3	1341
H3082B	390	1832	8.8	1209
H3082C	370	2017	10.0	1309
H3082D	419	2351	7.4	1499

Table 7-3

CHARACTERISTICS OF AIR VOID SYSTEM  
USING THE PLANE-INTERCEPT METHOD OF ANALYSIS

SAMPLE	AVERAGE DIAMETER OF VOID ( $\mu\text{m}$ )	SPECIFIC SURFACE ( $>25\text{mm}^2/\text{mm}^3$ )	VOIDS/ VOLUME ( $/\text{mm}^3$ )	PERCENT ENTRAINED AIR (%)	SPACING FACTOR ( $<0.2\text{ mm}$ )
CM051	119	33.6	25.2	2.7	.142
CM052	118	34.0	19.3	1.8	.159
CM053	112	35.7	28.6	2.7	.137
CM054	114	35.2	25.2	2.2	.143
CM081	116	34.4	32.1	2.9	.128
CM082	126	31.6	21.9	2.8	.148
CM083	130	30.8	27.1	3.5	.134
L2051	113	35.4	30.4	2.9	.133
L2052	115	34.8	28.1	2.7	.137
L3051	121	33.0	24.6	2.8	.143
L3052	120	33.3	20.8	2.4	.154
L2081	120	33.4	34.7	3.6	.123
L2082	119	33.6	36.9	3.4	.119
L3081	119	33.6	30.5	3.3	.131
L3082	121	32.9	32.8	3.4	.125
M2051	117	34.2	27.2	2.8	.138
M2052	114	35.2	31.0	2.8	.131
M3051	116	34.6	31.4	3.0	.130
M3052	116	34.5	28.0	2.8	.137
M2081	128	31.3	30.4	3.9	.128
M2082	125	32.0	30.5	3.7	.129
M3081	122	32.8	26.4	3.0	.138
M3082	128	31.2	28.5	3.5	.131
H2051	119	33.7	26.4	2.8	.139
H2052	123	32.5	23.1	2.8	.146
H3051	120	33.3	27.6	3.1	.136
H3052	108	37.1	26.1	2.2	.144
H2081	125	32.0	25.3	3.2	.140
H2082	118	33.9	29.9	3.1	.132
H3081	115	34.7	30.4	3.0	.132
H3082	121	33.0	28.6	3.4	.134

- 4) specific surface of the entrained-air-void system  
( $\text{mm}^2/\text{mm}^3$ ); and
- 5) spacing factor of the entrained-air-void system  
( $\mu\text{m}$ ).

The method of statistical analysis of the test results is described in Appendix A.

### 7.3 Statistical Evaluation of Image Analysis Data

The image analysis data is presented in Table 7-2. Within each test batch, four samples were individually analyzed. To compare data within each test group, a statistical comparison of means of total number of entrained voids was performed.

The comparison is given in Table 7-4. The only test group which indicates a significant variation is M208 (medium fly ash at 20% replacement and 8% air content). The variation cannot be explained in the batching procedure ( see Table 7-1). We can assume the difference is inherent to the M208 test group and is possibly due to experimental error during the preparation or microscopic analysis of the samples.

Table 7-4 Statistical Comparison of Means of Total Number of Entrained Voids in Table 7-2

	CM051	CM052	CM053	CM054
$\bar{x}$	1670	1313	1634	1547
s	359	307	198	293
n	4	4	4	4

Calculated "t"

CM051	-	1.5	0.17	0.53
CM052	-	-	1.76	1.10
CM053	-	-	-	0.49
CM054	-	-	-	-

"t" Critical @ 5% level of significance = 2.447

	CM052	CM053	CM054
$\bar{x}$	1441	1165	1292
s	153	144	154
n	4	4	4

Calculated "t".

CM081	-	1.86	0.97
CM082	-	-	1.20
CM083	-	-	-

"t" Critical @ 5% level of significance = 2.447

	L051	L2052	L3051	L3052	L2081	L2082	L3081	L2082
$\bar{x}$	1817	1655	1470	1426	1525	1533	1396	1425
s	207	145	181	359	151	331	46	193
n	4	4	4	4	4	4	3	4
Calculated "t"	1.28		0.22		.04		.21	

"t" Critical @ 5% level of significance = 2.447

	M2051	M2052	M3051	M3052	M2081	M2082	M3081	M2082
$\bar{x}$	1683	1806	1785	1698	1334	1481	1283	1401
s	115	155	55	119	43	41	30	263
n	4	4	4	4	4	4	3	4
Calculated "t"	1.27		1.33		*4.39		0.89.	

"t" Critical @ 5% level of significance = 2.447

\*This data group differs at the 5% significance level.

	H2051	H2052	H3051	H3052	H2081	H2082	H3081	H2082
$\bar{x}$	1679	1557	1755	1638	1260	1411	1410	1340
s	103	235	22	144	99	158	153	120
n	4	4	4	4	4	4	3	4
Calculated "t"	0.95		1.61		1.62		0.72	

"t" Critical @ 5% level of significance = 2.447

#### 7.4 Analysis and Discussion

##### 7.4.1 Air-Entraining Agent Demand

The required nominal air contents for the testing program were 5 and 8 percent with a tolerance of  $1\pm$  percent. The quantity of air entraining agent (AEA) added to the test batch to achieve the specified air content was determined by trial and error. In the process of determining the required amount of AEA a number of mixtures were batched. Only those mixtures which produced the desired nominal air content were used for image analysis.

The amount of AEA added to the test batches to produce 5 and 8 percent nominal air is recorded in Table 7-1. In the control mixes, the AEA requirement was 8 ml and 30 ml for 5 and 8 percent nominal air contents, respectively. With the addition of fly ash as a partial replacement of cement in the concrete mix, the demand for AEA increased. . .

In a number of test groups the amount of AEA added to the fly ash concrete mixtures varied. This is especially noticeable in the test groups with high air content and high percent replacement of fly ash. Gebler and Kleiger [45] found that the most significant components of fly ash affecting AEA requirements were organic matter content, carbon content, loss on ignition and alkali content. They also determined that a significant correlation existed between loss on ignition and carbon content and loss on ignition and organic matter content.

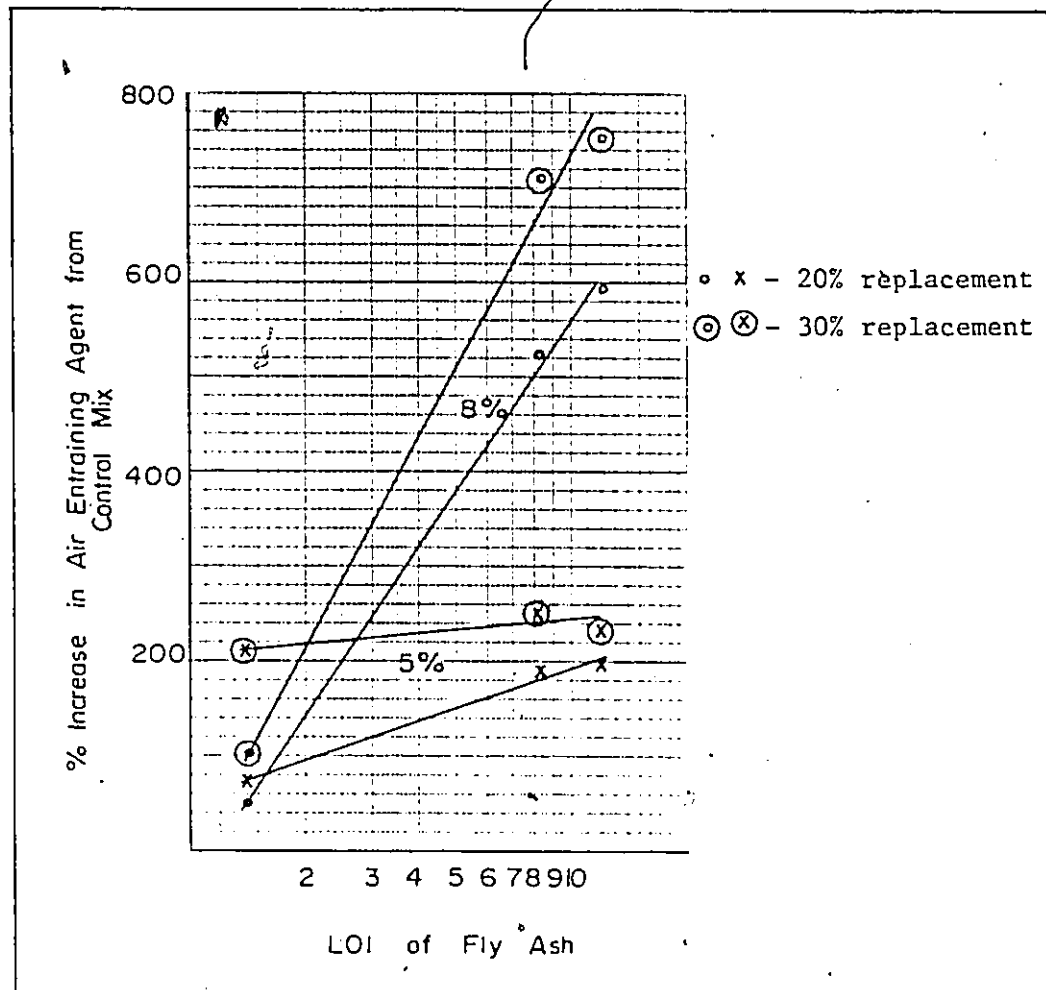


Figure 7-1 : Percent Increase in Air Entraining Agent Demand  
vs LOI of Fly Ash

Figure 7-1 graphically illustrates the log-normal trends between the percent increase in AEA and percent LOI for 5 and 8 percent nominal air content mixtures, having respectively 20 and 30 percent fly ash replacements. The



quantity of AEA increased in relation to the increase in LOI for the fly ash, however, as the LOI approaches the 12 percent level, the rate of increase in demand for AEA decreases, creating a non-linear trend. The increased demand for AEA in fly ash concrete is attributed to the high surface area of the carbon particles, which tends to adsorb the AEA. A fly ash with a finer particle size would also adsorb more AEA[39]. As shown below, the low LOI fly ash sample used in this research had a higher percent passing the 45 um sieve than the medium and high LOI fly ashes. The non-linear increase in demand for AEA observed in the fly ash concrete test batches may be attributed to the varying degrees of fineness for the three fly ash samples or the difference in LOI.

<u>Fly Ash</u>	<u>Percent LOI</u>	<u>Percent +325</u>
Low	1.4	1.7
Medium	8.2	28.3
High	12.1	12.1

#### 7.4.2 Compressive Strength

The results of compressive strength tests are presented in Table 7-1. Statistical analysis of these results is shown in Tables 7-5 and 7-6.

Table 7-5 Statistical Comparison of Means of 28 - day Compressive Strength for 5 and 8 Percent Nominal Air Content (Table 7-1)

	Control (MPa)	
	5%	8%
$\bar{x}$	34.3	27.0
s	4.01	1.04
n	4	3
calculated t	3.01*	

"t" critical @ 5 % significance level = 2.447

(Note: The table shown below uses a statistical comparison of paired means)

	Low LOI (MPa) 5% - 8%	Medium LOI (MPa) 5% - 8%	High LOI (MPa) 5% - 8%
$\bar{y}$	4.1	6.3	7.3
$S_{\bar{y}}$	1.34	0.86	0.90
n	4	4	4
calculated t	3.06	7.32**	8.07**

"t" critical @ 5 % significance level = 3.182

"t" critical @ 1 % significance level = 5.841

\* significantly different at the 5 % level of significance

\*\* significantly different at the 1 % level of significance

Table 7-6 Statistical Comparison of Paired Means of 28-day Compressive Strength for Fly Ash Concretes (Table 7-1)

	Low LOI vs Medium LOI (MPa)	Low LOI vs High LOI (MPa)
$\bar{y}$	4.2	3.2
$s_{\bar{y}}$	0.79	1.03
$n_{\bar{y}}$	8	8
calculated t	5.30**	3.11*

"t" critical @ 5 % significance level = 2.365

"t" critical @ 1 % significance level = 3.499

\* differs at the 5 % significance level

\*\* differs at the 1 % significance level

Table 7-7 Statistical Comparison of Paired Means of 56-day Compressive Strength for Fly Ash Concretes (Table 7-1)

	Low LOI vs Medium LOI (MPa)	Low LOI vs High LOI (MPa)
$\bar{y}$	4.0	3.7
$s_{\bar{y}}$	0.94	0.61
$n_{\bar{y}}$	8	8
calculated t	4.26*	6.06*

"t" critical @ 1 % significance level = 3.499

\* differs at the 1 % significance level

In Table 7-5 all test batches show that mixtures containing 5% air have significantly higher 28-day compressive strengths than mixtures containing 8% air. The control mix test batches had a 16 percent lower mean strength for the 8 percent nominal air content mixtures, than for the 5 percent nominal air content mixtures. In the fly ash concrete test groups, the mean of the differences in strength, between the 5 and 8 percent nominal air content mixtures, were compared. It is evident that the mean of the differences in strength increases as LOI increases to a maximum difference of 7.3 MPa observed in the high LOI fly ash test group.

In Table 7-6 the mean of the difference in strength for the low, medium and high LOI test groups are compared. A significant difference at greater than the 5 % level of significance was observed. The low LOI fly ash concrete attained the highest compressive strength. The greatest significant difference in means for 28-day compressive strength is shown between the low and medium LOI test groups. The low LOI fly ash has a finer particle size, therefore it is more reactive as a pozzolan.

A lower 28-day strength for the fly ash concrete mixture was anticipated; therefore, an additional set of two cylinders was cast and cured for a 56 day period. The results of the 28-day and 56-day compressive strengths are shown in Table 7-1. A comparison of the mean of the differences in strength at the 56-day curing period is

included in Table 7-7. As in the 28-day compressive strength results the low LOI specimens did differ significantly from the medium and high LOI specimens in compressive strength at the 1 % significance level.

Figures 7-2 and 7-3 illustrate the difference in strength at the 28-day and 56-day curing periods for 5 and 8 percent nominal air contents. The solid lines indicate the 28-day compressive strength for the control mixture. Figure 7-2 illustrates that although only one low LOI and one high LOI fly ash concrete test batch reached the 28-day strength of 34.3 MPa for the control mixture, all but two test batches had a 56-day strength above the 28-day strength for the control mixture. The lower 56-day strengths were obtained for the 30 percent fly ash replacement mixtures containing the medium and the high LOI fly ashes.

At 8 percent nominal air content the average strength for the control mixtures was 27.0 MPa. Three of the four low LOI fly ash concrete test batches exceeded this strength after the 56-day curing period. The remainder of the test samples had very low strengths even after the 56-day curing period.

When fly ash is added to concrete it acts as a pozzolanic material and to some extent exhibits its own cementitious properties. The degree to which a fly ash exhibits cementitious properties depends on the CaO content. The three fly ashes included in this testing program had CaO contents ranging from 4.9 to 5.3 percent. Fly ashes

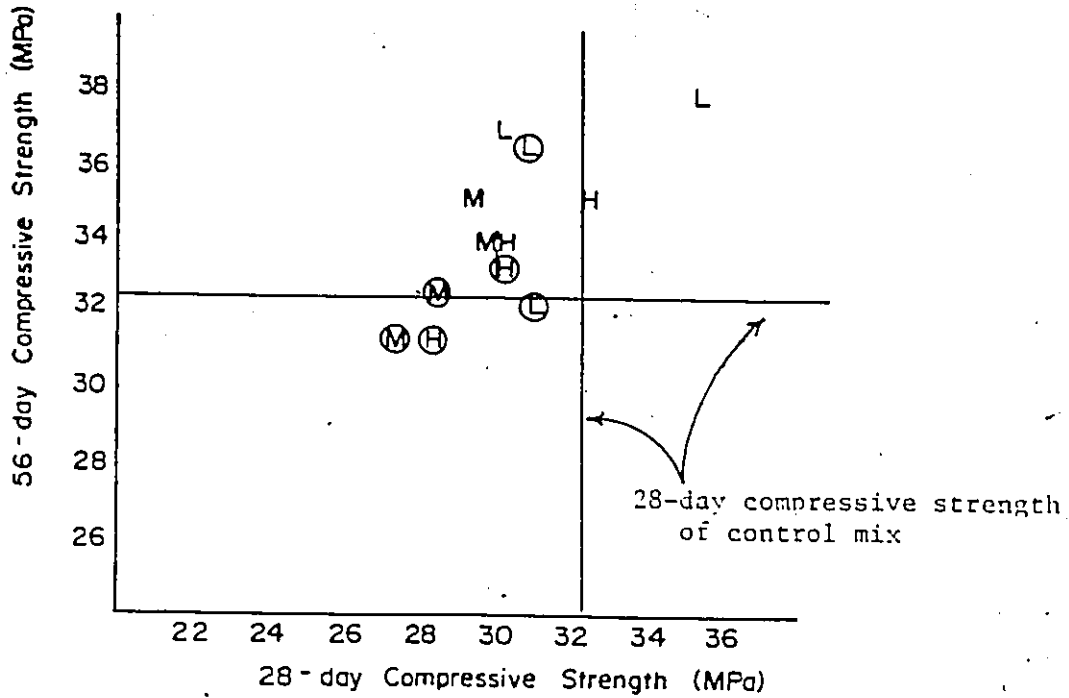


Figure 7-2 : Compressive Strength of Concrete at 5 % Nominal Air Content

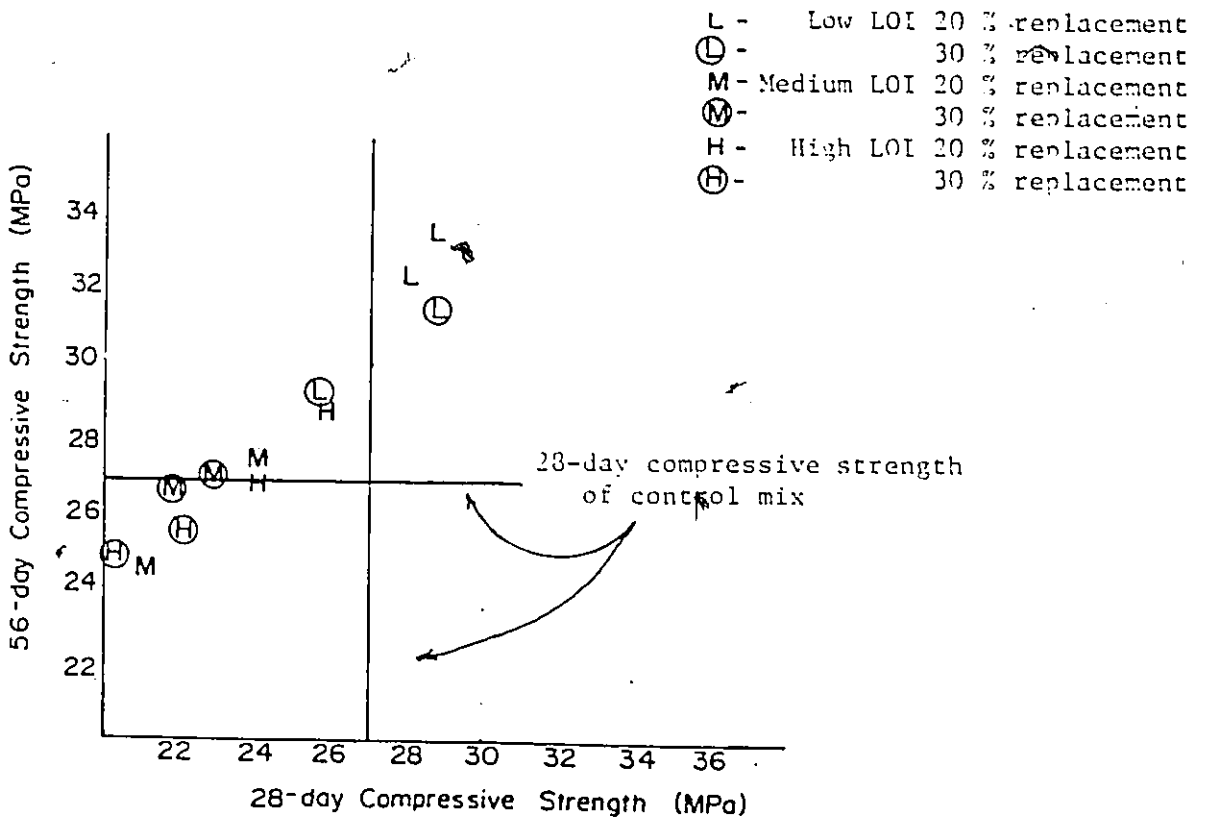


Figure 7-3 : Compressive Strength of Concrete at 3 % Nominal Air Content

with a CaO content less than 10 percent are considered to be a Class F fly ash and generally exhibit only slight pozzolanic properties. This explains the slow strength gain observed in the three fly ash concrete test batches. Concrete with pozzolans will continue to gain compressive strength long after the hydration of cement has slowed. The lower strength gain observed in some of the fly ash concrete test batches may have resulted from too short a curing period. It appears; that as the LOI, percent replacement, and air content increases, the concrete requires a much longer curing period to attain a given design strength.

#### 7.4.3 Air Content

The total air content for each test batch was measured in both the plastic and hardened states. In the hardened state, computerized image analysis was used to determine both the total air content and to classify the size distribution of the entrained air voids. The image analysis program was configured to distinguish between entrapped and entrained-air voids by the shape and section diameter. Entrained air was defined to include all air void sections with a circular shape and section diameter less than 1 mm.

Table 7-8 contains the measured total air content in the plastic and hardened states for each concrete test batch. Table 7-9 includes a statistical comparison of the mean air content measured in the plastic and hardened states for all test groups. The mean total air content of the

Table 7-8

Comparison of Measured Air Contents

<u>Test Batch</u>	<u>% Total Air Plastic State</u>	<u>% Total Air Hardened State</u>
CM051	5.0	6.7
CM052	4.8	4.4
CM053	5.2	6.6
CM054	5.1	5.2
CM081	7.7	8.0
CM082	7.5	8.0
CM083	7.5	10.2
L2051	5.1	6.8
L2052	4.5	5.7
L3051	5.3	6.6
L3052	4.9	5.5
L2081	7.1	9.1
L2082	10.0	8.2
L3081	7.0	8.5
L3082	8.1	7.8
M2051	5.8	6.6
M2052	5.0	6.3
M3051	5.5	7.7
M3052	5.6	6.6
M2081	8.5	11.2
M2082	8.5	9.3
M3081	7.0	9.1
M3082	8.0	9.3
H2051	5.6	6.5
H2052	5.8	6.0
H3051	6.0	7.3
H3052	5.0	4.7
H2081	8.0	9.1
H2082	8.4	8.3
H3081	7.3	8.8
H3082	8.4	8.9

---



Table 7-9 Statistical Comparison of % Total Air Content measured in the Plastic State and Hardened State (Table 7-7)

<u>Control Mixture (%)</u>				
	5%		8%	
	Plastic	Hardened	Plastic	Hardened
$\bar{x}$	5.0	5.7	7.6	8.7
s	0.17	1.11	0.12	1.27
n	4	4	3	3
calculated t	1.25		1.60	

"t" critical @ 5% significance level, ( = 6 ) = 2.447

"t" critical @ 5% significance level, ( = 4 ) = 2.776

(Note: The table shown below uses the statistical comparison of paired means)

	Low LOI (%)		Medium LOI (%)		High LOI (%)	
	Plastic/ Hardened		Plastic/ Hardened		Plastic/ Hardened	
$\bar{y}$	0.8		1.5		0.7	
$s_{\bar{y}}$	0.45		0.25		0.24	
n	8		8		8	
calculated t	1.78		5.97*		2.71*	

"t" critical @ 5% significance level = 2.365

\* differ significantly at the 5% level of significance

control group, measured in the hardened state, averaged 15 percent greater than the mean total air content determined in the plastic state. However, this difference did not prove to be statistically significant as indicated in Table 7-9. For the same comparison the medium LOI fly ash and the high LOI fly ash mixtures did show a significant difference.

When examining the hardened concrete by computerized image analysis the measured total air content value includes all pores regardless of the location within the concrete. The size and shape criteria used to filter out the entrained-air-void sections on the section sample surface eliminates the air voids within the aggregates and the larger entrapped air voids. In addition, aggregates which appear to be very porous were blackened after the sample surface was treated with the alumina oxide powder. Since it is the entrained-air-void system which is responsible for frost durability of the concrete, the evaluation of the characteristics of the air-void system is limited to the entrained rather than entrapped air void distribution.

The significantly higher air content determined in the hardened state for the fly ash concretes may be the result of the physical nature of the fly ash particles. Dolar-Mantauni [4] describes particles of fly ash as mostly solid or hollow spheres ranging in diameter from 1 to 150  $\mu\text{m}$ . The problem of analyzing a fly ash concrete in the

hardened state is in distinguishing between the air voids and the minute broken hollow spheres in the fly ash which may fill with the contrasting white powder.

In Table 7-9, the statistical analysis of the paired means for the two methods indicates the medium LOI fly ash mixture had differed at the highest significance level, followed by the high LOI fly ash mixture. This would be expected, since the medium LOI fly ash is the coarser of the three fly ash samples, followed by the high LOI and then the low LOI fly ash.

#### 7.4.4 Entrained-Air-Void System

Table 7-3 includes details of the characteristics of the entrained-air-void system as determined by the plane-intercept method. In general all test batches exhibited entrained-air-void characteristics believed to provide adequate protection against the deleterious effects of freeze-thaw action [48]. A statistical analysis of the data shown in Table 7-10 through 7-16 indicates that the addition of fly ash to the concrete did not have a significantly adverse effect on the parameters of the air-void system. Instead beneficial effects were observed in a majority of the fly ash concrete samples as discussed below.

In Table 7-10 it can be seen that the mean entrained air content for the control group at the 5% and 8% nominal air contents are 2.3% and 3.1%, respectively. The three fly

ash concrete test groups contained an entrained air content higher than the control group; however, the increase is not significant. A further statistical analysis in Table 7-11 of the entrained air content for the fly ash concretes at the 20% and 30% replacement levels indicate no significant difference in the percent entrained air produced. It is apparent from these data that the entrained-air-void system is unaffected by the addition of fly ash, when adjustments to the initial air entraining agent dosage are made.

As observed in the total air content analysis, the medium LOI fly ash group produced a higher entrained air content when compared to the other test groups. However as shown in Tables 7-10 and 7-12 this difference is not significant.

The number of entrained voids per volume of concrete for the control group at the 5% and 8% nominal air contents are 24.6 and 27.0, respectively. In Table 7-13, the voids per volume for the high LOI fly ash group are similar to the results of the control group. The low LOI and medium LOI groups have slightly higher voids per volume; however no significant differences were observed. The higher values may be attributed to the presence of hollow spherical particles in the fly ash, particularly for the coarser medium LOI fly ash as discussed previously. An alternative explanation for the higher number of entrained voids per volume evidenced in the fly ash concrete groups may be the

Table 7-10 Statistical Comparison of Means of Entrained Air Content for Control Mix with Fly Ash Concrete (Table 7-3)

Entrained Air Content (%)				
5% Nominal Air Content				
	Control	Low LOI	Medium LOI	High LOI
$\bar{x}$	2.3	2.7	2.9	2.7
s	0.45	0.21	0.09	0.38
n	4	4	4	4
Calculated "t"		1.38	2.31	1.35

"t" Critical @ 5% level of significance = 2.447

Entrained Air Content (%)				
8% Nominal Air Content				
	Control	Low LOI	Medium LOI	High LOI
$\bar{x}$	3.1	3.4	3.6	3.2
s	0.38	0.11	0.38	0.17
n	3	4	4	4
Calculated "t"		1.54	2.22	0.55

"t" Critical @ 5% level of significance = 2.571

Table 7-11 Statistical Comparison of Means of Entrained Air Content for 20% and 30% Fly Ash Mixtures (Table 7-3)

Entrained Air Content (%)						
	5% Nominal Air Content					
	Low LOI		Medium LOI		High LOI	
	20%	30%	20%	30%	20%	30%
$\bar{x}$	2.8	2.6	2.8	2.9	2.8	2.7
s	0.14	0.28	0.00	0.14	0.00	0.64
n	2	2	2	2	2	2
Calculated "t"	1.01		1.01		0.22	

Entrained Air Content (%)						
	5% Nominal Air Content					
	Low LOI		Medium LOI		High LOI	
	20%	30%	20%	30%	20%	30%
$\bar{x}$	3.5	3.4	3.8	3.3	3.2	3.2
s	0.40	0.07	0.14	0.35	0.07	0.28
n	2	2	2	2	2	2
Calculated "t"	0.35		1.88		0	

"t" Critical @ 5% level of significance = 4.303

Conclusion: No significant difference in entrained air content between 20% and 30% replacement.

Table 7-12 Statistical Comparison of Paired Means of Entrained Air Content for Fly Ash Concrete (Table 7-3)

Entrained Air Content (%)			
	Low LOI/ Medium LOI	Low LOI/ High LOI	Medium LOI/ High LOI
$\bar{y}$	.14	.10	.24
$s\bar{y}$	.087	.088	.126
n	8	8	8
Calculated "t"	1.61	1.11	1.89

"t" Critical @ 5% level of significance = 2.571  
for = 6

Conclusion: Entrained air contents for fly ash concrete do not differ at the 5% significance level.

Table 7-13 Statistical Comparison of Means of Voids per Volume for Control Concrete and Fly Ash Concrete (Table 7-3)

Voids per Volume ( $\text{in}^3/\text{mm}^3$ )

	5% Nominal Air Content			
	Control	Low LOI	Medium LOI	High LOI
$\bar{x}$	24.6	25.9	29.4	25.8
s	3.86	4.19	2.11	1.91
n	4	4	4	4
Calculated "t"		0.46	2.18	0.56

"t" Critical @ 5% level of significance = 2.447

Voids per Volume ( $\text{in}^3/\text{mm}^3$ )

	8% Nominal Air Content			
	Control	Low LOI	Medium LOI	High LOI
$\bar{x}$	27.0	33.7	28.9	28.6
s	5.10	2.72	1.93	2.29
n	3	4	4	4
Calculated "t"		2.28	0.70	0.57

"t" Critical @ 5% level of significance = 2.571

Conclusion: No difference observed in voids per volume for control or fly ash concrete mixture at the 5% significance level.



additional dosage of air entraining agent added to the fly ash concretes during batching to attain the desired air content.

The slightly higher number of voids per volume in the fly ash concrete test groups is accompanied by a reduction in the spacing factor. Again, no significant difference was observed, as shown in Table 7-14. The spacing factor for all test groups is considerably lower than the recommended maximum of 0.2 mm.

The mean specific surface for all data groups shown in Table 7-15, exceeded the minimum recommended value of 25 mm<sup>2</sup>/mm<sup>3</sup> by an average of 35 percent. The average specific surface for the 5 and 8 percent nominal air control mixture was 34.6 mm<sup>2</sup>/mm<sup>3</sup> and 32.3 mm<sup>2</sup>/mm<sup>3</sup>, respectively. All three fly ash concretes produced comparable values for specific surface with no significant differences from the control group. The 5% nominal air content mixtures have higher specific surface values than the nominal 8% air-content mixtures. A higher specific surface is favorable to frost-resistant concrete.

The lower specific surface values of the 8% nominal air content mixtures are accompanied by a greater average air-void diameter shown in Table 7-3 and 7-16. As image analysis is performed on the surface of the sample, the section diameters for the encountered air-voids are measured and recorded according to size into one of seven size groups. Table 7-17 presents the number of air-voids in each

Table 7-14 Statistical Comparison of Means of Spacing Factor for Control Concrete and Fly Ash Concrete (Table 7-3)

Spacing Factor (mm)				
5% Nominal Air Content				
	Control	Low LOI	Medium LOI	High LOI
$\bar{x}$	0.145	0.139	0.134	0.141
s	.0095	.0100	.0041	.0046
n	4	4	4	4
Calculated "t"		0.87	2.13	0.76

"t" Critical @ 5% level of significance = 2.447

Spacing Factor (mm)				
8% Nominal Air Content				
	Control	Low LOI	Medium LOI	High LOI
$\bar{x}$	.137	.125	.132	.134
s	.0103	.0050	.0045	.0038
n	3	4	4	4
Calculated "t"		2.07	0.89	0.55

"t" Critical @ 5% level of significance = 2.571

Conclusion: No difference observed in spacing factor for control or fly ash concrete mixture at 5% significance level.

Table 7-15 Statistical Comparison of Means of Specific Surface for Control Concrete and Fly Ash Concrete (Table 7-3)

Specific Surface ( $\text{mm}^2/\text{mm}^3$ )

	5% Nominal Air Content			
	Control	Low LOI	Medium LOI	High LOI
$\bar{x}$	34.6	34.1	34.6	34.2
s	0.99	1.16	0.42	2.03
n	4	4	4	4
Calculated "t"		0.66	0	0.35

"t" Critical @ 5% level of significance = 2.447

Specific Surface ( $\text{mm}^2/\text{mm}^3$ )

	8% Nominal Air Content			
	Control	Low LOI	Medium LOI	High LOI
$\bar{x}$	32.3	33.4	31.8	33.4
s	1.89	0.33	0.74	1.16
n	3	4	4	4
Calculated "t"		1.18	0.49	1.60

"t" Critical @ 5% level of significance = 2.571

Conclusion: The specific surface of the control concrete does not significantly differ from the fly ash concrete at the 5% level of significance.

Table 7-16 Statistical Comparison of Means of Average Void Diameter for Control Mix with Fly Ash Concrete (Table 7-8)

Average Void Diameter (um)				
5% Nominal Air Content				
	Control	Low LOI	Medium LOI	High LOI
$\bar{x}$	116	117	116	118
s	3.3	3.9	1.3	6.6
n	4	4	4	4
Calculated "t"		0.39	0	0.54

"t" Critical @ 5% level of significance = 2.447

Average Void Diameter (um)				
8% Nominal Air Content				
	Control	Low LOI	Medium LOI	High LOI
$\bar{x}$	124	120	126	120
s	7.2	1.0	2.9	4.3
n	3	4	4	4
Calculated "t"		1.13	1.17	1.57

"t" Critical @ 5% level of significance = 2.571

Conclusion: The average void diameter of the control concrete does not significantly differ from the fly ash concrete at the 5% level of significance.

size group. The average diameter of air-voids is calculated from the distribution of section diameters shown in Table 7-17. Figure 7-4 graphically depicts the percent distribution of section diameters less than 188  $\mu\text{m}$ , for each data group, at the 5 and 8 percent nominal air contents. It is apparent that 5% nominal air content produced a higher percentage of entrained air voids with section diameters less than 19  $\mu\text{m}$  for all data groups than the 8% nominal air content. This would account for the slightly lower specific surface values. However, a cumulative addition of the percent entrained-air voids in Table 7-17 indicate approximately 95 percent of the air voids have a section diameter less than 160  $\mu\text{m}$ . It is generally believed that the very fine entrained-air voids, in the order of 10 to 50  $\mu\text{m}$ , contribute most significantly to the resistance against frost action in concrete. The results of this research indicate that 40-50% of the entrained air voids fall within this size range.

Table 7-17 Size Distribution of Entrained Air Voids

SAMPLE	Percent of Total Number of Entrained Voids						
	0 - 19	19 - 47	47 - 94	94-188	188-282	282-376	>376
	(µm)						
CM051	22	24	30	17	5	2	2
CM052	33	23	23	15	4	1	1
CM053	21	24	31	17	4	1	1
CM054	32	22	26	14	4	1	1
CM081	32	23	24	15	4	1	1
CM082	29	19	26	18	4	2	2
CM083	30	19	26	17	5	2	2
L2051	23	22	31	18	4	1	1
L2052	22	24	31	16	4	1	2
L3051	26	20	27	19	5	1	2
L3052	22	20	31	20	4	2	2
L2081	30	20	26	17	5	2	1
L2082	36	18	24	14	4	1	1
L3081	25	19	29	18	4	2	2
L3082	32	19	25	16	5	2	1
M2051	27	20	29	18	5	1	1
M2052	28	22	27	16	4	1	1
M3051	28	22	27	17	4	1	1
M3052	24	21	30	18	4	1	1
M2081	27	18	29	17	5	2	2
M2082	28	17	27	19	5	2	2
M3081	28	17	29	19	5	1	2
M3082	31	16	27	17	4	2	2
H2051	25	19	30	18	5	2	1
H2052	22	22	30	18	4	2	2
H3051	23	20	30	19	4	2	2
H3052	22	23	32	18	4	1	1
H2081	25	18	30	19	5	2	2
H2082	27	18	30	18	5	2	1
H3081	27	19	28	19	4	1	1
H3082	23	18	31	21	5	2	2

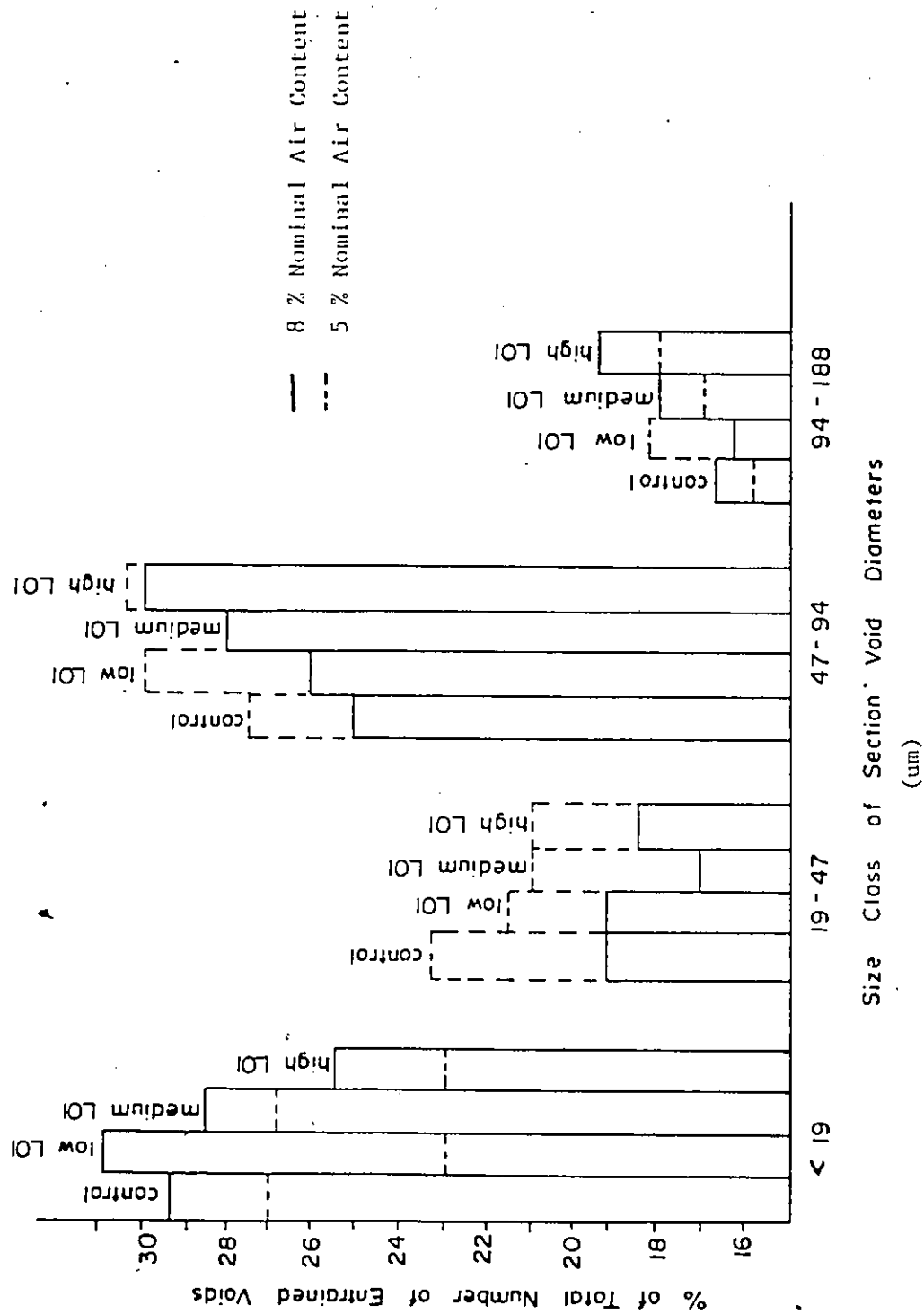


Figure 7-4 : Bar Graph of Percent Distribution of Section Diameters



## CHAPTER 8

### CONCLUSIONS AND RECOMMENDATIONS

[1] The addition of fly ash to air-entrained concrete increases the demand for air-entraining agent to maintain a given air content. The demand for air-entraining agent was also found to increase as the adsorptive characteristics of the fly ash increase. The degree of adsorption of a fly ash is dependent on the loss on ignition and fineness of the fly ash.

[2] The fly ash concrete test batches produced lower 28-day compressive strengths than the control mixture. However after a curing period of 56 days a majority of the fly ash concrete had exceeded the 28 day strength of the control mixture. The fly ash concrete test batches which did not reach the 28 day compressive strength of the control mixture contained the medium and high LOI fly ash samples at 30 percent replacement and 8 percent air. The additional strength gain which occurs after the 28-day curing period is a result of the pozzolanic activity which continues long after the hydration of cement has slowed down. As the % LOI of the fly ash and % replacement of the cement increases, the concrete requires a much longer curing period to attain the specified design strength.



[3] Microscopic analysis of the air void system in hardened concrete using image analysis techniques may indicate a higher total air content than actually exists. If the fly ash has a coarse particle size distribution with a large number of hollow spheres, the image analysis may interpret the spheres as air voids. A recommended solution to eliminate this error would be to carry out a standard method of microscopic analysis on a representative number of samples, so as to determine the percentage of hollow spheres in the void system. All test data would then be standardized to accomodate the presence of the hollow spheres.

[4] All test groups produced an entrained-air-void system which met the requirements for effective resistance to frost damage. The addition of fly ash to air-entrained concrete did not produce a significant difference in the parameters of the entrained-air-void system. However, to maintain a proper air void system in fly ash concrete, care must be exercised to ensure that adequate air-entraining agent is added to the concrete mixture during batching.

[5] The 5% nominal air content mixtures for all test groups tended to produce a larger percentage of entrained air voids less than 19  $\mu$ m, resulting in smaller average void diameter when compared to the 8% nominal air content mixtures.

However all test groups produced an entrained air void system with 40-50% of the voids having a section diameter less than 50  $\mu\text{m}$ .

[6] Image analysis has been found to be a more efficient, cost effective and more reliable method of air content determination. Computerized image analysis produces results beyond the capabilities of the conventional methods, such as, a means of filtering out entrapped air measurements, determining pore sizes and pore size distribution. With greater magnification and better surface preparation, the smaller voids that are considered to be an integral part of concrete durability can be detected.

[7] The results of this research indicate that the development of an image analysis system for air content measurement using a personal computer is a very promising approach considering the present cost and inaccessibility of the larger main frame image analysis systems. The continuation of the development of personal computer image analysis systems and its application to concrete technology is recommended.

## APPENDIX A

The statistical analysis for this research was based on the following statistical methods.[69]

Sample Mean      $x = \frac{x_1 + x_2 + \dots + x_n}{n}$      [1]

where  $x$  = observation

$n$  = number of observations

Standard Deviation      $\sigma = \frac{\sum_{i=1}^n (x_i - \mu)^2}{n}$      [2]

where  $\mu$  = true mean or sample mean

Correlation      $r = \frac{\sum xy}{\sqrt{\sum x^2 \sum y^2}}$      [3]

where  $x$  and  $y$  are variables

Linear Regression      $y = a + bx$      [4]

where  $a = \frac{\sum x^2 \sum y - \sum x \sum xy}{n \sum x^2 - (\sum x)^2}$

$b = \frac{n \sum xy - \sum x \sum y}{n \sum x^2 - (\sum x)^2}$

t - test : test to prove the null hypothesis that the two samples being compared are drawn from the same population.

$$S_c^2 = \frac{S_1^2(n_1 - 1) + S_2^2(n_2 - 1)}{(n_1 - 1) + (n_2 - 1)}$$

$$S_c = S_c \sqrt{\frac{n_1 + n_2}{n_1 n_2}}$$

$$t = \frac{|x_1 - x_2|}{S_c} \quad [5]$$

t - test for Paired Data - a test in which the mean difference between two samples is compared with the standard deviation.

$$\bar{x} = \frac{\sum x}{n} ; \quad y = x_2 - x_1 ; \quad \bar{y} = \frac{\sum y}{n}$$

$$S = \sqrt{\frac{\sum (y - \bar{y})^2}{n-1}} ; \quad S_{\bar{y}} = \frac{S}{\sqrt{n}}$$

We determine whether there is a difference between sample sets by comparing the mean difference,  $\bar{y}$ , to a zero mean difference using the t test.

$$t = \frac{|\bar{y} - 0|}{S\sqrt{n}}$$

- [6]

The values of the distribution of  $t$  is taken from Table III of Fisher and Yates, Statistical Tables for Biological, Agricultural, and Medical Research, published by Oliver & Boyd Ltd., Edinburgh, Scotland.

APPENDIX B

Image Analysis Software Program

```
#include <oc200.h>
```

```
#include <fcntl.h>
```

```
#include <stdio.h>
```

```
/* This program, written in C language enables the user to  
identify the various features of a prepared concrete surface and in  
turn quantify three important parameters of air voids in concrete:  
% air content, specific surface and spacing factor. In addition,  
the user has access to the characteristics of each individual air  
void, which may be used to determine void section diameter  
distributions.
```

```
*/
```

```
/* This program is an application of Gray library program  
DFEAT.C and is to be used as an image analysis system for determining  
air void parameters in hardened concrete.
```

```
*/
```

```
/**
```

```
matrix[y][x]: the window selected on the OCULUS 200 board is  
transferred in matrix[][] in two separate fields :  
matrix[0][x] to matrix[y3][x] is the first field of the  
window.
```

```
matrix[y3+1][x] to matrix[2*y3+1][x] is the second field  
of the window.
```

```
y3 = maximum index number for the y coordinate in matrix[y][x]  
it represents the line number of the last line in a field
```

x3 = maximum index number of the x coordinate in matrix[][]  
x3 = xword-1  
xword = number of words requested in window  
ylen = the number of lines requested. It is expanded to an even  
number of lines in matrix, by padding it with a blank at the  
end if ylen is odd

\*/

```
int _stack=64500;
int matrix[480][32];
main()
{
int ok,stop,er,startlin,i, display,nentree;
int curflag,winflag,objflag,imaflag;
int threshold,mode,lut,gmode,field,protect;
int ylen, xword;
int inter,grload();
int xadj,xlen,mask,y;
int imax,maxnb,noob,jmax,j,ret,x3, y3,totvds,totent;
FILE *fp,*dp;
int *nexti,*ob,*preanc,*predes,*line,*xdeb,*lon,*firsti;
int *anc,*des;
int reponse,n,x1 , y1 , x2 , y2,ac;
int flag,flag2,nc,ne[10],nclass,nfeat[12],c,k;
char label1[17],label2[10][17],sample[9];
float m[10][12],s[10][12],feat[12],air,scal;
char function[20],*malloc();
```



```
unsigned int nbyte,diff;
char *p,*data1,*data2,*name;
float n_black,n_white,totblk,totwht,total,dia,totdia,entdia,totarea;
float area, width;
float class1,class2,class3,class4,class5,class6,class7;
long int grcntp();
/*-----dynamic memory allocation -----*/
maxnb=1750;
nbyte = maxnb*2;
nexti =(int *)malloc(nbyte);
if (nexti == NULL)    {er=1; goto endstop;}
ob = (int *)malloc(nbyte);
if (ob == NULL)      {er=2 ; goto endstop;}
preanc = (int *)malloc(nbyte);
if (preanc == NULL)  {er=3 ; goto endstop;}
predes = (int *)malloc(nbyte);
if (predes == NULL)  {er=4 ; goto endstop;}
line = (int *)malloc(nbyte);
if (line == NULL)    {er=5 ; goto endstop;}
xdeb = (int *)malloc(nbyte);
if (xdeb == NULL)    {er=6 ; goto endstop;}
lon = (int *)malloc(nbyte);
if (lon == NULL)     {er=7 ; goto endstop;}
firsti = (int *)malloc(nbyte);
if (firsti == NULL)  {er=8 ; goto endstop;}

nbyte = maxnb*3*2 ;
```

```
anc = (int *)malloc(nbyte);
if (anc == NULL)      {er=9 ; goto endstop;}
des = (int *)malloc(nbyte);
if (des == NULL)      {er=10; goto endstop;}

/*-----*/

lut=4;      /* lut is the look-up table used */
protect=0 ; /* bit7 or graphic plane protected */
mode=1;     /* grab mode positive */
gmode=0;    /* continuous grabs */
threshold=56; /* threshold for grab */
startlin=20; /* beginning of display */
stop=0;     /* enable grab and display functions*/
field=0;
display=x1=y1=x2=y2=ok=curflag=winflag=objflag=imaflag=0;
grclo(0);
cls();
printf ("          IMANLYS.C \n");
printf ("          MEASURING AIR CONTENT IN \n");
printf ("          HARDENED CONCRETE(1986)\n");
for (i=0; i<32000; i++);
maxnb=500;
flag2=0;
menu:
if (display)
```

```
locate (1,1);
else
    cls ();
printf ("MAIN MENU FOR IMAGE ANALYSIS\n");
printf ("COMMANDS\n");
printf ("A:% air voids\n");          /*% air content only*/
printf ("D:obtain & transfer data\n");/*characteristics of air*/
printf ("Q:quit\n");                /*void section diameters*/

while (ok==0)
{
    reponse=getch ();
    switch (reponse)
    {
        /*****/
        case 'a':    /* % air voids in window */
        case 'A':
            if (winflag==1)
            {
                fp=fopen("PRN:", "w");
                n_black = grcntp(x1,y1,xlen,ylen,0);
                n_white = grcntp(x1,y1,xlen,ylen,1);
                fprintf(fp,"%1f %1f %1f\n",n_black,n_white,n_black+n_white);
                total = n_black / (n_black+n_white);
                fprintf(fp,"% air voids: %.2f\n",total*100);
            }

            else{locate(20,1);printf("window not set\n");}
```

```
fclose(fp);
locate (20,1);
for (i=1; i<2; i++) printf("                \n");
break;
/*****
case 'd': /*obtain and transfer data to outside file*/
case 'D':
    /* enter names of data files*/

    locate (15,1);
    printf ("sample identification = ");
    scanf ("%s",&sample); /* sample name*/
    printf ("number of pixels/micron = ");
    scanf ("%f",&scal); /* set pixel scale */
    printf ("Expected % air content? ");
    scanf ("%d",&ac); /* nominal air content*/

    /* initializing */
    n=totblk=totwht=totvds=area=width=0;
    dia=totdia=diff=totent=entdia=totarea=0;
    class1=class2=class3=class4=class5=class6=class7=0;
    output:
    n=n+1;

    /* specify window coordinates according to */
    /* nominal air content */
    if(ac > 5) {x1=140;y1=140;x2=360;y2=360;}
    else {x1=120; y1=120; x2=380; y2=380;}
```

```
/*grabbing image*/
cls();
locate (13,1);
printf ("GRABBING IMAGE\n");
grthrs(lut,threshold,mode);
printf ("Strike any key to end grab\n");
grgrab(lut,field,gmode,protect);
c = getch();
printf ("Grabbing image has ended\n");

data:

/*set window*/
grbox(x1,y1,x2,y2);

/*load window*/
xlen=x2-x1+1;      /* from the box coordinates */
ylen=y2-y1+1;      /* we calculate dimensions */
if (ylen &1) ylen-=1 ;/* test if number is even*/
                        /* adjust if not */
xword=(int)xlen/16; /* for encoding in the */
                        /*matrix*/
xadj=xlen-xword*16;/* xadj is the number of emp-*/
if (xadj!=0) xword+=1; /* ty bytes in the leftmost */
                        /* word to be filled with 1 */
if (xword>32) xword=32;
```

```
x3=xword-1;
xadj=xword*16-xlen;
y3=ylen-1;
grwindo (matrix,x1,y1,xword,ylen);/*load the matrix */
if (xadj!=0) /* mask the unused bit with */
{ /* 1 in the window */
mask=0xffff ;
mask= mask >> (16-xadj) ;
for (y=0; y<=y3; y++)
    matrix[i][xword]=matrix[i][xword] | mask;
for (y=y3+1; y<=2*y3+1; y++)
    matrix[i][xword]=matrix[i][xword] | mask ;
}
winflag=1;
locate (17,1);
printf("FRAME # %-3d\n",n);

/*encoding window*/
printf ("ADVANCE SAMPLE WHEN BEEP SOUNDS\n");
er=grencod(matrix,y3,x3,line,xdeb,lon,&imax,maxnb);
if(er == 705)
{
printf("TOO MANY PIXEL GRPS FOR ENCODING\n");
printf("WILL REDUCE FRAME SIZE\n");
grebox (x1,y1,x2,y2);
x1=x1+20; y1=y1+20; x2=x2-20; y2=y2-20;
grgrab(lut,field,mode,protect);
```

```
        goto data;
    }
    else if(er) goto endstop;

    /* link the window objects */
    er=link(line,xdeb,lon,ob,firsti,nexti,imax,preanc,
            predes,anc,des,&noob);
    if (er == 1351 || er == 1352)
    {
        noob = 0; imax = 0; n_black = 0;
        n_white = (x2-x1)*(y2-y1);
        sound (400,30);
        goto calculate;
    }
    else if(er) goto endstop;
    sound(400,30);

    /* determine total air content */
    /*calculating # of black & white pixels*/
    n_black = grcntp(x1,y1,xlen,ylen,0);
    n_white = grcntp(x1,y1,xlen,ylen,1);

    calculate:
    totblk=totblk+n_black;
    totwht=totwht+n_white;
    totvds=totvds+noob;
    width = (x2-x1)*scal/1000.0;
```

```
f area = area + (width*width);
```

```
/*analyse individual voids*/
```

```
if (flag2 == 0) /*FOR FIRST TIME ONLY*/
```

```
{  
/* assign the list of features */
```

```
nfeat[1]=10; nfeat[2]=11; /* feature 10 : width of */
```

```
nfeat[0]=2; /* smallest box enclosing object */
```

```
} /* feature 11: height of smallest box enclosing*/
```

```
/* object feature 2: number of objects where */
```

```
/* objects are void/sections */
```

```
/******- FEATURES -******/
```

```
k=1;
```

```
for (k=1; k<=noob; ++k) /* learn the # of voids */
```

```
{  
er=features(firsti[k],line,xdeb,lon,nexti,preanc,  
predes,anc,des,nfeat,feat,0.8);
```

```
if (er==852) goto cont;
```

```
if (er) goto endstop;
```

```
cont:
```

```
dia=(feat[1] + feat[2])/2;
```

```
totdia=totdia + dia;
```

```
diff=feat[1]-feat[2];
```

```
if (diff<=0.2*feat[1])./* check for width height */
```



```
{
    /* if true process as */
    totent = totent + 1; /* entrained air void */
    entdia = entdia + dia;
    totarea = totarea + (3.14 *(dia*dia)/4);

    /* classification of void section diameters */
    /* into size range */
    if (dia <= 2) class1 = class1 + 1;
    else if (dia > 2 && dia <= 5 ) class2 = class2 + 1;
    else if (dia > 5 && dia <= 10) class3 = class3 + 1;

    else if (dia > 10 && dia <= 20) class4 = class4 + 1;
    else if (dia > 20 && dia <= 30) class5 = class5 + 1;
    else if (dia > 30 && dia <= 40) class6 = class6 + 1;
    else class7 = class7 + 1;
}

flag2=1;
grebox(x1,y1,x2,y2);
locate(20,1);

/* check for end of sample analysis */
printf ("Hit S to continue with same sample\n");
printf ("Hit E to end and print data\n");
test:
reponse=getch();
if (reponse=='s' || reponse=='S') goto output;
else if (reponse=='e' || reponse=='E')
```

```
{ /* Printing data*/  
    fp=fopen("PRN:", "w");  
    if((fp=fopen("PRN", "w"))==NULL)  
    { locate (19,1);  
      printf(stderr, "cannot access printer");  
      goto test;  
    }  
  
    total = totblk/(totblk+totwht);  
  
    /* print out data */  
    fprintf(fp, "\n");  
    fprintf(fp, "SAMPLE : %s\n", sample);  
    fprintf(fp, "AREA OF SAMPLE ANALYSED : %.1f sq mms\n", area);  
    fprintf(fp, "NUMBER OF FRAMES : %-3d\n", n);  
    fprintf(fp, "TOTAL # OF VOIDS : %-4d\n", totvds);  
    fprintf(fp, "AVG DIAM OF TOTAL VOIDS : %.1f um\n", totdia/totvds*scal);  
  
    fprintf(fp, "PERCENT TOTAL AIR : %.2f %%\n", total*100);  
    fprintf(fp, "NUMBER OF ENTRAINED VOIDS : %-4d\n", totent);  
    fprintf(fp, "AVG DIAM OF ENTRAINED VOIDS : %.1f  
              um\n", entdia/totent*scal);  
    fprintf(fp, "PERCENT ENTRAINED AIR : %.2f  
              %%\n", totarea/(totblk+totwht)*100);  
    fprintf(fp, "CLASSIFICATION OF VOIDS\n");  
    fprintf(fp, "0.0 - %.1f : %.1f %%\n", 2*scal, class1/totent*100);  
    fprintf(fp, "%.1f - %.1f : %.1f %%\n",  
            2*scal, 5*scal, class2/totent*100);
```

```
fprintf(fp,"%0.1f - %0.1f : %0.1f
        %%\n",5*scal,10*scal,class3/totent*100);
fprintf(fp,"%0.1f - %0.1f : %0.1f
        %%\n",10*scal,20*scal,class4/totent*100);
fprintf(fp,"%0.1f - %0.1f : %0.1f
        %%\n",20*scal,30*scal,class5/totent*100);
fprintf(fp,"%0.1f - %0.1f : %0.1f
        %%\n",30*scal,40*scal,class6/totent*100);
fprintf(fp,"> %0.1f : %0.1f %%\n",40*scal,class7/totent*100);
        fclose(fp);
```

```
/* Decision to continue or return to main menu */
```

```
printf("DO YOU WISH TO CONTINUE WITH SAME SAMPLE
        (Y/N)?\n");
```

```
decision:
```

```
reponse=getch();
```

```
if(reponse == 'y' || reponse == 'Y') goto output;
```

```
else if(reponse == 'n' || reponse == 'N') goto menu;
```

```
else {sound (400.30);
```

```
        locate (24,1);
```

```
        printf ("bad key\n");
```

```
        locate (24,1);
```

```
        for (i=1; i<2; i++) printf ("\n");
```

```
        goto decision;
```

```
}
```

```
} /* Finish for response to End*/
```

```
else {  
    sound (400,30);  
    locate (24,1);  
    printf ("bad key\n");  
    locate (24,1);  
    for (i=1; i<2; i++) printf ("\n");  
    goto test;  
}  
break;
```

```
/******  
}
```

## REFERENCES

1. Canadian Standards Association, CAN3-A23.1-M77, "Concrete Materials and Methods of Concrete Construction", December 1977, Rexdale, Ontario.
2. Canadian Standards Association, CAN3-A23.2-M77, "Methods of Test for Concrete", December 1977, Rexdale, Ontario.
3. Neville, A.M., "Properties of Concrete", Third Edition, Pitman Publishing Limited, 39 Parker Street, London, 1981.
4. Dolar-Mantuani, L., "Handbook of Concrete Aggregates - A Petrographic and Technological Evaluation", Hoyes Publications, Park Ridge, New Jersey, 1983.
5. Annual Book of ASTM Standards 1986, ASTM Designation C618-85, "Standard Specification for Fly Ash and Raw or Calcined Natural Pozzolan for Use as a Mineral Admixture in Portland Cement Concrete", American Standard for Testing Materials, Philadelphia, Section 4, Volume 04.02, pp 385-388.
6. Mindess, S. and Young, J.F., "Concrete", Prentice-Hall, Inc., Englewood Cliffs, New Jersey, 1981.

7. Canadian Standards Association Publication,  
CAN3-A266.1-M.
8. Munro, E., "Concrete durability in a free market system",  
Concrete International, October, 1986.
9. American Concrete Institute, "Guide to Durable Concrete",  
ACI Committee 201, Detroit, 1977.
10. Powers, T.C., "A Working Hypothesis for Further Studies of  
Frost Resistance of Concrete", American Concrete  
Institute Journal, Proceedings, Volume 41 N4, February  
1945, pp 245-272.
11. Powers, T.C., "The Air Requirement of Frost-Resistant  
Concrete", Proceedings, Highway Research Board, V29,  
1949.
12. Powers, T.C., "Void Spacing as a Basis for Producing  
Air-Entrained Concrete", American Concrete Institute  
Journal, Proceedings, V50 N9, May 1954, pp 741-760.
13. Powers, T.C., "Basic Considerations Pertaining to Freezing  
and Thawing Tests", Proceedings, American Standards for  
Testing Materials, V55, 1955, pp 1132-1155.

14. Powers, T.C., "The Mechanism of Frost Action in Concrete", Stanton Walker Lecture Series on Material Sciences, Lecture No. 3, University of Maryland, November, 1965.
15. Litvan, G.G., "Frost Action in Cement Paste", Materials and Structures, No. 34, July-August, 1973.
16. Powers, T.C., "The Bleeding of Portland Cement Paste, Mortar and Concrete", Research Department Bulletin No. 2, Portland Cement Association, July 1939.
17. Klieger, P., "Something for Nothing - Almost", Concrete International, January 1980.
18. Berry, E.E., Hemmings, R.T., and Burns, J.S., "Coal Ash in Canada Summary Report", Canadian Electrical Association, Montreal, Quebec, March 1983.
19. Lea, F.M., "The Chemistry of Cement and Concrete", 3rd Edition, Chemical Publishing Company, Inc., New York, 1971.
20. Malquori, G., "Portland-Pozzolan Cement", Paper VIII - 3, Proceedings of the Fourth International Symposium, Chemistry of Cement, Washington, pp 983-1000, 1960.

21. Colleparidi, M., et. al., "The Effect of Pozzolans on the Tricalcium Aluminate Hydration", Cement and Concrete Research, 8, pp 741-752, 1978.
22. Berry, E.E., "Fly Ash for use in concrete Part I - A Critical review of the chemical, physical and pozzolanic properties of fly ash", CANMET, Energy, Mines and Resources Canada, CANMET Report, 1976.
23. Watt, J.D. and Thorne, D.J., "Composition and Pozzolanic Properties of Pulverized Fuel Ashes.  
Part I, Journal Applied Chemistry, 1965  
Part II, Journal Applied Chemistry, 1965  
Part III, Journal Applied Chemistry, 1966.
24. Lane, R.O. and Best, J.F., "Properties and Use of Fly Ash in Portland Cement Concrete", Concrete International, July 1982.
25. Manz, O., "Lignite Production and Utilization, Paper A4, Preprints to Fourth International Ash Utilization Symposium, 1976, St. Louis, Missouri.
26. Davis, R.E., Carlson, R.W., Kelly, J.W. and Davis, H.E., "Properties of Cements and Concretes Containing Fly Ash", Journal ACI, V 33, May 1937.



27. Davis, R.E., Davis, H.E. and Kelly, J.W., "Weathering Resistance of Concretes Containing Fly Ash Cements", Proc. ACI, V 37, 1941.
28. Davis, R.E., "Use of Pozzolans in Concrete", Journal ACI, V 46, January 1950.
29. Blanks, R.F., "Fly Ash as a Pozzolan", Proc. ACI, V 46, May 1950.
30. Minnick, J.L., "Investigations Relating to the Use of Fly Ash as a Pozzolanic Material and as an Admixture in Portland Cement Concrete", Proc. ASTM, V 54, 1954.
31. Mather, B., "Discussion of Minnicks paper", Proc. ASTM, V 54, 1954.
32. Clendenning, T.G. and Durie, N.D., "Properties and Use of Fly Ash from a Steam Plant Operating Under Variable Load", Proc. ASTM, V 62, 1962.
33. Hester, J.A. and Smith, O.F., "Use of Fly Ash in Concrete by the Alabama Highway Department, NRC Symposium, 1964.
34. Hughes, R.D., "Experimental Concrete Pavement Containing Fly Ash Admixtures, NRC Symposium, 1964.

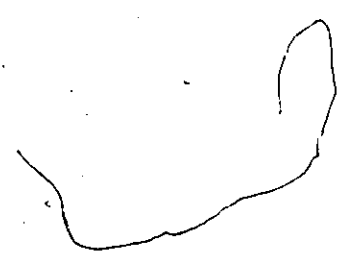
35. Sutton, C.A., "Use of Fly Ash in Concrete Pavement Constructed in Newbraska", NRC Symposium, 1964.
36. Stingley, W.M. and Peyton, R.L., "Use of Fly ASH as an Admixture in an Experimental Pavement in Kansas", NRC Symposium, 1964.
37. Legg, F.E., "Experimental Fly Ash Concrete Pavement in Michigan", NRC Symposium, 1964.
38. Stirrup, V.R. and Clendenning, T.G., "The Evaluation of Concrete by Outdoor Exposure", Highway Research Record, PCC, HRR268, USA, 1969.
39. Mardulier, F.J., "Particle Size of Dispersed Carbon Black Affects Entrainment of Air in Concrete", Civil Engineering, V 18, 1948.
40. Larson, T.D., "Air Entrainment and Durability Aspects of Fly Ash Concrete", Proc. ASTM V 64, 1964.
41. Gebler S. and Klieger, P., "Effect of Fly Ash on the Air-Void Stability of Concrete", Proc. of the CANMET/ACI First International Conference, Montbello, Quebec, July-August 1983.

42. Dodson, V., "Foam Index Test", presented at the  
Transportation Research Board, Washington, D.C.,  
January 1980.
43. Meininger, R., "Use of Fly Ash in Concrete--Report of  
Recent NSGA-NRMCA Research Laboratory Studies",  
Presented at NRMCA Quality Control Conference, St.  
Louis, MO, July 1980.
44. Stirrup, V.R., Hooton, R.D. and Clendenning, T.G.,  
"Durability of Fly Ash Concrete", Proc. of the  
CANMET/ACI First International Conference, Montbello,  
Quebec, July-August 1983.
45. Gebler S., and Klieger, P., "Effect of Fly Ash on the  
Durability of Air-Entrained Concrete", Proc. of the  
CANMET/ACI Second International Conference on the Use  
of Fly Ash, Silica Fume, Slag and Natural Pozzolans in  
Concrete, Madrid, Spain, April 1986.
46. Klieger, Paul, "Studies of the Effect of Entrained Air on  
the Strength and Durability of Concretes Made with  
Various Maximum Sizes of Aggregates", Research  
Department Bulletin RX040, Portland Cement Association,  
1952.

47. ACI Manual of Concrete Practice, Part I - 1985, Cement and Concrete Terminology, ACI 116R - 78.
48. Canadian Portland Cement Association, Design and Control of Concrete Mixtures, Metric Edition, 160 Bloor St. East, Toronto, Ontario.
49. Kosmatka, S.H. and William, C.P., "Design and Control of Concrete Mixtures", Thirteenth Edition, 5420 Old Orchard Road, Skokie, Illinois.
50. Annual Book of ASTM Standards 1986, ASTM Designation C138-81, "Test Method for Unit Weight, Yield, and Air Content of Concrete", American Society for Testing Materials, Philadelphia, Section 4, Volume 04.02.
51. Annual Book of ASTM Standards 1986, ASTM Designation C173-78, "Test Method for Air Content of Freshly Mixed Concrete by the Volumetric Method", American Society for Testing Materials, Philadelphia, Section 4, Volume 04.02.
52. Annual Book of ASTM Standards 1986, ASTM Designation C231-82, "Test Method for Air Content of Freshly Mixed Concrete by the Pressure Method", American Society for Testing Materials, Philadelphia, Section 4, Volume 04.02.

53. Chayes, F., "A Simple Point Counter for Thin-Section Analysis", American Mineralogist, V. 34, 1949.
54. Annual Book of ASTM Standards 1986, ASTM Designation C457-82, "Practice for Microscopical Determination of Air-Void Content and Parameters of the Air Void System in Hardened Concrete", American Society for Testing Materials, Philadelphia, Section 4, Volume 04.02.
55. Brown, L.S. and Pierson, C.U., "Linear Traverse Technique for Measurement of Air in Hardened Concrete", ACI Journal, Proceedings V.47, No.2, Oct. 1950.
56. Willis, T.F., "Discussion of "Linear Traverse Technique for Measurement of Air in Hardened Concrete", ACI Journal, Proceedings V.47, Part 2, Dec. 1951.
57. Lord, G.W. and Willis, T.F., "Calculation of Air Bubble Size Distribution from Results of a Rosiwal Traverse of Aerated Concrete", ASTM Bulletin No.177, Oct 1951.
58. Verbeck, George J., "The Camera Lucida Method for Measuring Air Voids in Hardened Concrete", ACI Journal, Proceedings V.43, May 1947.

59. Rexford, Elliot.P., Discussion of a paper by George Verbeck: "The Camera Lucida Method for Measuring Air Voids in Hardened Concrete," ACI Journal, Dec. 1947, Part 2, Proc. V. 43.
60. Willis, T.F., "Remarks on a Paper by T.C. Powers Entitled 'The Air Requirement of Frost Resistant Concrete', Missouri State Highway Department, Bureau of Materials, Research Division (1949).
61. Warren, C., "Determination of Properties of Air Voids in Concrete", Bulletin No. 7, Highway Research Board, 1953.
62. Chatterji, S. and Gudmundsson, H., "Characterization of Entrained Air Bubble Systems in Concretes by Means of an Image Analysing Microscope", Cement and Concrete Research, V.7, 1977.
63. Kernigham, B.W. and Ritchie, D.M., "The C Programming Language", Prentice-Hall, 1978.
64. Annual Book of ASTM Standards 1986, ASTM Designation C311-87, "Test Method for Sampling and Testing Fly Ash or Natural Pozzolans for Use as a Mineral Admixture in Portland Cement Concrete, American Society for Testing Materials, Philidelphia, Section 4, Volume 04.02.

65. Benton, Elton J., "Cement-Pozzolan Requirements" Highway Research Board #239, pp.56-65.
  66. Dunn, J.R. and Hudec, P.P., "Frost and Sorption Effects in Argillaceous Rocks", Highway Research Record No. 393, 1972.
  67. Meyer, L.P.H., "Determination of Air Content in Hardened Concrete Using Image Analysis", Masters Thesis, University of Windsor, 1983.
  68. Racic, D., "An Investigation of the Effect of Superplasticizers on the Entrained Air Void System in Concrete Using Image Analysis", Masters Thesis, University of Windsor, 1984.
  69. Kennedy, J.B. and Neville, A.M., "Basic Statistical Methods for Engineers & Scientists", A Dun-Donnelley Publisher, New York, New York, 1976.
  70. Cook, J.E., "Research and Application of High-Strength Concrete Using Class C Fly Ash", Concrete International, July 1982.
- 

VITA AUCTORIS

- 1961 Barbara Yvette Sellars was born on December 18, 1961 in Western Bay, Newfoundland.
- 1966 In September 1966, she began her early education at Western Bay Elementary, Newfoundland.
- 1975 Her secondary education, which included Grades 10 and 11, was obtained at Bishops College, St. John's, Newfoundland.
- 1977 In September, 1977, she attended Memorial University of Newfoundland, St. John's, Newfoundland, where two years of General Science prepared her for entry into the Faculty of Engineering in September of 1979.
- 1984 In May, 1984, she successfully completed a Bachelors degree in Civil Engineering from Memorial University of Newfoundland. In July, 1984, she enrolled as a graduate student at the University of Windsor, Windsor, Ontario, to attain the degree of Master of Applied Science in Civil Engineering.
- 1987 In April, 1987, she left full-time graduate studies, to pursue a career at Dominion Soil Investigation Inc. Her graduate studies was continued on a part-time basis.